

**An Easy to Manufacture Non-Contact Precision Linear
Motion System And Its Applications**

by

Roger Shapley Cortesi

S.B., Mechanical Engineering
Massachusetts Institute of Technology, 1999

SUBMITTED TO THE DEPARTMENT OF MECHANICAL ENGINEERING
IN PARTIAL FULFILLMENT OF THE DEGREE OF

MASTER OF SCIENCE

at the

MASSACHUSETTS INSTITUTE OF TECHNOLOGY

August 2000

[September 2000]

© 2000 Massachusetts Institute of Technology
All rights reserved




Signature of Author



.....
Department of Mechanical Engineering
August 1, 2000

Certified by

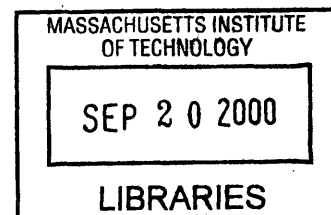
.....

Professor Alexander Slocum
 Thesis Supervisor

Accepted by

.....

Professor Ain A. Sonin
Chairman, Department Graduate Committee



BARKER



An Easy to Manufacture Non-Contact Precision Linear Motion System And Its Applications

by

ROGER CORTESI

Submitted to the Department of Mechanical Engineering
on August 1st, 2000 in Partial Fulfillment of the
Requirements for the Degree of Master of Science
at the Massachusetts Institute of Technology

ABSTRACT

The Axtrusion is a new linear motion element developed by Professor Alexander Slocum and Roger Cortesi of the Massachusetts Institute of Technology's Mechanical Engineering Department. It is an easy to manufacture non-contact linear motion system. The prototype uses porous graphite air bearings and an open face permanent magnet linear motor to support and propel the carriage. Since there is no contact between the carriage and the way, the Axtrusion is ideal for high speed where reliability is at a premium. Initial testing of the prototype carriage indicates that it has the following performance specifications: a vertical load capacity of 2000 N (450 lbs); horizontal load capacity of 4000 N (900 lbs); a carriage pitch error of 12 micro-radians (2.5 arc seconds); a yaw error of 7.7 micro-radians (1.6 arc seconds); a vertical straightness at the center of the carriage of 0.3 microns (0.000012 inches); and a vertical stiffness of the carriage of 422 Newtons per micron (2,400,000 lbs/in).

Thesis Supervisor:
Prof. Alexander H. Slocum
Dept. of Mechanical Engineering

ACKNOWLEDGMENTS

I would like to thank my thesis advisor Professor Alex Slocum for all of his help and criticism. I would also like to thank Eli Razon of Anorad Corporation (www.anorad.com), Drew Devitt of Newway Bearings (www.newwaybearings.com), Phillip Greene of Dover Instruments (www.doverinstruments.com), and Claire "the measurement goddess" Johnson also of Dover Instrument for all of their help in making this project a success. A big thanks to the summer UROPS Sean Montgoery and Kelly Harper for all their help in machining the parts. Finally to Jen Kelly for her proof reading help.

Abstract	3
Acknowledgments	5
Nomenclature	13
Chapter 1. Designing the Axtrusion	14
1.1 Axtrusion Components	15
1.2 How the Axtrusion Works	17
1.3 The Bench Level Prototype	19
1.4 Bearing Selection	21
1.4.1 Rolling Elements	21
1.4.2 Hydrostatic Bearings	21
1.4.3 Orifice Air Bearings	21
1.4.4 Porous Graphite Air Bearings	21
1.5 Way Surface Selection	23
1.5.1 Granite	23
1.5.2 Polymer Concrete	23
1.5.3 Metal	23
1.5.4 Aluminum Oxide	23
1.6 Motive Power Selection	25
1.6.1 Linear Motors	25
1.6.2 Ball Screw	25
1.6.3 Belt Drive	25
1.7 Sizing the Carriage (Load Capacity)	27
1.8 Sizing the Carriage (Roll and Normal Stiffness)	29
1.8.1 Stiffness of the Individual Bearing Pads	29
1.8.2 Stiffness Normal to the Direction of Travel	29
1.8.3 Rotational Stiffness	29
1.9 Casting the Carriage Base	31
1.10 Machining the Carriage Base	33
1.11 The Carriage Fixturing	35
1.12 Replicating the Bearing Pads to the Carriage Base	37
1.13 Assembly Lessons Learned	39
1.14 Modal Analysis Setup	41
1.15 Modal Analysis Results	43

1.16 The Dynamic Stiffness	45
1.17 Measurement Setup	47
1.18 The Pitch Data	49
1.19 The Yaw Data	51
1.20 The Linear Position Accuracy Data	53
1.21 The Vertical Straightness Data	55
1.22 The Vertical Stiffness Data	57
Chapter 2. The MiniMill	60
2.1 Some Competing Machines	61
2.1.1 Small Hobbyist Machines	61
2.1.2 Small CNC Machining Centers	61
2.2 Some Initial Concepts	63
2.3 Two “L”s To Make a Machine	65
2.4 The Error Budget	67
2.4.1 Static Deflection Errors	67
2.4.2 Thermal Expansion Errors	67
2.4.3 Control and Alignments Errors	67
2.5 MiniMill Major Components	69
2.6 Simple Stiffness Check	71
2.7 A Finite Element Check	73
2.8 An FEA Check of the Z Axis	75
2.9 Displacement Errors Due to Gravity	77
2.9.1 Error Inducing Displacements	77
2.9.2 Non Error Inducing Displacement	77
2.10 Remaining Work on the Minimill	79
Chapter 3. Axtrusion Part Drawings	80
Chapter 4. Axtrusion Supplementary Materials	113
A.1 Carriage Stiffness Estimates	113
A.1.1 Air Bearing Stiffness Calculations	113
A.1.2 Estimating the Stiffness of the Axtrusion	115
A.1.3 Translation and Rotation of Points Not at the C.O.S.	117
A.2 Detail Bearing Replication Steps	117

A.3 Performance Data from the Prototype	123
A.3.1 Carriage Pitch Data	123
A.3.2 Carriage Yaw Data	127
A.3.3 Linear Position Accuracy Data	131
A.3.4 Straightness Data	133
A.4 The Stiffness Data	135

TABLE 1.1	Carriage Floating Modes	43
TABLE 1.2	Carriage Not Floating Modes	43
TABLE 1.3	Modal Equipment Conversion Factors	45
TABLE 2.1	Equivalent Young's Modulus for Air Pad Models	73
TABLE A.1	Carriage Pitch Data Results	124
TABLE A.2	Carriage Yaw Data Results	128
TABLE A.3	Linear Position Accuracy Results	131
TABLE A.4	Vertical Carriage Displacements Under Load	135
TABLE A.5	Vertical Carriage Stiffness Data	136

NOMENCLATURE

A	area [m ²]
\vec{C}	carriage compliance matrix (6 x 6)
$\vec{D}_{carriage}$	the displacement and rotational vector (1 x 6) of the carriage
E	Young's modulus [Pa]
\vec{E}	The displacement vector (1 x 4) of the point \vec{P}
f	frequency [Hz]
F	force [N]
F_m	attractive force between the motor coil and magnet track [N]
F_s	force on each side bearing [N]
F_{top1}	force on each inboard top bearing [N]
F_{top2}	force on each inboard top bearing [N]
g	gravitational acceleration [m/s ²]
h	air gap between air bearing and way surface [m] or [microns]
\vec{HTM}	The Homogenous Transformation Matrix (4 x 4)
K	stiffness [N/m]
K_{50x100}	stiffness of the 50 x 100 mm bearings [N/m]
K_{75x150}	stiffness of the 75 x 150 mm bearings [N/m]
L	load [N]
L_{50x100}	load on 50 x 100 mm bearing [N]
L_{75x150}	load on 75 x 150 mm bearings [N]
$L_{bmaxside}$	the maximum load that can be supported by a side bearing [N]
$L_{bmaxtop}$	the maximum load that can be supported by a top bearing [N]
L_{cmaxh}	the maximum working load of the carriage in the horizontal direction [N]
L_{cmaxv}	the maximum working load of the carriage in the vertical direction [N]
L_{lr}	the distance between the left and right pairs of top bearings [mm]
\vec{P}	The vector (1 x 4) containing the coordinates of a point with respect to the carriage's center of stiffness.
P_s	supply pressure [Pa]
θ	motor angle [degrees]
w_m	width of the motor track [mm]
Y_1	location of the inboard pair of top bearings in the Y direction [mm]
Y_2	location of the outboard pair of top bearings in the Y direction [mm]
Y_m	motor coil location in the Y axis [mm]
Z	the center of the side bearings in the Z direction [mm]
Z_m	motor coil location in the Z axis [mm]

Chapter 1

DESIGNING THE AXTRUSION

The Axtrusion is a new linear motion concept developed by Professor Alexander Slocum and Roger Cortesi of the Massachusetts Institute of Technology's Mechanical Engineering Department.

It is intended for applications where the emphasis is on high speed, no wear, and very low error motions. It is designed to enable air bearing systems to be competitive in price with high performance ball bearings systems. At the same time, it exploits all the advantages of a non-contact motion system.

Envisioned applications include:

- Precision high speed material handling
- Machining and turning centers
- Optical equipment.

The functional requirements of the Axtrusion system are:

- **No Contact:** No contact between the way and the carriage allows for very high speed operation and NO wear. The elimination of grease will reduce machine downtime and mess. Non-contact is also the primary means of reducing error motion.
- **Moderate Stiffness:** The exact stiffness requirement will be determined by the specific application.
- **Thermal Robustness:** Many linear guide systems are very sensitive to large changes in temperature due to the very tight tolerances between the parts. The Axtrusion should be insensitive to temperature changes.
- **Minimal Precision Surfaces and Parts:** The geometry should remain simple, and minimal precision parts should be used to keep the manufacturing inexpensive and easy.

1.1 Axtrusion Components

1. **The Way:** This is the base of the Axtrusion. It is the surface on which the carriage slides back and forth.
2. **The Top and Side Precision Surfaces:** These are the two critical surfaces of the way. The air bearings slide over these two surfaces, hence the necessity for higher tolerances on straightness and surface finish.
3. **Linear Motor Permanent Magnet Track:** This component is bolted to the angled groove in the top surface.
4. **Position Encoder Scale:** This component is a piece of tape that allows the position encoder read head to measure the carriage's position.

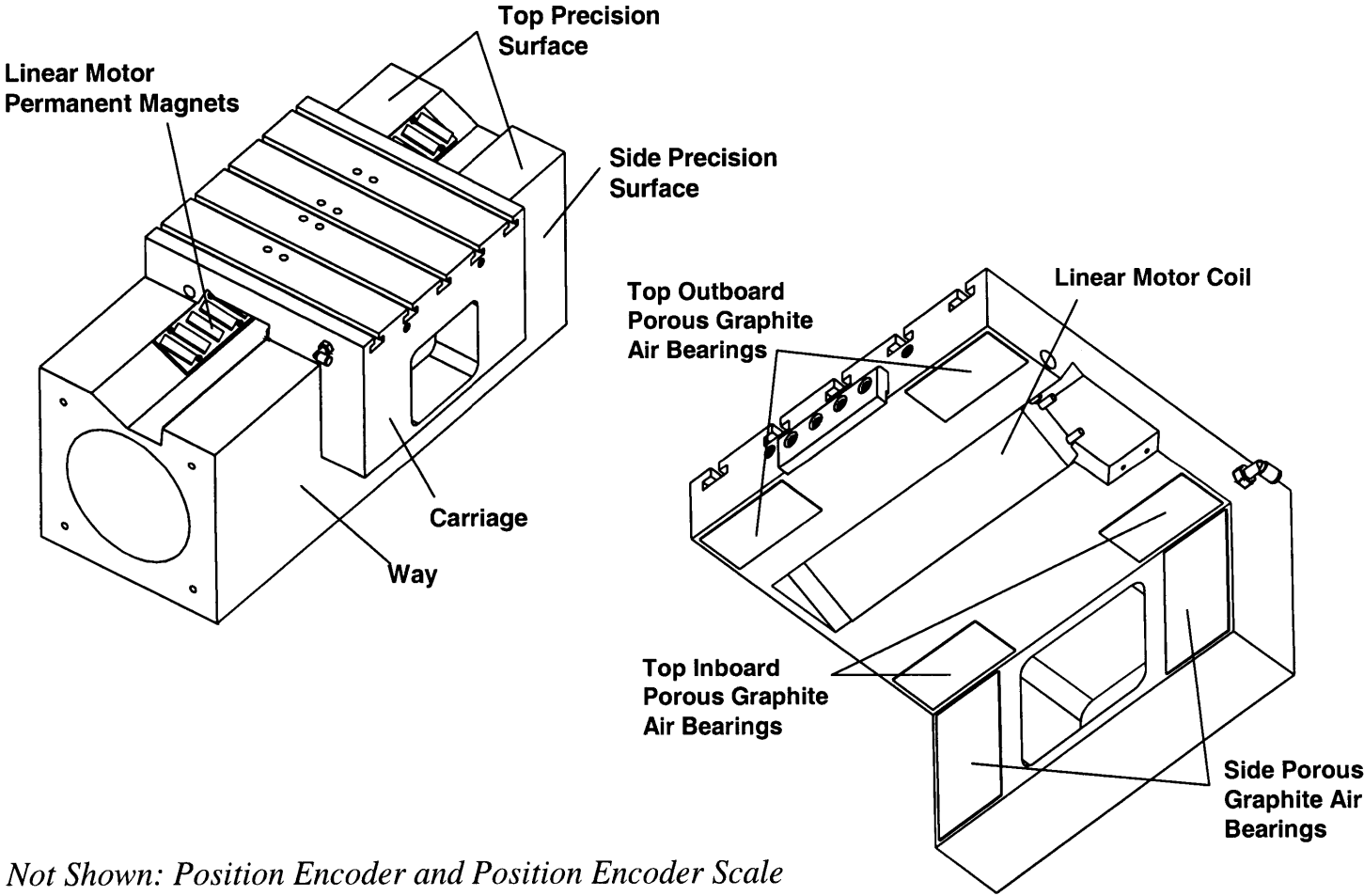
The carriage is made up of a number of smaller components.

1. **The Carriage Base:** This is the structure to which the other carriage components are attached.
2. **Porous Graphite Air Bearings:** These six (6) bearings allow the carriage to slide with no friction over the way surfaces. They also determine the maximum load capacity of the carriage.
3. **The Linear Motor Coil:** Since this component is essentially a large block of iron with coils of

wire inside, it is very strongly attracted to the magnet track on the way. This attractive force preloads the air bearings. When the coils are energized by the controller, the motor coil provides the motive force to move the carriage.

4. **Position Encoder Read Head:** This is what senses the position of the carriage and transmits it to the motor controller.

Axtrusion Components



Not Shown: Position Encoder and Position Encoder Scale

1.2 How the Axtrusion Works

The attractive force between the motor coil and the magnet track preloads the bearings, which support the vertical and horizontal loads. By choosing the groove angle (θ) and motor location (y_m, z_m) the designer can specify the amount of preload on each bearing pair. The pairs are the top outboard pair, the top inboard pair and the side pair.

Summing the forces in the horizontal direction yields,

$$F_{side} = \frac{-F_m \sin \theta}{2}, \quad (1.1)$$

where F_{side} is the preload forces on each of the side bearings, F_m is the motor attractive force, and θ is the motor angle. Summing the forces in the vertical direction yields,

$$F_{top1} + F_{top2} = \frac{-F_m \cos \theta}{2}, \quad (1.2)$$

where F_{top1} and F_{top2} are the forces on each of the inboard and outboard pairs of top bearings. Summing the moments yields,

$$F_{side}z - F_{top1}y_1 - F_{top2}y_2 = \frac{F_m}{2}(\cos(\theta)y_m - \sin(\theta)z_m), \quad (1.3)$$

where y_m and z_m are the motor location in the horizontal and vertical directions. In the prototype configuration the vertical motor location is determined by

$$z_m = w_m \sin \theta, \quad (1.4)$$

where w_m is the width of the motor track.

Equations 1.1 through 1.3 have not taken into account the 20 kg (44 lbs) mass of the carriage. It is not significant compared to the magnetic preload force. If the mass of the carriage is significant with respect to the linear motor attractive force, then it must be included in the calculations.

Equations 1.1 through 1.3 can be solved as a linear system for $F_{side}, F_{top1}, F_{top2}$, yielding

$$\begin{bmatrix} -2 & 0 & 0 \\ 0 & -2 & -2 \\ 2y & -2x_1 & -2x_2 \end{bmatrix}^{-1} \begin{bmatrix} F_m \sin \theta \\ F_m \cos \theta \\ F_m(\cos(\theta)y_m + \sin(\theta)z_m) \end{bmatrix} = \begin{bmatrix} F_{side} \\ F_{top1} \\ F_{top2} \end{bmatrix}. \quad (1.5)$$

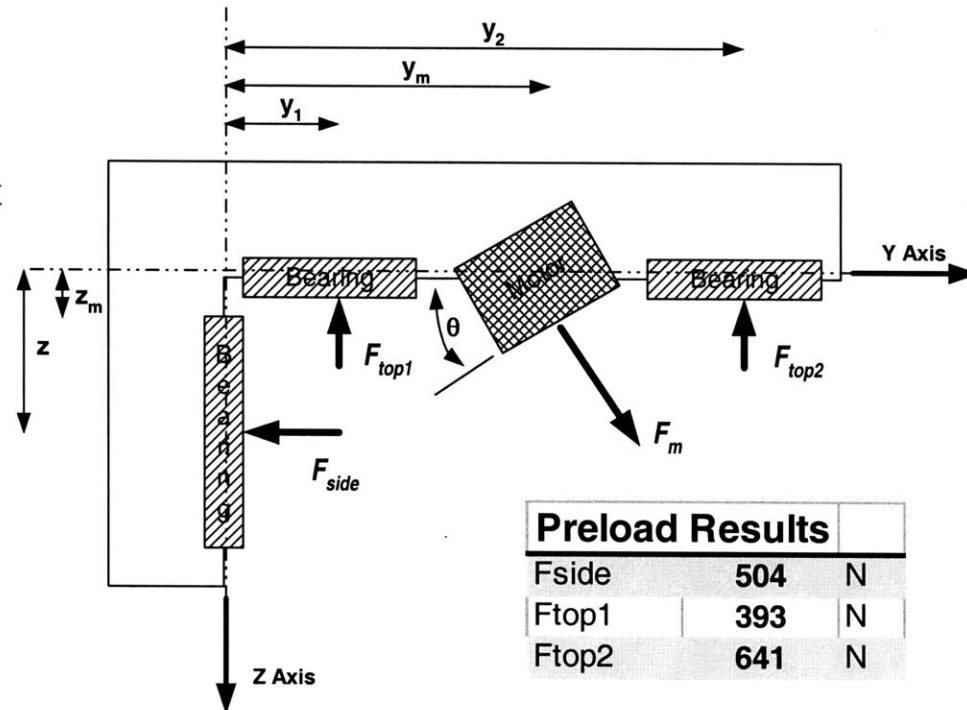
The values for $F_{side}, F_{top1}, F_{top2}$ will determine the preload, and hence air gap and stiffness, of the three pairs of bearings.

How the Axtrusion™ Works

The attractive force between the motor coil and magnets preload the air bearings.

Changing the values of θ , y_m , and z_m the values for F_{side} , F_{top1} , and F_{top2} can all be set independently

Prototype Parameters		
Theta	26	degrees
Fm	2300	N
Y1	30	mm
Y2	260	mm
Ym	145	mm
Z	81	mm
Zm	25	mm



Preload Results		
Fside	504	N
Ftop1	393	N
Ftop2	641	N

1.3 The Bench Level Prototype

The bench level prototype (BLP) of the Axtrusion uses five cam rollers as the bearings: three (3) on the top surface and two (2) on the side surface.

The gap between the magnet and the way can be adjusted using the magnet adjustment screw. This adjusts the amount of attractive force preloading the bearings.

This BLP demonstrates the viability of the Axtrusion concept, and justifies further development.

The five (5) rolling element bearings are a good setup to demonstrate the Axtrusion concept. However, they leave a lot to be desired for precision applications, including:

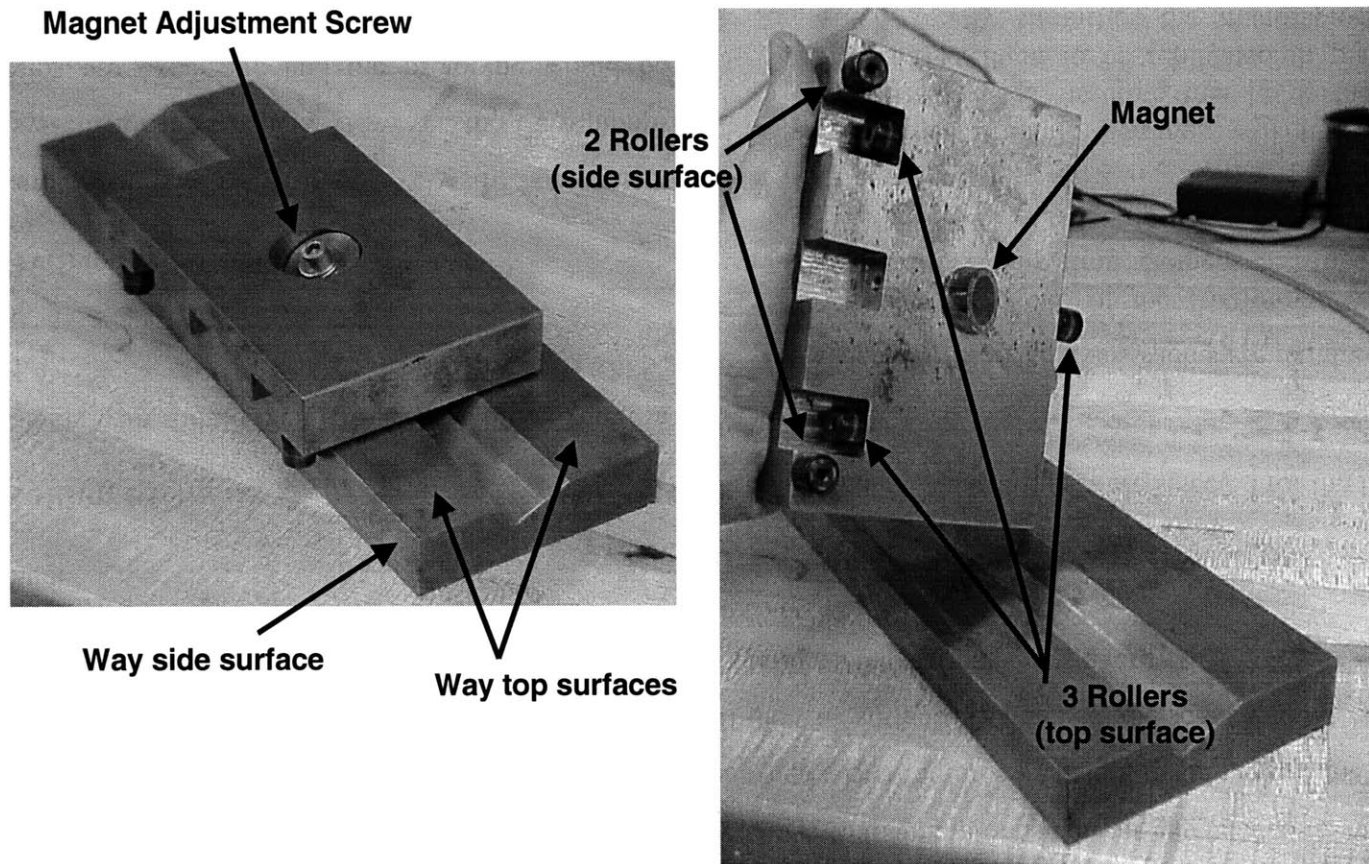
1. The five point contacts will make the carriage extremely sensitive to surface roughness and way straightness. Any dirt on the way will affect the motion of the carriage as the rollers roll over it.
2. The load capacity is limited by the hertz contact stress between the roller and the way. If the stress is too high, the way will be damaged, especially under impact loads.

3. The roundness of each roller directly affects the motion of the way.

These problems can be reduced by using more rollers, but this increases the complexity of the system and its sensitivity to dirt remains.

Other bearings considered for use in the Axtrusion are discussed in Section 1.4.

The Bench Level Prototype



The first Axtrusion ever built! It uses 5 CAM rollers as bearings

1.4 Bearing Selection

The functional requirements for the bearing system are:

- Easy to mount in the carriage assembly
- Robust with respect to dirt and surface scratches
- Robust when the carriage is “unpowered”
- Independent from extensive support equipment

1.4.1 Rolling Elements

The problems with rolling element bearings are covered in Section 1.3.

1.4.2 Hydrostatic Bearings

Hydrostatic bearings would provide a very stiff non-contact bearing system for the carriage. However, the fluid pumping systems are expensive and the prototype would be messy. Hydrostatic bearings would be worth considering if the application was submerged in a fluid environment.

1.4.3 Orifice Air Bearings

Orifice Air Bearings require a very smooth underside of the carriage to maintain the small air gap needed to support the carriage. This requires precision machining of the carriage. If the way surface is scratched, the scratch could “short” the bearing as the orifice passes over it.

1.4.4 Porous Graphite Air Bearings

Porous graphite air bearings were selected for the following reasons:

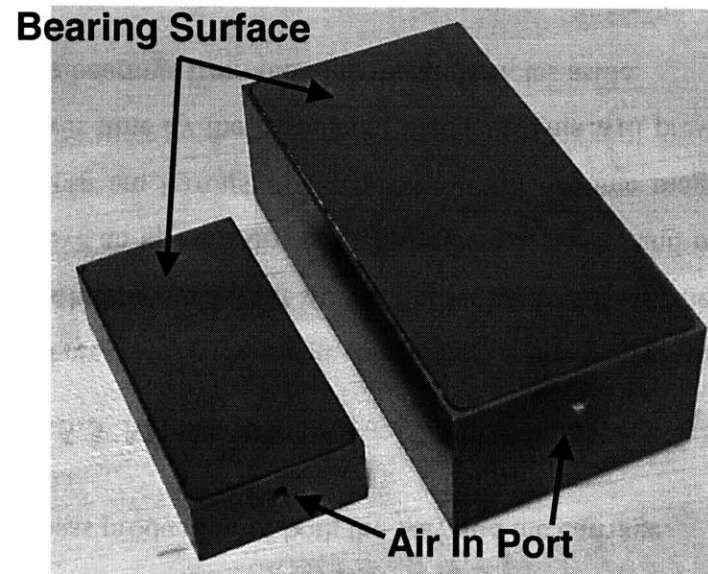
1. Clean: No fluid captive systems are required.
2. Non-Contact: None of the friction or wear associated with rolling element bearings is experienced.
3. Self-contained: Unlike the orifice bearings, the porous graphite bearings will function regardless of the structure that holds them. This allows them to be replicated in place, which greatly simplifies the manufacturing process.
4. Large Discharge Area: This allows bearings to travel over scratches and craters without shorting.

Bearing Selection

Bearing Types	Design Considerations			Additional Equipment	Mess
	Non-Contact	Stiffness	Sensitivity to way surface		
Porous Graphite Air	no contact	ok	ok	some	none
Orifice Air	no contact	ok	poor	some	none
Rolling Element	contact	good	good	none to minimal	none
Hydrostatic	no contact	excellent	poor	a lot	a lot

Modular Air Bearings (**porous graphite bearings**) help make the Axtrusion a cost effective **high performance** linear motion system.

*Left: Newway™ Porous graphite air bearings in the two sizes used in the Axtrusion Prototype.
[Http://www.newwaybearings.com/](http://www.newwaybearings.com/)*



1.5 Way Surface Selection

The functional requirements for the way material are:

- No upward divots when the way is cratered
- Nonferrous
- Easy to finish to the needed tolerances

1.5.1 Granite

Granite has some of the best divot properties. If cracked, the granite will fracture completely downward. This allows the air bearings to continue to slide over the fracture unimpeded. In single piece quantities, the granite base for the prototype cost \$2800.

1.5.2 Polymer Concrete

Polymer Concrete cratering resistance is inferior to granite's, but it is better than metal's. A wood prototype mold for the base costs about \$3800, and makes 3 to 4 parts. A steel production mold costs about \$12,500, and makes 600 to 800 parts. It might be possible to cast the parts to the required surface finish, thereby eliminating the need for additional grinding. The price per casting is \$1000. Polymer

concrete is an area that should be researched further for mass production of both the way and the carriage.

1.5.3 Metal

There is a wide range of metals available for the way, including steel, cast iron, and aluminum. All of these will have an upward divot when they are cratered, and many of these are ferrous. A ferrous way will become magnetized over time by the permanent magnets. This will prevent the air bearings from blowing metal particles aside.

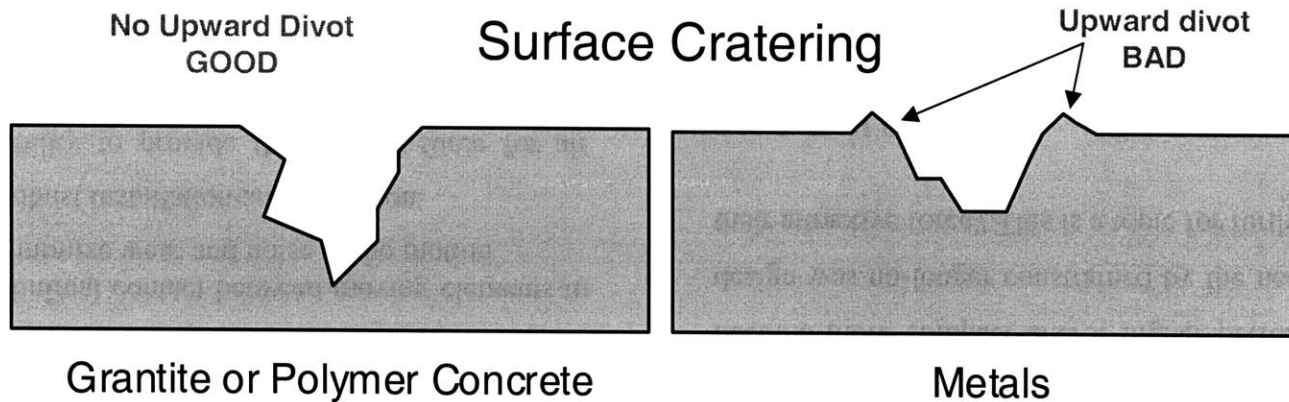
One of the most promising ways to get a light weight low cost way is to extrude the Axtrusion profile from aluminum, grid the top and side precision surfaces to the correct shape, and finally hard anodize them.

1.5.4 Aluminum Oxide

Because the geometry of the way is very simple, it could be cold pressed in aluminum oxide. This would provide a way that is 4 times stiffer than aluminum, and whose surface is virtually indestructible.

Way Surface Selection

Material	Design Considerations			
	Divot Properties	Mass Producible	Stiffness	Process
Granite	Excellent	Medium	OK	Cutting/Grinding
Polymer Concrete	Good	Excellent	Poor	Casting/Grinding
Aluminum	Poor	Excellent	OK	Extrusion/Grinding
Aluminum Oxide	Are there any?	Medium	Excellent	Cold Pressing



1.6 Motive Power Selection

The motive power functional requirements are:

- Minimal contact between moving elements to minimize wear and noise in the motion.
- Robust installation and operation
- Ability to provide the preload force for air bearings.

1.6.1 Linear Motors

Open face permanent magnet linear motors meet all the motive power functional requirements. There is no contact between the motor coil and magnet tracks so there is no wear. The strong attractive force between the coil and magnet track provides the force to preload the bearings. The tolerances for the alignment of the motor coil and magnet track are much looser than that of a gear drive or ballscrew system.

Currently linear motors are designed to minimize the attractive force between the coil and the magnets. In conventional rolling element linear bearing systems, this high attractive force causes increased wear. In the Axtrusion, the higher

attractive force is a benefit, because the higher preload force improves air bearing stiffness. Whether linear motors would become more compact and/or higher performance if their design was no-longer constrained by the need to minimize their attractive force? This is a topic for further study.

1.6.2 Ball Screw

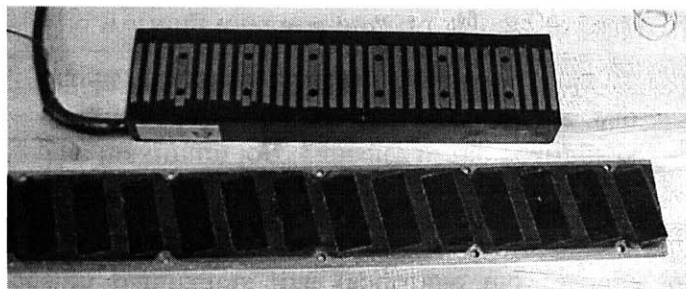
It is possible to design an Axtrusion that uses a ball screw for motive power. This would increase the number of moving parts. A magnet track would still be required to preload the air bearings. And mounting the ballscrew in the vicinity of the magnets and motors presents some tricky design issues. This choice of motive power increases the error and repeatability of the carriage motion.

1.6.3 Belt Drive

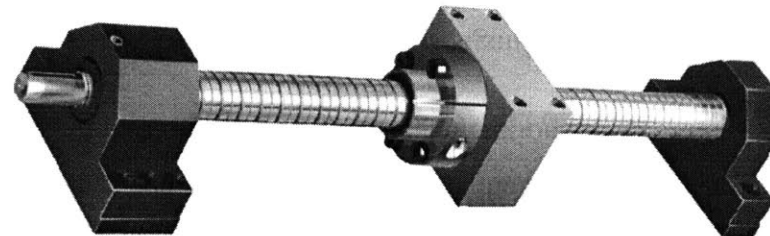
If stiffness in the direction of motion is not a major concern, a belt drive can be used to move the Axtrusion. This is considerably easier to mount than the ball screw option, and is the least expensive per unit length of the three options. However, it is also the least precise of the three.

Motive Power Selection

Motors	Design Considerations			
	Contact	Scalable	Stiffness	Wear
Linear Motor	None	Few Discrete Sizes	Excellent	None
Ball Screw	Many	Excellent	Excellent	Most
Belt Drive	Some	Excellent	poor	Yes
Rocket Motor	None	Poor	N/A	Yes



An open face linear motor



Typical ballscrew assembly

1.7 Sizing the Carriage (Load Capacity)

The design parameters that determine the carriage load capacity are:

- The maximum load capacity of the bearings is determined by the minimum allowable gap height between the bearings and way.
- The working load and preload applied to each bearing must not exceed its maximum load.

The maximum load capacity of the air bearings is determined by their surface area and their air pressure. The bearings reach their maximum capacity when the gaps decrease to about 3-4 microns.

The carriage working load capacity in the horizontal direction is determined by

$$2L_{bmaxside} - F_m \sin \theta = L_{cmah}, \quad (1.6)$$

where $L_{bmaxside}$ is the maximum load each of the side bearings can support, $F_m \sin \theta$ is the preload component in the direction in question, and L_{cmah} is the maximum load capacity of the carriage in the horizontal direction. The carriage load capacity in the vertical direction is estimated by

$$4L_{bmaxtop} - F_m \cos \theta = L_{cmav}, \quad (1.7)$$

where $L_{bmaxtop}$ is the maximum load each of the top bearings can support, and L_{cmav} is the maximum load capacity of the carriage in the vertical direction.

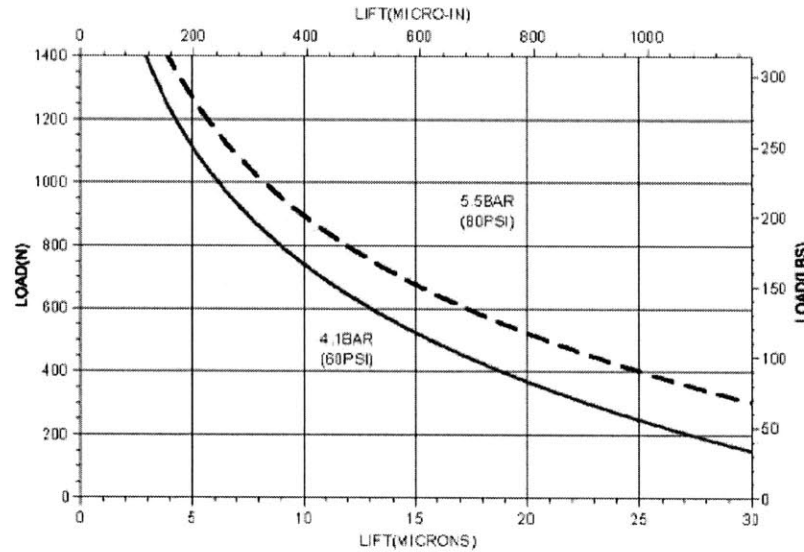
If the mass of the carriage is significant with respect to the preloading or anticipated forces then it should be included in equation 1.6 or 1.7.

NOTE: The values used for $L_{bmaxside}$ and $L_{bmaxtop}$ are determined by the minimum allowed gap between the air bearing and the way. The estimates in the prototype assume that the minimum gap is 3-4 microns. If this gap is too small then one should use the load vs. gap charts supplied by the bearing vendor to calculate the correct values for $L_{bmaxside}$ and $L_{bmaxtop}$.

Carriage Load Capacity

Carriage Load Capacity is determined by:

- Air Pressure
- Bearing Surface Area
- Minimum Tolerated Gap
- The Amount of Preload



This plot shows the load vs. gap for a single 50x100 mm Air Bearing

Prototype Extrusion Carriage Load Capacity							
	n	Max Bearing Load (N)	Total (N)	Preload (N)	Angle	Preload Component (N)	Carriage Capacity (N)
Vertical	4	1400	5600	2300	26	2067	3533
Horizontal	2	3000	6000	2300	26	1008	4992

These values assume that the carriage can run with an air gap of 3 to 4 microns

1.8 Sizing the Carriage (Roll and Normal Stiffness)

The design parameters that determine the rotational and the normal stiffness of the carriage are:

- The stiffness of the individual air bearings
- The number of air bearings
- The bearing's distance from the center of stiffness of the carriage.

Carriage stiffness is a function of the stiffness of each individual air bearings and the distance between them. We are interested in stiffness in two directions normal to the direction of travel (horizontal and vertical), and the roll, yaw, and pitch stiffness.

1.8.1 Stiffness of the Individual Bearing Pads

The stiffness of an individual bearing pad is the derivative of the load capacity vs. the gap thickness function for each bearings. The stiffness of the bearings is approximately

$$K_{50 \times 100} = -0.0258h^3 + 1.489h^2 - 29.196h + 223.35 \quad (1.8)$$

or

$$K_{75 \times 150} = -0.158h^3 + 7.543h^2 - 122.644h + 786.51, \quad (1.9)$$

where h is the gap height [microns] and K is the stiffness [Newtons per micron]. Section A.1 gives the full derivation.

1.8.2 Stiffness Normal to the Direction of Travel

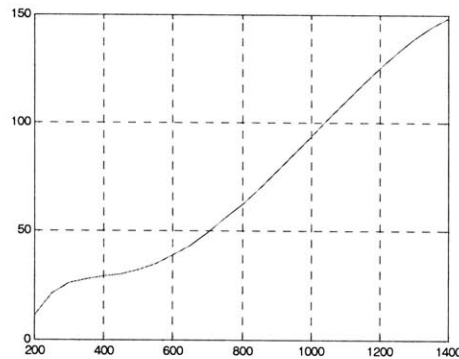
The stiffness normal to the direction of travel is simply the sum of the individual stiffnesses of each bearing in the direction in question. Given a load in a particular direction. Equations 1.8 and 1.9 can be used to calculate the stiffness of the individual bearings.

1.8.3 Rotational Stiffness

There are three axes of rotation that the stiffness needs to be computed about. The rotational stiffness of the carriage is proportional to the distance between the bearings squared. Therefore increasing the distance between the bearings pads can increase the roll stiffness dramatically. See Section A.1 on page 113 for more detailed information on the theoretical stiffness of the carriage. See Section 1.22 on page 57 for the measured stiffness data and its implications.

Carriage Stiffness

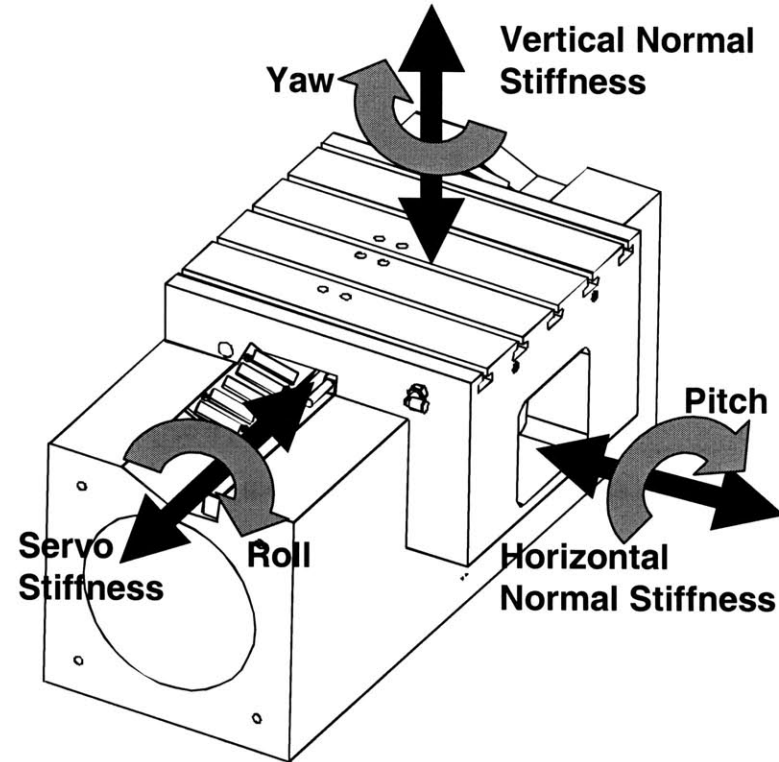
Calculate the bearing load vs. stiffness curves for the individual bearings



From the preload values calculate the stiffness of each bearing pair.

Enter the individual stiffnesses in the carriage compliance model (see appendix)

Calculate the displacement at other points



1.9 Casting the Carriage Base

The functional requirements of the carriage base are:

- To provide a ridged mount for the linear motor and air bearings.
- Light weight to allow rapid accelerations.
- Nonferrous, so the carriage does not become magnetized by the magnet track over time.

The rough shape of the carriage for the prototype was cast in Magnesium AZ91-T6 alloy. Magnesium's density is 60% of Aluminum's and is about half the Young's Modulus. The drawings for the prototype casing are in Chapter 3. The pattern for the casting costs \$2300 and each casting costs \$600.

The cross section of the carriage had to be large enough to provide plenty of stiffness despite the low Young's Modulus of the Magnesium.

The carriage casting was then cleaned up and detailed features were added on a milling machine. The drawings for the carriage machining are in Chapter 3.

Other options for manufacturing the casting base considered include:

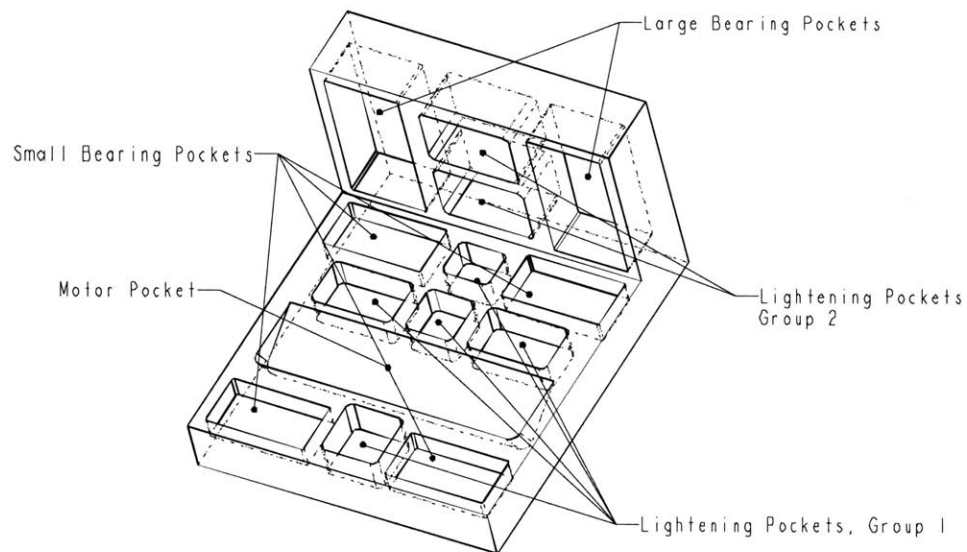
1. Hogging the base out of a solid metal block. This method was discarded because it offers no time saving when making multiple copies of the carriage.
2. Machining the top and side pieces out of separate pieces of metal and then welding or bolting them together. Again this method offered no time savings when making multiple copies.

It is important for the carriage to be made of a nonferrous material. A ferrous carriage is more difficult to assemble. Additionally, the strong permanent magnets on the way will magnetize a ferrous carriage over time.

Manufacturing the Carriage Base

(the casting)

It is important that the carriage base be made of a stiff **nonferrous** material



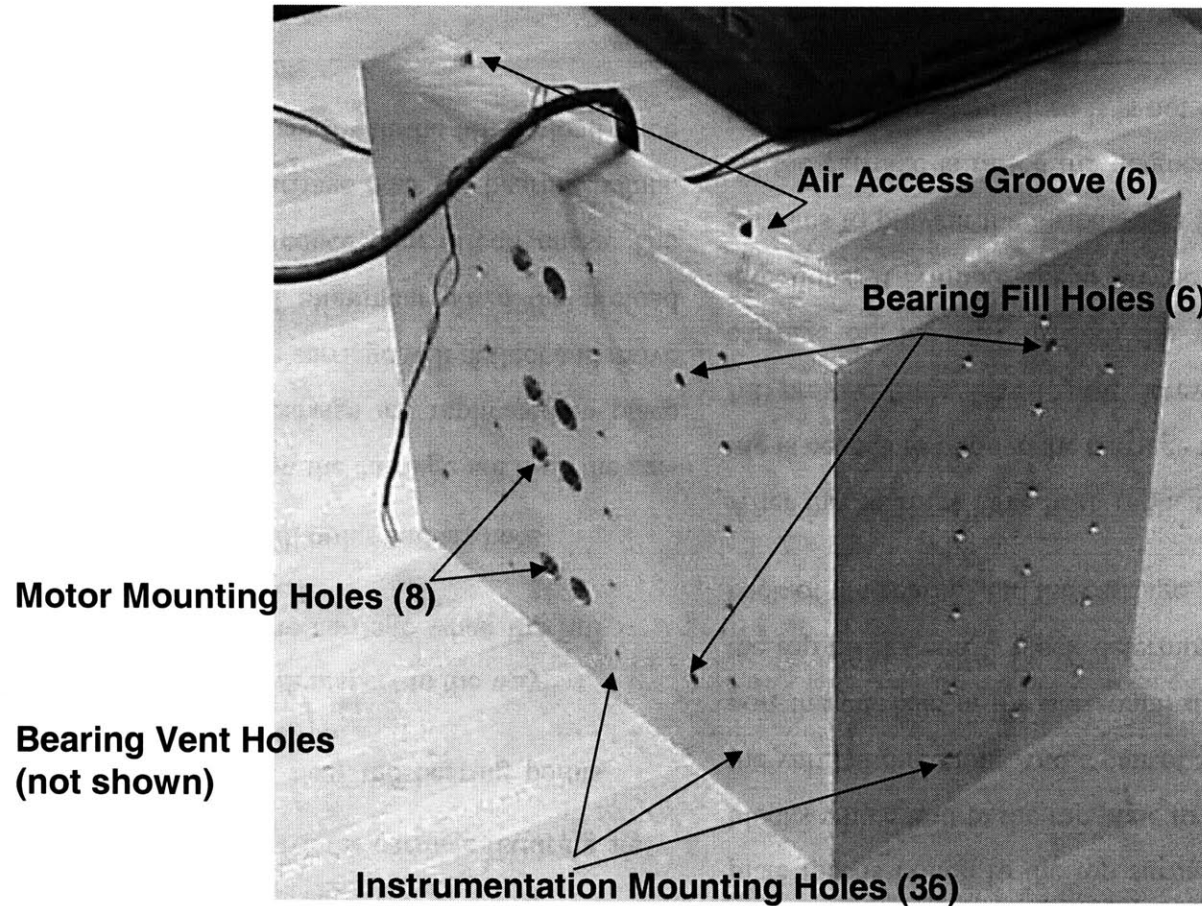
1.10 Machining the Carriage Base

The carriage base casting had more features machined into it. These features include:

1. Mounting holes on the linear motor.
2. Access grooves for the air fittings for each of the air bearings.
3. Fill and Vent holes for replicating the air bearings in place.
4. Threaded holes on the two outside faces for mounting test instrumentation.

Manufacturing the Carriage Base

(the machining)



1.11 The Carriage Fixturing

The functional requirements for the carriage fixturing are

- Support the carriage near the bearing points during bearing replication.
- Align the carriage with respect to the way
- Be able to remove the carriage when the full preload force is applied.
- Allow access to the fill holes and air lines

Because the preload forces on the carriage are high the carriage will deflect. If the bearings are replicated in place without the preload force, the carriage will deflect and move the bearings slightly out of alignment when the preload force is applied. This will reduce their effectiveness. The solution is to support the carriage near the bearing points, while the bearings are replicated with the full preload force in place.

The fixturing will also determine how parallel the carriage top and sides are with respect to the way. This parallelism was not a major concern in the prototype Axtrusion, so the prototype fixturing was not very precise.

The prototype fixturing consists of the following: A top plate that is bolted to the top surface of the carriage; Top blocks which bolt to the top plate to support the carriage in the vertical direction; And a pair of side “L” blocks to support the carriage in the horizontal direction. The height of the top blocks and L block determine the gap between the back of the bearing and the carriage.

After the bearings have been replicated in place the fixturing is needed to remove the carriage from the way under the full preload force. Five (5) M6 screws are used to raise the carriage off the way in both the vertical and horizontal directions. It is important to lift the carriage off both way surfaces to prevent the air bearings from getting scratched. As the carriage is raised the magnetic preload force drops by the distance squared, so it is not difficult to get the preload to a manageable level.

The next generation carriage should be designed to take advantage of standard fixturing (i.e. a 1-2-3 block or parallels) during replication. This would allow the carriage to be aligned with greater accuracy in less time.

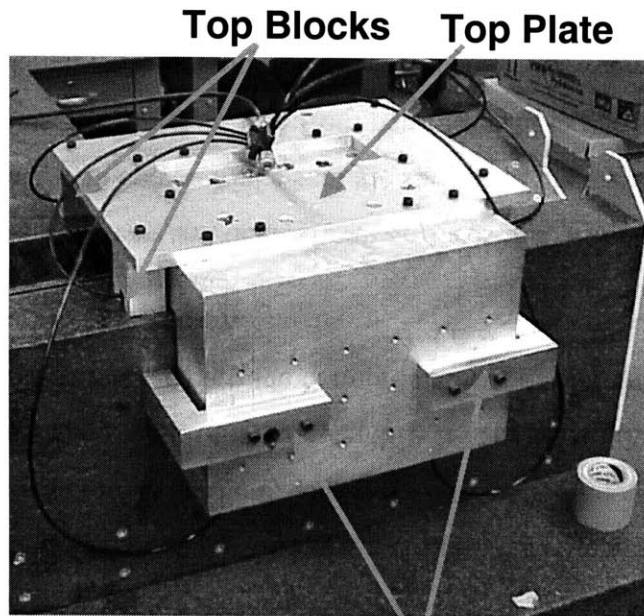
Carriage Fixturing

Replicating Fixturing Features:

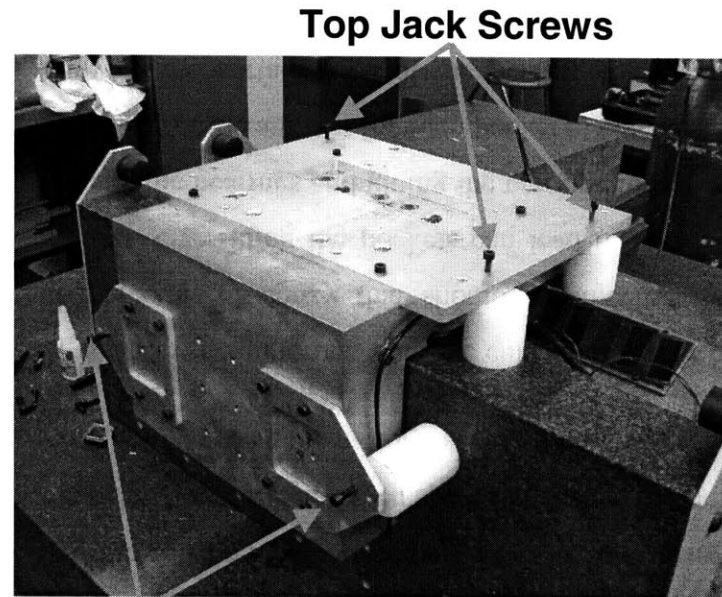
- “Correct” Stress Distribution
- Square’s Carriage with respect to the Way

Removal Fixturing Features:

- Removes Carriage vertically and horizontally to prevent scratch of the bearings



Top Blocks **Top Plate**
Side "L" Blocks
Replicating Fixturing



Top Jack Screws
Side Jack Screws
Removal Fixturing

1.12 Replicating the Bearing Pads to the Carriage Base

Appendix Section A.2 contains all the details available on replicating the bearings into the carriage. The important points are summarized here. This procedure took 2 hours 15 minutes during the prototype assembly. It is expected that it will get faster as the carriage is improved. An outline of the procedure is listed below.

Thoroughly clean and degrease all surfaces that will come in contact with epoxy. Make sure the surface of the way and bearings are completely free from particles. These particles could damage the bearings if they are caught between the bearings and way.

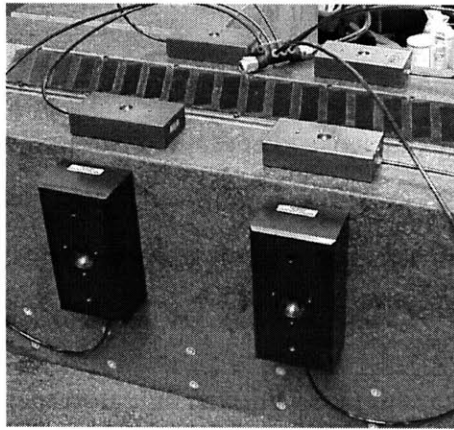
Draw a vacuum through the bearings when they are positioned correctly on the way to ensure that they remain in contact and aligned with the way as the epoxy cures.

A means of lowering the motor coil to the correct air gap must be provided. At full preload force (500+ lbs) the carriage assembly will be difficult to handle by hand. In the prototype this is accomplished by drawing the motor coil

completely up into its pocket. Once the carriage is in place and aligned, the coil is lowered to the correct air gap (measured using a piece of non-ferrous shim stock), thus applying the full preload to the carriage. Then the bearings are replicated in place, and then space behind the motor is filled with epoxy giving the motor a secure mounting face.

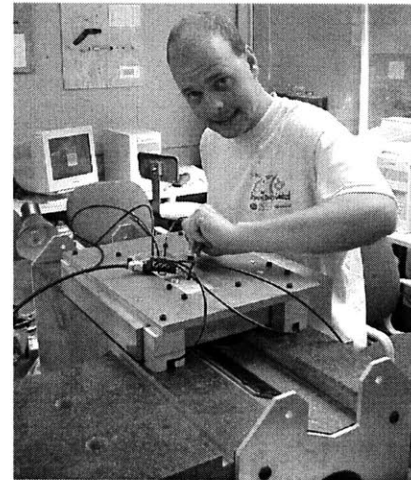
It is also very important that one calculates an estimate for the amount of epoxy that should be injected into each pocket. Overfilling the pockets can lead to epoxy leaking around the bearings and gluing the carriage to the way. The estimate for the amount for each pocket is obtained by multiplying the surface area of the bearing face by the gap between the pocket and back of the bearing. It highly suggested the hat distance between the bearing and the pocket be measured as a double check to any estimate from CAD models.

Replicating the Bearing Pads into the Carriage



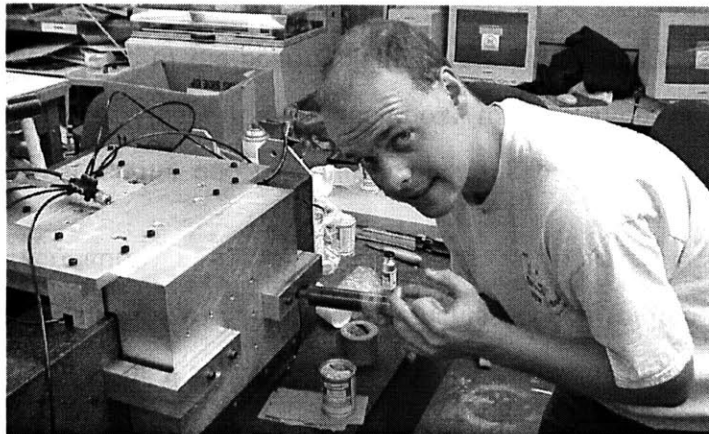
1

Place Bearings on the way. Draw a vacuum through them to temporarily secure them in place.



2

Lower motor coil to the correct air gap. This applies the full preload force to the carriage.



3

Inject epoxy into bearing and motor pockets. Calculate the amount of epoxy needed before injection to prevent gluing the carriage to the way!!

Please see the text for a more detailed description of the bearing replication process.

1.13 Assembly Lessons Learned

The assembly of the prototype carriage went well. However, there are quite a few improvements needed for the next generation.

Rather than having one fill hole per bearing pocket there should be two. This will allow the epoxy to cover more of the back surface of the bearing. The hemispherical feature on the back of the bearing would not need to be covered because they will no longer be under the injection holes. Furthermore, the bearing vent holes can be eliminated.

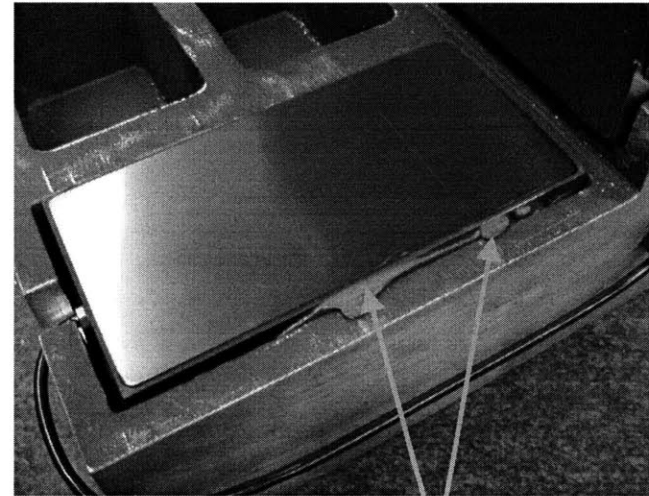
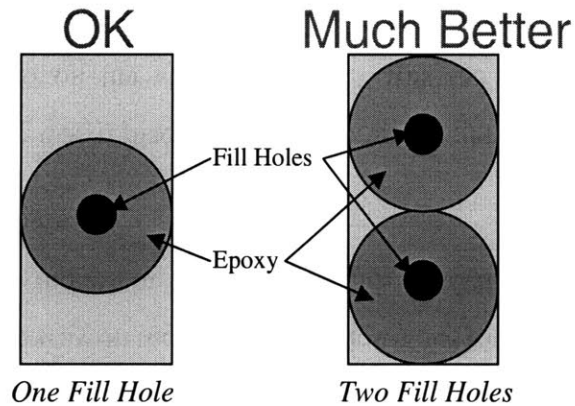
The distance from top and side faces of the carriage from the way surface in its final position should be the height of some standard form of fixturing (1-2-3 block for example). This will make it less expensive and easier to square the carriage with respect to the way without custom made fixturing.

Once the motor and bearings have been replicated into the carriage, removing carriage without mechanical assistance is impossible. In the prototype the alignment fixturing was modified to allow the carriage to be removed. It may be

desirable to have the removal features built into the carriage in the future.

DO NOT overfill one of the bearing pockets and glue the carriage to the way. However, should this occur it can be corrected by removing the carriage and filing down the place where the epoxy made contact with way.

Assembly Lessons Learned



DON'T GLUE THE CARRIAGE TO THE WAY! It had to be filed down to allow the carriage to slide.

- Center Fixturing Holes on Bearings
- Two Fill Holes Per Bearing
- No Vent Holes Needed
- Design Carriage to use 1-2-3 Blocks for Fixturing
- Build removal features into carriage base
- DO NOT overfill the one of the bearing pockets and glue the carriage to the way.

1.14 Modal Analysis Setup

The first performance analysis of the prototype was a modal analysis. The data was collected using a three axis accelerometer and a Hewlett Packard 35670 Dynamic Signal Analyzer. The data was analyzed in the Star Modal software package. The impact hammer was a PCB model 086C03, and the accelerometer was a PCB model 356A08 three axis accelerometer.

First the carriage was removed from the base and the accelerometer was glued to the way. The vibration modes were found for the way on the table. This allows one to differentiate between modes in the carriage and those in the way/table combination.

The carriage was replaced on the way, and eight (8) points were marked on the surface. Point 1 was the excitation point. This is where the carriage was struck with a hammer for all tests. Points 2 through 8 were measurement points. The accelerometer was glued to each point in turn while the carriage was excited.

Measurements were made when the carriage was both floating and not floating.

The data was then imported into the Star Modal software. A stick figure model of the carriage was made where each vertex is one of the measurement points.

The data was analyzed by finding the frequency, damping percent, magnitude, and the dynamic compliance of prominent vibration modes. The stick figure carriage model was animated to show the vibration modes.

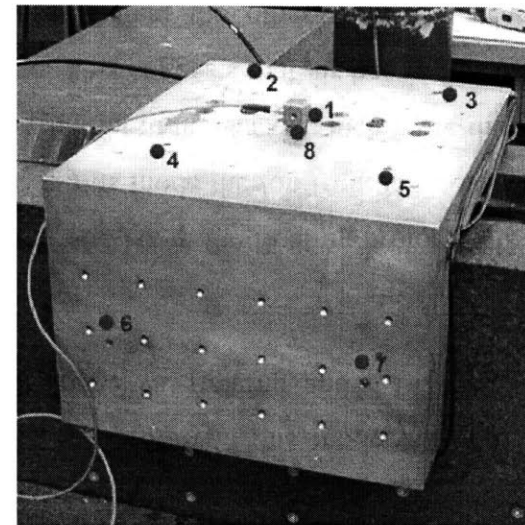
The Modal Analysis Setup

Measurements were taken for:

- Way Only
- Carriage Floating
- Carriage Not Floating

Point 1: Impact point
Points 2-8: Measurement Points

Data Measured with 3
Axis Accelerometer



1.15 Modal Analysis Results

Several interesting modes were found in the Axtrusion. These are summarized in the tables below.

TABLE 1.1 Carriage Floating Modes

Frequency [Hz]	Damping [%]	Magnitude [Output/ Input]	Comments
362	3.8	48	Top left front air bearing oscillates much more than others
608	3.3	33	Carriage deformation is like a “hinge” and top center vibrates a lot
487	1.9	5	Carriage deformation is like a “hinge” and top center vibrates less

TABLE 1.2 Carriage Not Floating Modes

Frequency [Hz]	Damping [%]	Magnitude [Output/ Input]	Comments
1430	0.6	300	Top center of carriage oscillates up and down
501	1.3	2.3	Whole carriage moves up and down

Some important results of the modal analysis are:

In almost all the dominant modes the top center of the carriage vibrates in the Z axis much more than the rest of the carriage. In the prototype this mode occurred at 607 Hz while the carriage was floating, and at 1430 Hz while it was not.

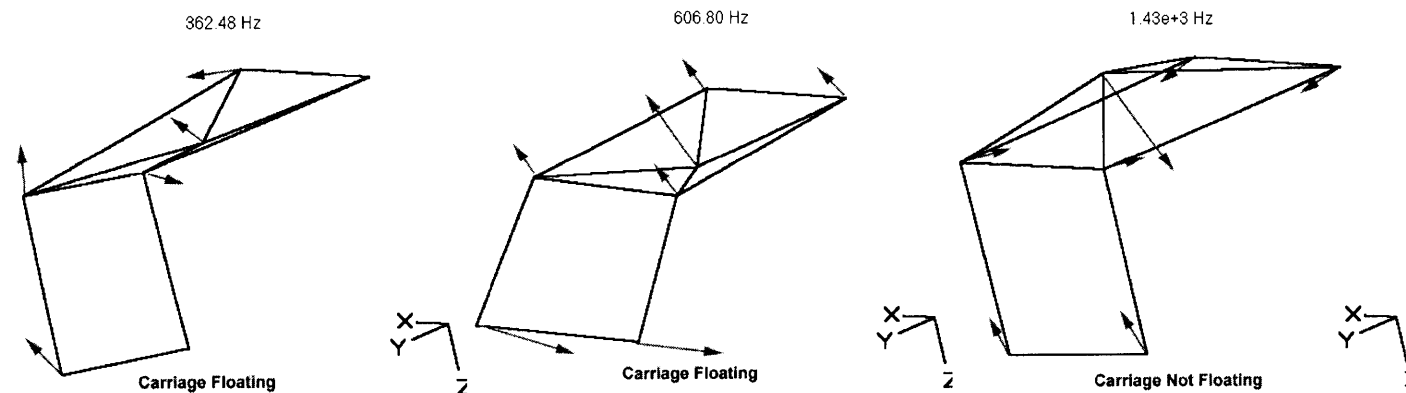
The mode at 362 Hz in the floating prototype is very interesting too. In this mode the top front left corner of the carriage is oscillating in the Z axis much more than the rest of the carriage. This suggests that air bearing in this corner is much less stiff than the other three top bearings. This reduced stiffness could be caused by uneven preloading. It is expected that the inboard top bearings will be preloaded less (therefore less stiff) than the outboard pair. See the Vertical Stiffness Section 1.22 on page 57 for explanation of what might be causing the left or right sides of the carriage to be preloaded unevenly.

The modal analysis also shows the effect on the angled preload by the linear motor. Even though the carriage was excited only in the Z direction, the carriage oscillates normal to the angled motor track.

The Modal Analysis Results

The modal analysis provided the following information:

- Resonant frequencies of the carriage.
- Which bearings are not preloaded equally
- Good and poor locations for mounting sensitive equipment.



See text or web page for table of modes.

Go to the Axtusion web site <http://pergatory.mit.edu/cortesi/index.htm> for the modal animations.

1.16 The Dynamic Stiffness

The modal data was also used to calculate a dynamic stiffness of the carriage in the floating and not floating configurations. The dynamic stiffness was calculated for the top center of the carriage (point #8 when the model data was taken).

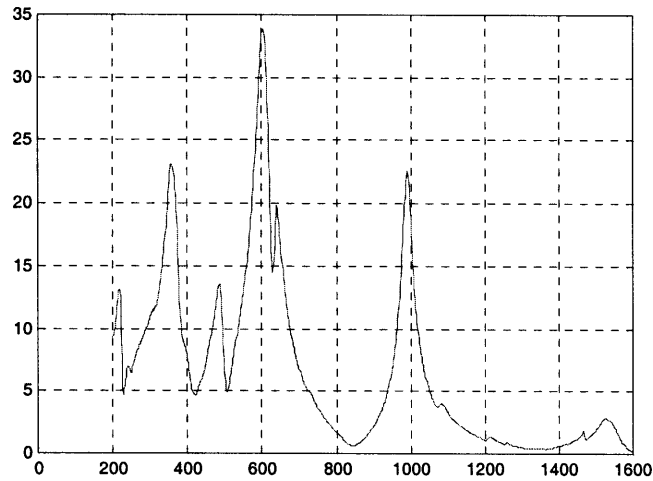
The raw data from the accelerometer is in volts. This must be converted to an acceleration by multiplying it by an appropriate conversion factor for the accelerometer used. Then the data must then be divided by the conversion factor for the impact hammer. Now the data has units of $\frac{Ns^2}{m}$. Dividing the data by the frequency (in Hz) squared yields stiffness as a function of frequency.

TABLE 1.3 Modal Equipment Conversion Factors

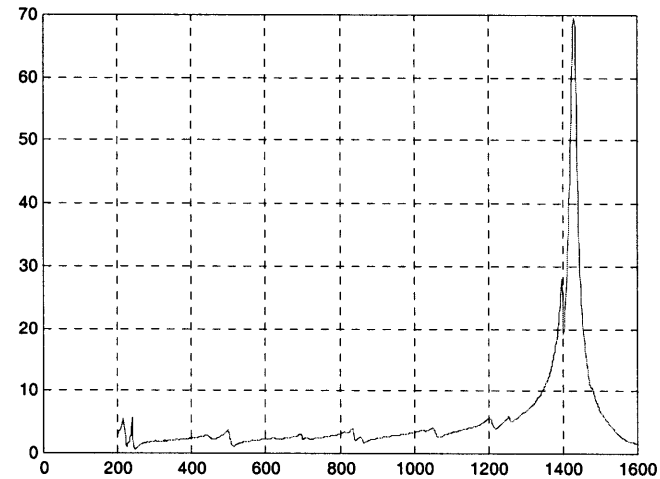
Equipment	Factor
PCB 3 Axis Accelerometer	10 mV/(m/s ²)
PCB model 086C03 Impact Hammer	2.3 mV/N

The Dynamic Stiffness

The modal analysis also revealed the dynamic stiffness of the carriage over a range of frequencies.



Top center of the carriage while floating



Top center of the carriage while not floating

1.17 Measurement Setup

The pitch, yaw, linear accuracy, straightness, and stiffness measurements were done at Dover Instruments in Westboro Massachusetts. All data was taken with the air bearings running at 60 psi (4.14 Bar).

The pitch, yaw, and linear accuracy measurements were made with a Hewlett Packard 5519A Laser System. Four data sets were taken for both pitch and yaw. The first three data sets consisted of six (6) passes, three (3) in each direction, using 320 mm of travel (the carriage has a total travel of 330 mm). The measurements were taken every 10 mm. Two data sets were run with the carriage at continuous speeds of 10 mm/s, 40 mm/s. A third data was run with the carriage stopping every 10 mm to take a measurement at rest. Finally for both pitch and yaw, a fourth pass was made to take measurements every 0.1 seconds, while the carriage traveled at a continuous speed of 10 mm/s. This provided a higher resolution image of what the carriage was doing in pitch and yaw.

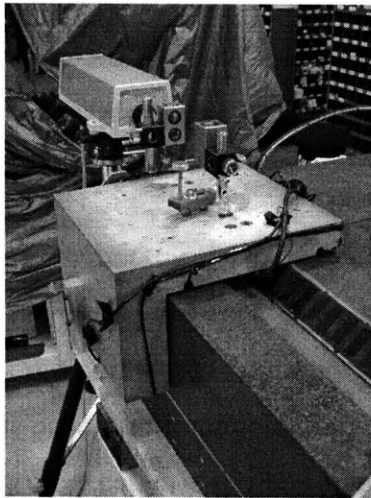
The linear accuracy test was done to determine the difference between where the controller thought the carriage was and its actual position. The same HP laser system was used with slightly different optics. The carriage was moved in 10 mm increments and the difference between the controller position and the actual position was recorded.

The vertical straightness measurements were made by suspending a capacitance probe (ADE-2102 probe with ADE Microsense 3401 Amp) above a plane mirror on the carriage. As the carriage moved back and forth (10 mm/s) the vertical displacement of the carriage was recorded at 0.1 second intervals.

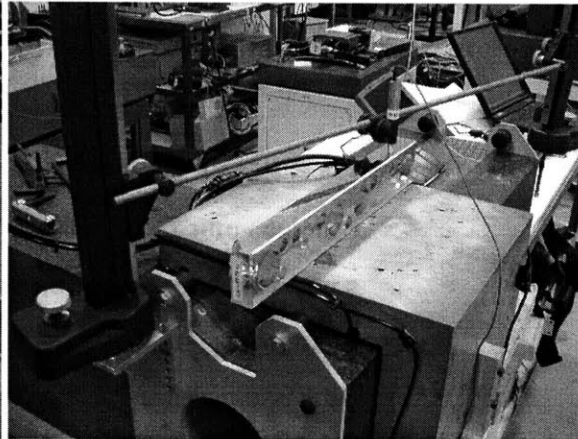
The stiffness measurements were fairly crude. A pair of 25 lb. (111.2 N) weights were placed on the center of the carriage (single and together). The displacement was measured above each of the four (4) top bearings pads by a dial indicator. From the known force and displacement the vertical stiffness of the carriage was estimated.

Due to a lack of fixturing, horizontal straightness and horizontal stiffness were not measured.

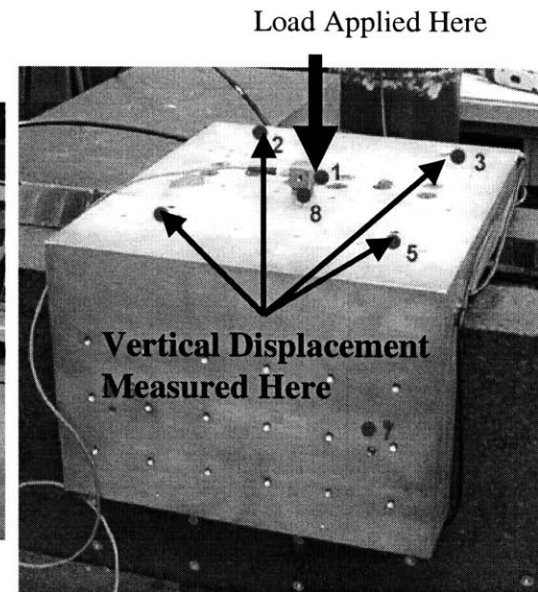
The Pitch, Yaw, Position Accuracy, Vertical Straightness, and Vertical Stiffness Setup.



The basic setup for the pitch, yaw, and accuracy measurements. A laser and a variety of optics was used to make each measurement.



The basic setup for the vertical straightness measurement. The probe is suspended above the straight edge on the carriage.



The basic setup for the vertical stiffness measurements. The load is applied in the center of the carriage and measurements made above each of the top bearing pads.

1.18 The Pitch Data

The pitch of the carriage, as it traveled down the length of the way, varied between 2.38 and 2.44 arc seconds, with a repeatability of between 0.19 and 0.50 arc seconds.

The pitch error has a couple of obvious components. The most noticeable is the periodic oscillations. These oscillations have a period of approximately 29.9 mm and a magnitude of about 1.4 arc seconds. These oscillations are due to the motor coil traveling over the alternating magnetic poles of the magnet track. These poles are spaced 31 mm center to center.

The other significant component of the pitch data is that at the beginning of the carriage (position 0 mm) it starts out with an average pitch of -0.5 arc seconds. Over the length of travel this value changes to +0.5 arc seconds. This indicated that the top surface of the way is slightly concave.

Please see Section A.3.1 on page 123 for the complete plots of all the pitch data taken.

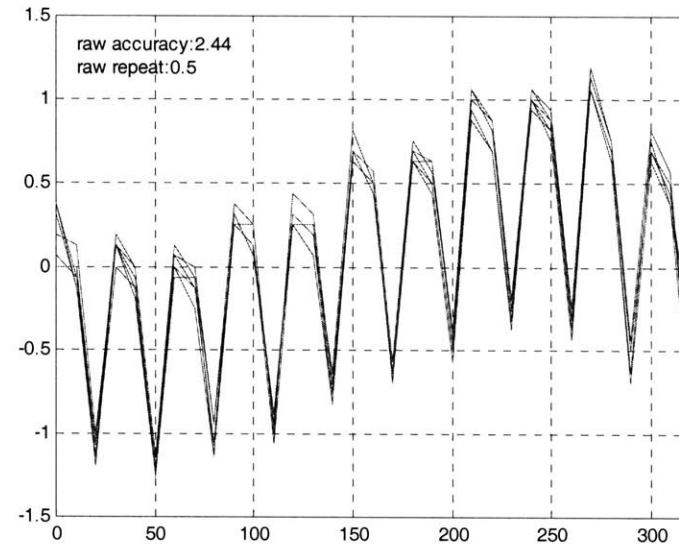
The Pitch Data

Raw Accuracy:	2.44 arc sec
Raw Repeatability:	0.50 arc sec

Period of Variation 29.9 mm

This period is half the pitch of the magnet track!

The way also appears to be slightly curved (from -0.5 arc seconds to $+0.5$ arc seconds).



Measurements every 10 mm
Carriage Speed of 10 mm/sec
6 passes (3 in each direction)

Pitch data was also taken at a carriage speed of 40 mm/s, after incremental movements, and as a function of time. There were no major differences. Please see the appendix for the complete data.

1.19 The Yaw Data

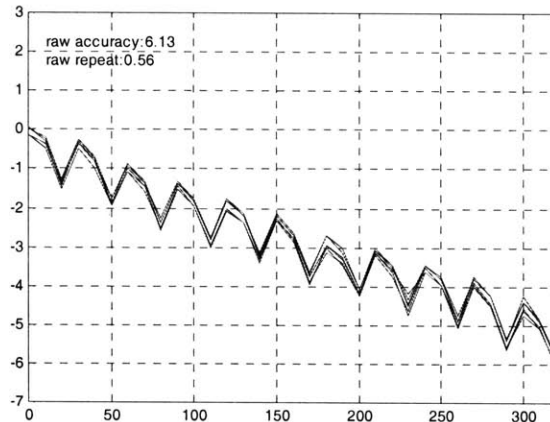
The yaw data was collected in the exact same manner as the pitch data, except the optics of the inferometer were reoriented to measure the angular displacement about the vertical axis of the carriage.

The most striking feature of the raw yaw data is the very linear trend from 0 arc seconds to about 6 arc seconds. If this linear trend is removed the yaw error motion ranges from 1.59 to 1.70 arc seconds, with a repeatability of between 0.26 to 0.56 arc seconds. It is not clear at this time whether this linear change in yaw is due to instrumentation error or an actual change in yaw. Having the controller map out such a linear error and compensate for it is fairly straightforward, but is not even necessary if the trend is an artifact of the instrumentation.

Again the oscillation with a period of about 30 mm due to the magnet poles is visible.

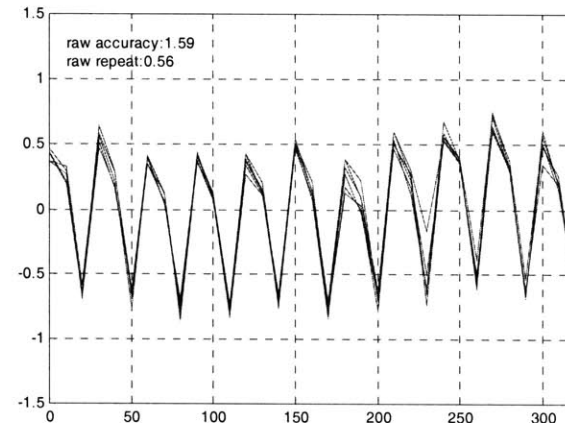
Please see Section A.3.2 on page 127 for the all the yaw data taken.

The Yaw Data



Raw Yaw Data

Measurements every 10 mm
 Carriage Speed of 10 mm/sec
 6 passes (3 in each direction)



Yaw Data with Linear Slope Removed

Raw Accuracy:	1.59 arc sec
Raw Repeatability:	0.56 arc sec

Period of Variation 30.1 mm

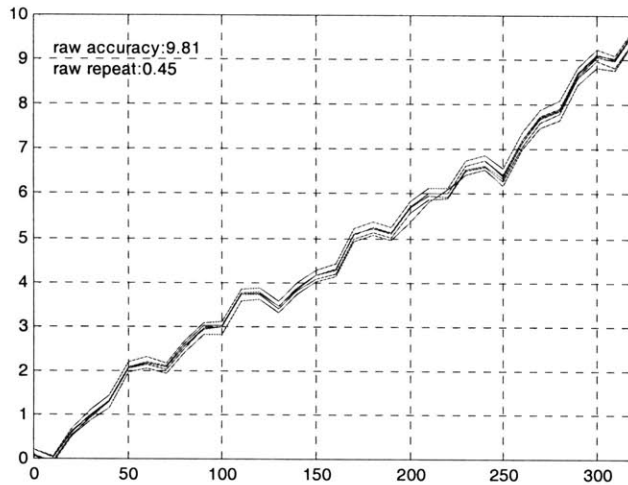
Pitch data was also taken at a carriage speed of 40 mm/s, after incremental movements, and as a function of time. There were no major differences. Please see the appendix for the complete data.

1.20 The Linear Position Accuracy Data

The linear position accuracy measures how accurately the controller can position the carriage. This data had a strong linear trend. Since this linear trend is very easy to correct within the controller, the real significance is in the position errors that are left once this trend is removed.

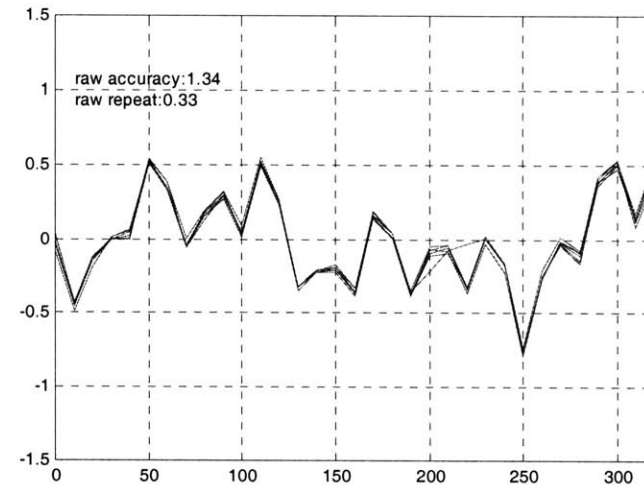
With the linear trend in the data removed, the carriage was consistently positioned to within 1.34 microns, with a repeatability of about 0.33 microns. The 0.33 micron repeatability seems to be an artifact of one or two data points. The repeatability over most of the travel is closer to 0.1 microns. The position encoder has a number resolution of 0.1 microns.

The Linear Accuracy Data



Raw Linear Accuracy Data

This is the difference between the actual carriage position and the position that the controller thinks it is in.



Linear Accuracy with Linear Slope Removed

Raw Accuracy:	1.34 micron
Raw Repeatability:	0.33 micron

1.21 The Vertical Straightness Data

The raw vertical straightness data also had a strong linear trend. This was due to the plane mirror not being level. The slanted mirror gave a vertical displacement reading as it traveled with the carriage under the capacitance probe. This linear trend was removed from the data.

The carriage was moved at 10 mm/s and a measurement was taken every 0.1 seconds. Four (4) passes were made two (2) in each direction. The data from one forward and one reverse pass was filtered by the data collection software to remove the noise; the other two passes were not filtered.

To plot both filtered plots on the same graph, it was necessary to reverse the data taken in the reverse direction and to shift it in time to align the common features on the single plot.

Notice the hour glass shape of the data. Due to a lack of fixturing the plane mirror had to be placed on the carriage with the probe suspended above it. Due to the Abbe error caused by the pitching of the carriage, larger vertical displacements were measured as the measurement point was moved fur-

ther away from the center of rotation of the carriage. This is confirmed by multiplying the pitch by the distance from the center of the carriage to the edge, yielding

$$\frac{1.5[\text{arcsec}]}{3600} \frac{\pi}{180} 152\text{mm} = 1.1\mu\text{m}. \quad (1.10)$$

The vertical translation of the carriage can be estimated by looking at the displacements when the probe was near the middle of the carriage. From the data gathered this appears to be on the order of 0.3 microns.

This test should be redone with the probe attached to the middle of the carriage and the plane mirror suspended above the carriage to get a much better picture of the vertical translation of the carriage over its length of travel.

The Vertical Straightness Data

An Abbe error of 1.2 microns vertical displacement at both edges of the carriage.

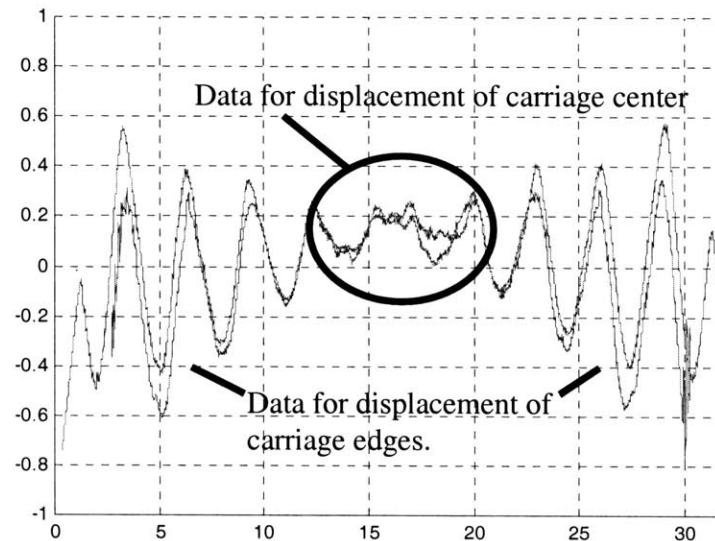
Period of Variation is 28.6 mm

Notice that the hourglass shape of the data is due to pitch errors measured away from the center of pitch rotation.

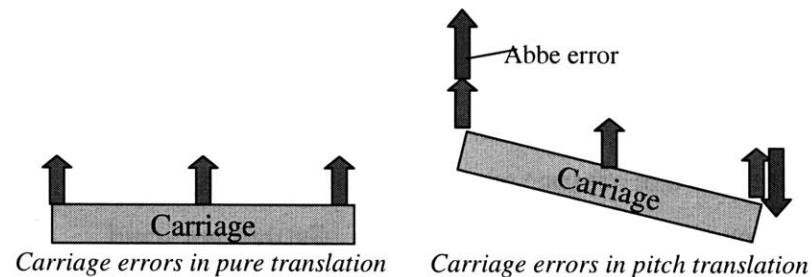
To get better data, the test must be rerun with the probe mounted in the middle of the carriage and the mirror suspended above it.

The data from the center of the carriage shows the pure translation of the carriage to be **about 0.3 microns**.

Because the plane mirror could not be leveled perfectly, any linear slope in the data was removed.



Two passes are shown for a carriage speed of 10 mm/s



1.22 The Vertical Stiffness Data

The vertical stiffness of the carriage was measured by placing weights on the top center of the carriage, and measuring the displacement above each of the four top bearing pads.

Because of more preloading on the outboard bearing pair it is expected that the outboard side of the carriage (points 2 and 3) should have a higher stiffness than the inboard side (points 4 and 5). The measured data supports this. Point 2 is stiffer than point 4, and point 3 is stiffer than point 5.

Another interesting feature of the data, is that the left side of the carriage (2 and 4) is much stiffer than the right side (3 and 5). This effect was not predicted. One can see a possible explanation by looking at the pitch data. There are periodic attractive forces that pitch the carriage forward and backwards. This changes the loading on the left and right pairs of top bearings and increases the stiffness of the bearing on the loaded side. The position that the carriage was placed in to perform the stiffness test was chosen without considering this effect. So it is no surprise that the left and right sides are loaded unevenly. This hypothesis is easy to test. Moving the

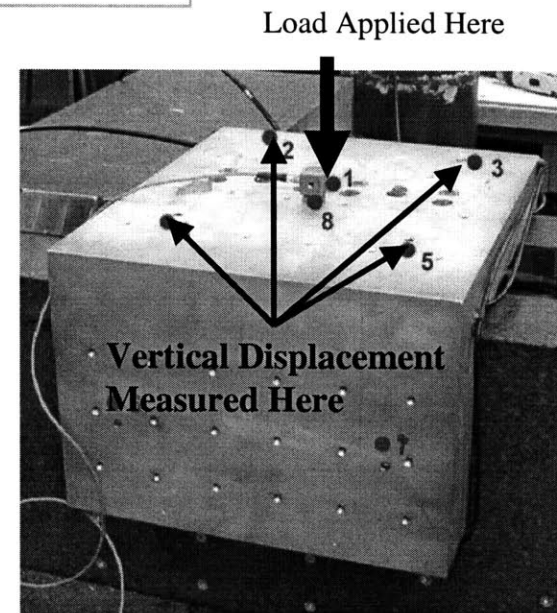
carriage half a period (15 mm) in either direction should pitch the carriage to the other extreme and load the right side of the carriage. Moving the carriage to a position where the pitch is zero should allow both bearing pairs to be preloaded evenly.

Averaging the stiffness measured at the four point yields a vertical stiffness of **422 Newtons per micron**. Therefore each of the top bearings has a stiffness of 106 N/ μm . Using the estimates for bearing load vs. stiffness derived in Section A.1.1 (illustrated in Figure A.1 on page 115 for the bearings in the prototype) each top bearing is loaded with, approximately 1000 N (225 lbs). The resulting total vertical load on the carriage is about 4000 N (900 lbs) or twice the predicted vertical load of 2000 N (550 lbs). Since the magnetic attractive force varies inversely to the distance *squared*, setting the motor coil 0.2 mm closer to magnet track could be enough to almost double the attractive force. This hypothesis could be checked by collecting data for the horizontal stiffness of the carriage, and comparing the measured load to the preload.

The Vertical Stiffness Data

Point	Deflection [microns]		Average Stiffness [N/micron]
	25 lbs (111 N)	50 lbs (222 N)	
2	0.15	0.4	649
3	0.4	1.0	250
4	0.2	0.4	556
5	0.5	0.9	235
Average Vertical Stiffness of Carriage 422 N/micron			

Masses were placed on the top center of the carriage and the displacement above the four (4) top air bearings was measured.



Chapter 2

THE MINIMILL

With the concept of the Axtrusion complete, it was decided to showcase the Axtrusion with a small milling machine.

The machine is called the Minimill

The basic functional requirements of the Minimill are:

- It should be a three (3) axis machine.
- It should have a minimum work volume of 300 mm x 300 mm x 300 mm (12 in x 12 in x 12 in).
- There should be additional clearance in the Z axis direction for tooling and fixturing.
- The machine should be able to cut parts to with an accuracy of at least 25.4 microns (0.001 in).

2.1 Some Competing Machines

After searching the web and reading trade publications it was concluded that small milling machines currently available can be divided in to two categories.

2.1.1 Small Hobbyist Machines

These machines range in price from about \$500 to about \$2000. They may or may not be computer controlled. Most of them are glorified drill presses with an XY stage. Few of these machines appear to be stiff enough to do precision work in materials other than wax.

2.1.2 Small CNC Machining Centers

These machines range in cost from about \$20,000 to upwards of \$50,000. These are small production machines typically used in prototyping and making injection molding dies. They have optional tool changers and a variety of size and speed spindles. All the vendors surveyed list their machines' accuracies in terms of the servo/controller accuracy. I.E. how accurately the machine can move the tool, but they do not give an estimate for how accurately the

machine will cut the parts. Determining a machine's accuracy requires an knowledge of how the machine will deflect under the load of the cutting forces. None of the engineers spoken to at these companies knew how large those deflections might be.

Some Competing Machines



The Compact DMC™ (left), and the XV Tabletop™ (middle) Machining Centers by Defiance. The Benchman™ Series (right) by Light Machines.

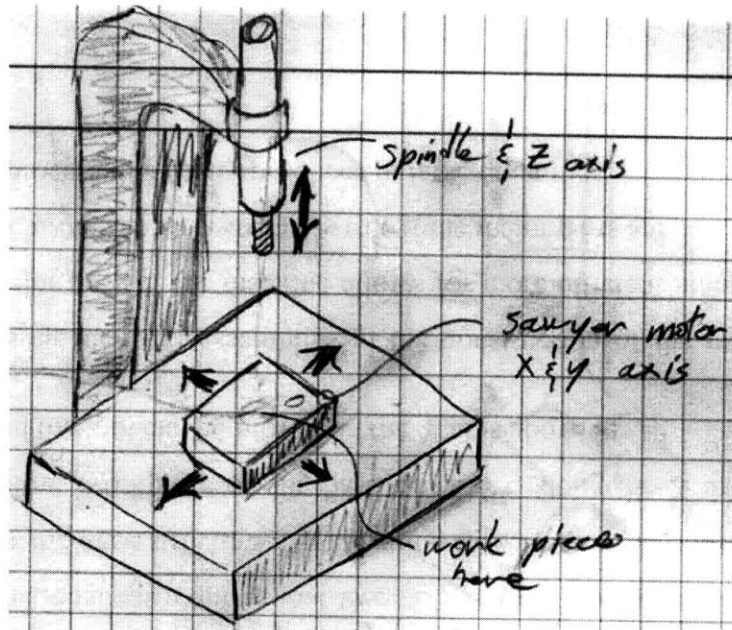
2.2 Some Initial Concepts

Some stick figure sketches were made for several machine concepts. The main criteria at this point for eliminating concepts are the distance between the tool tip and the linear motion points on the axis. Designs that have excessively long distances between the tool tip and motion points will be more susceptible to Abbe error. These designs are eliminated for this reason.

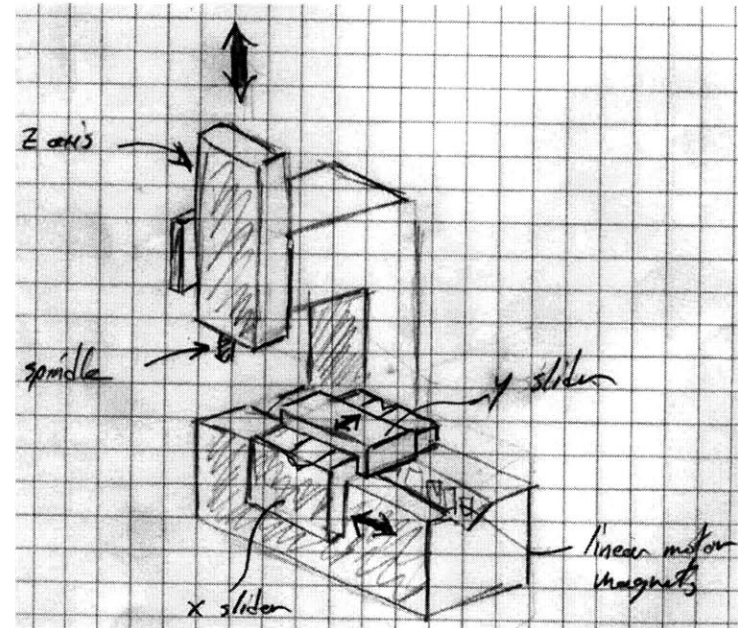
Some other considerations in the initial design of the machine was whether the tool should be vertical or horizontal. A vertically mounted tool requires less fixturing to hold the workpiece. A horizontally mounted tool is convenient for cutting chip removal (they can fall straight down). In a small machine, the spindle is likely to be one of the heavier components, so there is an advantage in mounting this lower down (as in a horizontally mounted spindle).

It is difficult to stack all three degrees of freedom on only the tool or the workpiece. The right-hand sketch below shows a concept where the tool moves in one degree of freedom (Z) and the workpiece moves in two (X and Y).

Some Initial Concepts



Sawyer Motor for the X & Y Directions. Traditional or Combined Unit for the Z axis and Spindle



Two Axtrusions on the base (X & Y) and an Axtrusion for the Z axis.

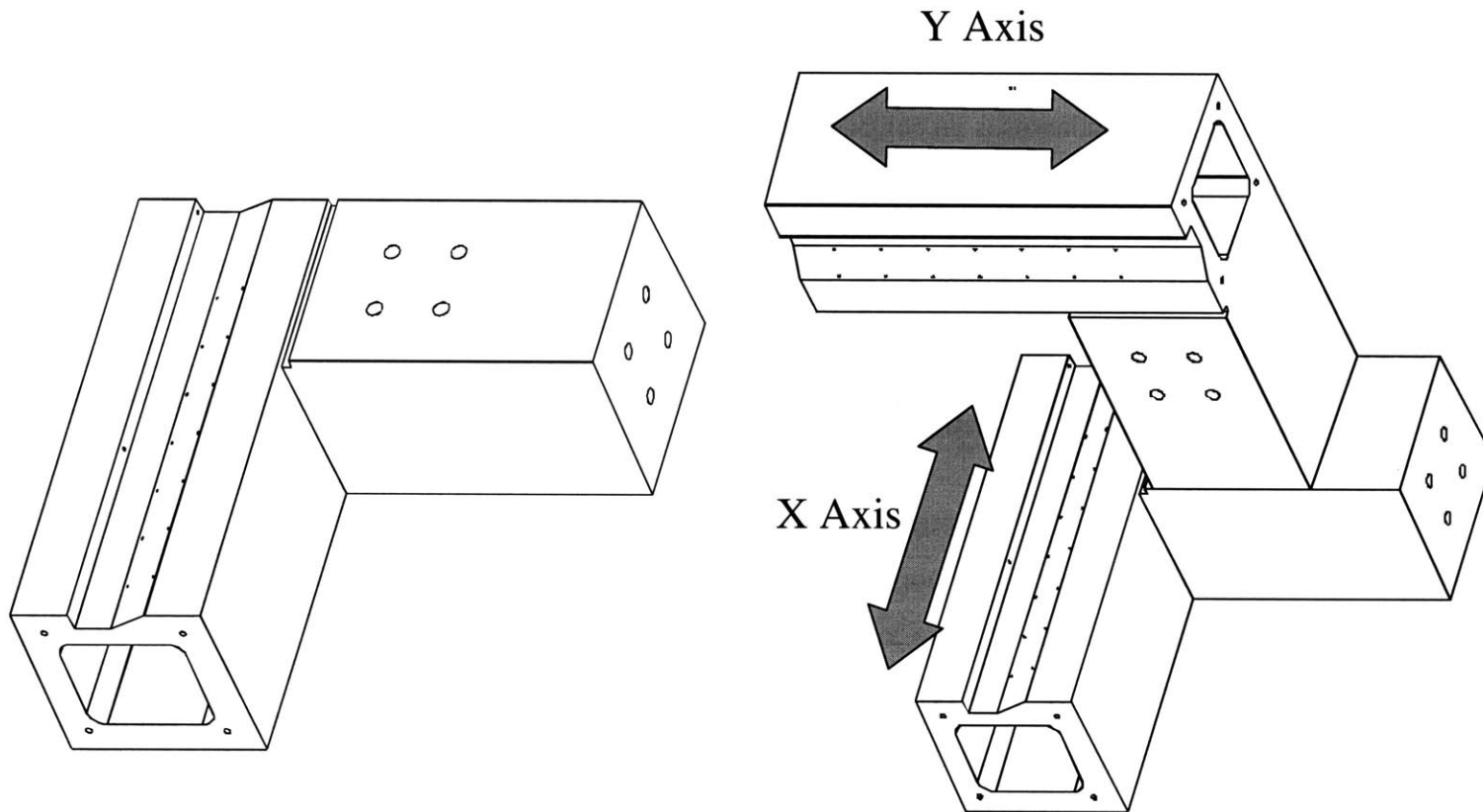
2.3 Two “L”s To Make a Machine

In the process of trying to decide whether the tool or the work piece should have two degrees of freedom, it was realized that two identical assemblies could be used to make a the X and Y axis of the machine.

This concept requires that two “L” shaped blocks be used for the base structure. By attaching these blocks, as shown below, workpiece on the base can move along the X axis and the tool can be moved on the Y axis above it.

Using identical assemblies in the construction of the two major axes of the machine allows for more efficient manufacturing. This is especially true if the major parts are cast in a process that easily produces in large quantities.

Two L's Used to Make Machine



2.4 The Error Budget

The formulation of an error budget is an important step in ensuring that the machine will meet its accuracy goals. The types of errors were broken down into three main categories. Each of these categories is initially allotted an equal share, $8.47\ \mu\text{m}$ (0.0003 in), in the target accuracy of $25.4\ \mu\text{m}$ (0.001 in).

2.4.1 Static Deflection Errors

These are the errors associated with compliance in the machine structure, bearings, spindle, and tools. It is important to keep in mind that the target accuracy only needs to be met on the finish pass of the cut, when the machine is not running at full power. Therefore the cutting forces will be much lower. The final cutting forces were assumed to be no greater than 30 N (6.7 lbs). The cutting tool was assumed to have a deflection of 3 microns. The compliance in the carriage bearings causes the carriage to rotate when a moment is applied. This carriage rotation will cause a displacement error at the tool tip. The maximum allowable magnitude of this displacement determines the maximum allowable car-

riage rotation. For the worst case error budget the carriage rotation was estimated for when the Z way was fully extended. When the Z way is completely extended the carriage rotation in the Y and Z carriages causes the greatest amount of error. In this state the error caused by the X carriage rotation is minimized because the tool tip is very close to the X carriage.

2.4.2 Thermal Expansion Errors

Heat generated by the machine components and changes in the ambient temperature will cause the machine to expand and contract. The errors associated with these changes should be no more than 8.47 microns (0.0003 inches). The parts of the machine most susceptible to thermal errors are the ways.

2.4.3 Control and Alignments Errors

This category includes all the errors caused by the pitch and yaw of the linear motion elements, the errors in the position encoders and controller, the misalignment of an axis, and any error motions in the X, Y, and Z carriages. The magnitude of these error motions were not known until the prototype Axtrusion was built.

The Error Budget

With an overall machine goal of 25.4 microns (0.001 inches) the allowable errors are split among three main errors sources.

Static Deflection Errors	[microns]
Tool Deflection	3.0
X Carriage Roll	0.5
Y Carriage Roll (@ full extension)	1.5
Z Carriage Roll (@ full extension)	1.5
X Way Deflection	0.0
Y Way Deflection	0.2
Z Way Deflection	1.6
Total Static Deflection	8.3

Maximum Carriage Roll	
Due to Deflection	[arc sec]
X	0.3
Y (@ full extension)	1.0
Z (@ full extension)	1.0

Thermal Expansion Errors

$$\alpha_{al} := 6 \frac{\mu\text{m}}{\text{m}\cdot\text{K}}$$

The coefficient of expansion of granite

$$L := 600\text{mm}$$

The maximum length of one of the ways

$$\delta L := 8\mu\text{m}$$

The maximum length a way may change

$$\Delta T := \frac{\delta L}{\alpha_{al} \cdot L}$$

$\Delta T = 2.2\text{K}$ The maximum temperature change that the machine can tolerate

Control and Alignment Errors

Maximum error motion in carriage roll, pitch, and yaw for each axis is 2 arc seconds

2.5 MiniMill Major Components

A convenient feature of the MiniMill is that there are only three major moving parts: the X carriage, the Y carriage, and the Z way.

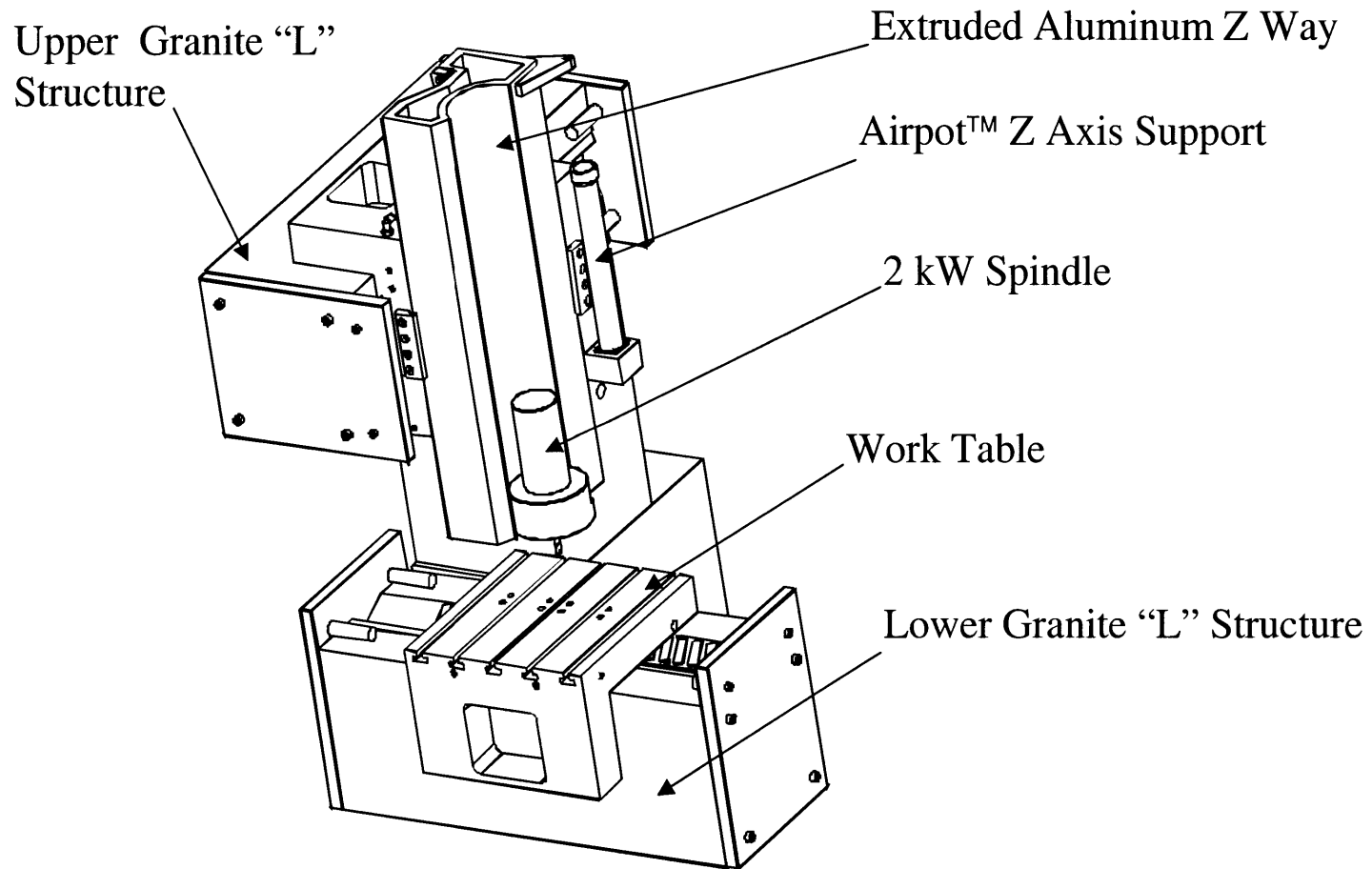
The Z way is an extruded piece of Aluminum. The two precision surfaces are ground and then the whole piece is hard anodized. The linear motor magnet track is attached to the Z axis and the motor coil and air bearings are attached to the Y carriage. The only wiring that has to move with the Z axis is the spindle wiring.

The Airpot™ piston is used to support the weight of the Z axis while it is floating.

The 2 kW (2.7 hp) spindle could be supplied by a company like Fisher Precision Spindle of Berlin CT, USA.

The work table is 300 mm (12 inches) square and the X and Y axis are configured to allow the tool to reach any point on the table.

MiniMill Major Components



2.6 Simple Stiffness Check

The largest sources of compliance in the Minimill are the air bearings. A quick check of the machine stiffness is performed early in the design process. This check only accounts for the tool tip error due to compliance in the air bearings. If the air bearings can meet the performance criterion specified in the error budget, this aspect of the design is likely to succeed. The displacement of the tool tip can be no more than 1.5 microns (0.000059 in) each for the Y and Z carriages.

When the Z axis is completely extended there will be a moment arm of about 500 mm (19.6 inches) on both the Z and Y carriages. With a maximum cutting force of 30 N this results in a torque on the Y and Z carriage of 15 Nm (11.3 ft.-lbs). Using the bearing stiffness measured on the prototype extrusion of 100 N/micron (570,000 lbs/in), these parameters are entered into the basic stiffness model shown below. This model indicates that the tool displacement due to the rotation of each carriage at full Z extension under the 30 N load is about 1.4 microns. This is within the specifications of the error budget.

Axtrusion MiniMill™ Quick Check of Bearing Compliance

$L_b := 230\text{mm}$ Distance Between Bearing Centers

$L_t := 500\text{mm}$ Distance From Center of Stiffness to Tool Tip

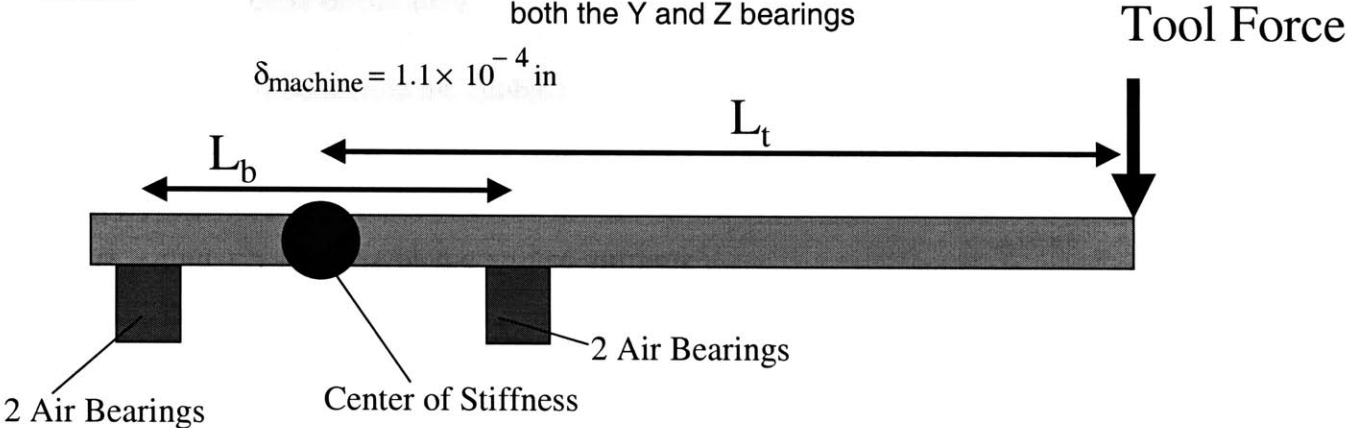
$K := 200 \frac{\text{N}}{\mu\text{m}}$ Stiffness of a Pair of Air Bearings

$F := 30\text{N}$ Force Applied at Tool Tip

$\delta := \frac{L_t^2 \cdot F}{0.5 \cdot K \cdot L_b^2}$ $\delta = 1.4\mu\text{m}$ Deflection at Tool Tip due to one set of bearings

$\delta_{\text{machine}} := 2 \cdot \delta$ $\delta_{\text{machine}} = 2.8\mu\text{m}$ Deflection at Tool Tip due to both the Y and Z bearings

$\delta_{\text{machine}} = 1.1 \times 10^{-4} \text{ in}$



2.7 A Finite Element Check

The stiffness results were checked with a finite element analysis (FEA) of the machine. The displacement predicted by the FEA is within 1.2 microns of the simple stiffness check. The FEA results shown below use an estimated individual bearing stiffness of 40 N/μm (it agrees with the simple check when 40 N/μm is entered in the simple model).

One of the most critical parts of the FEA model is to correctly model the air bearings. The air bearings are modeled as blocks of equivalent stiffnesses. The size of the air gap in the actual machine is on the order of 10 to 20 microns. If the actual dimensions of the air pad model were used they would be 100 mm x 50 mm x 12 μm and 150 mm x 75 mm x 19 μm. The finite element size is approximately the air pad model's smallest dimension. If the actual dimensions were used the air pad models would have approximately 30 million elements each. The CAD software also has trouble creating features so thin compared to the rest of the machine. So for the FEA model the air gap was made 4 mm thick. This reduces the number of elements in each pad by 5 orders of magnitude, allowing the program to solve it.

The air is modeled as an solid with a Young's Modulus such that the air pad model will have the same stiffness as the actual air bearing. The equivalent modulus is calculated by

$$E_{equiv} = \frac{K \cdot t}{A}, \quad (2.1)$$

where K is the desired stiffness of the air pad model, t is the thickness of the model, and A is the area of the air pad.

TABLE 2.1 Equivalent Young's Modulus for Air Pad Models

Parameter	100 x 50 mm	150 x 75 mm
K [N/μm]	40	110
t [mm]	4	4
A [mm ²]	5000	11,250
E_{equiv} [MPa]	32	39

Air bearings modeled in this way provide stiffness in all directions. Actual air bearings only provide stiffness normal to the surface that they are running on.

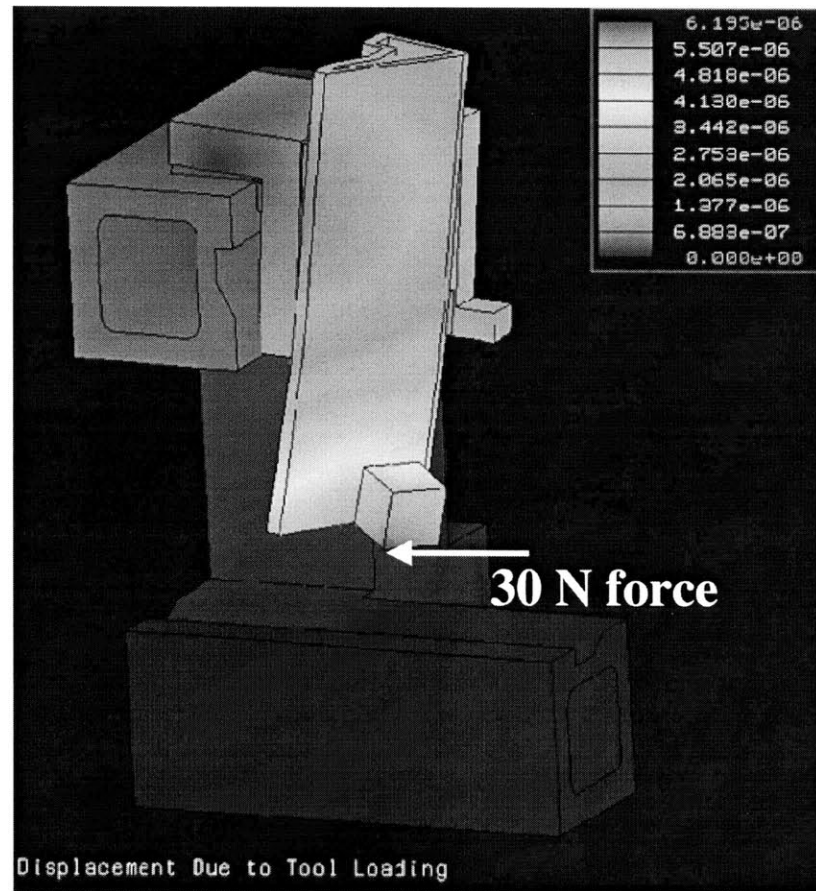
Axtrusion MiniMill™ Displacement Due to Tool Loading

A 30 Newton tool load was applied to the Z axis at full extension in the negative X direction.

The FEA estimated 6.2 microns of displacement with this load, when the bearing stiffness was estimated to be 40 N/micron.

This yields a machine stiffness of:
5 N/micron (27,000 lbf/in)

The quick stiffness check (previous slide) gives an estimate of 5 μm for deflection at the tool tip (w/ a bearing stiffness of 40 N/ μm .) Did the extra 1.2 μm come from the deflection of the Z axis itself?



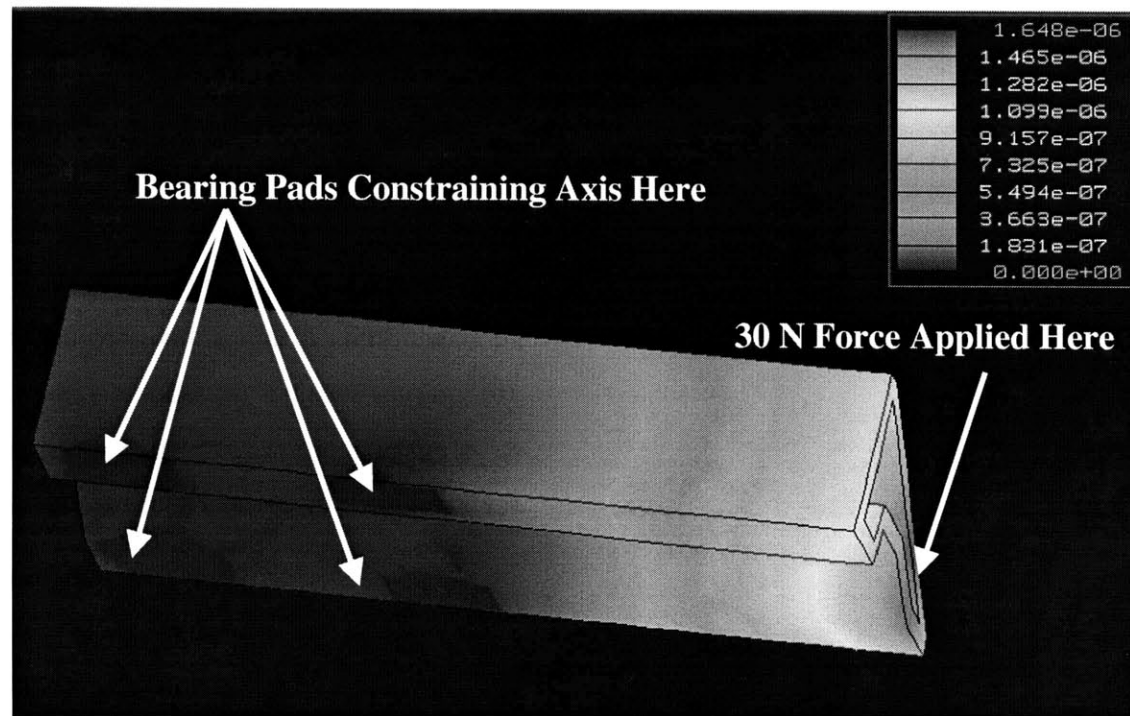
2.8 An FEA Check of the Z Axis

After the air bearings in the carriage the next most compliant component in the structural loop is the Z way. The Z way is an extruded aluminum piece.

It is hypothesized that the difference in displacement between the simple stiffness model and the FEA of the machine can be rectified by checking the displacement due to the deflection of the Z axis.

A Finite Element Analysis of the Z axis was run and confirmed the hypothesis.

Checking the Compliance of the Z Axis



Under a 30 N force at full extension the Z Axis deflects 1.6 microns.

This rectifies the difference between the simple stiffness calculation and the FEA of the whole machine.

2.9 Displacement Errors Due to Gravity

The Finite Element Analysis in Section 2.7 only calculated the displacement due to a tool force. Gravity will also cause displacements in the machine. The FEA was rerun to estimate the magnitude of these displacements. The results of this second FEA run can be divided into two categories.

2.9.1 Error Inducing Displacements

As the Y carriage moves out the Y axis, its mass deflects the Y way further. When the Y carriage is at the extreme of its travel, the Y axis will droop about 20 microns (0.0008 in). This error in the vertical deflection can be eliminated by mapping it out and having the controller drive the Z axis way to compensate for it.

2.9.2 Non Error Inducing Displacement

The compliance of the Y and Z carriage bearings will cause the Y and Z carriages to rotate under the load induced by gravity. Because this rotation is constant for all Y and Z positions it does not contribute to the errors in the machine.

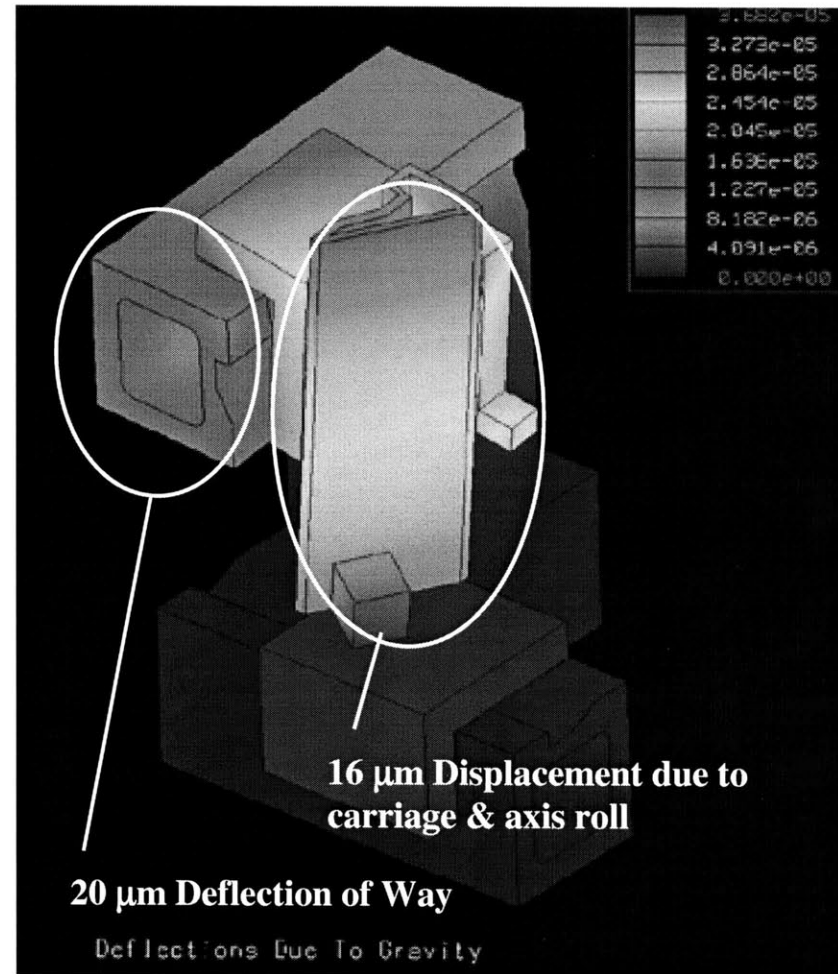
Axtrusion MiniMill™ Deflection Due to Gravity

There are two components:

- The deflection of the Y way
- The Roll of the YZ Carriage

The deflection of the Y way is proportional to the position of the YZ Carriage on the axis. When the YZ Carriage is at the end of the Y way there will be a deflection of about 20 microns for the polymer concrete version. Solutions are listed on the next slide.

The Roll of the YZ Carriage is independent of either the YZ Carriage Position or the Z Axis position, So it should not effect the accuracy of the machine much.



2.10 Remaining Work on the Minimill

The Minimill design is not complete. However, it has been demonstrated that the Axtrusion linear motion element makes the design very simple. The work remaining to be done on the Minimill includes:

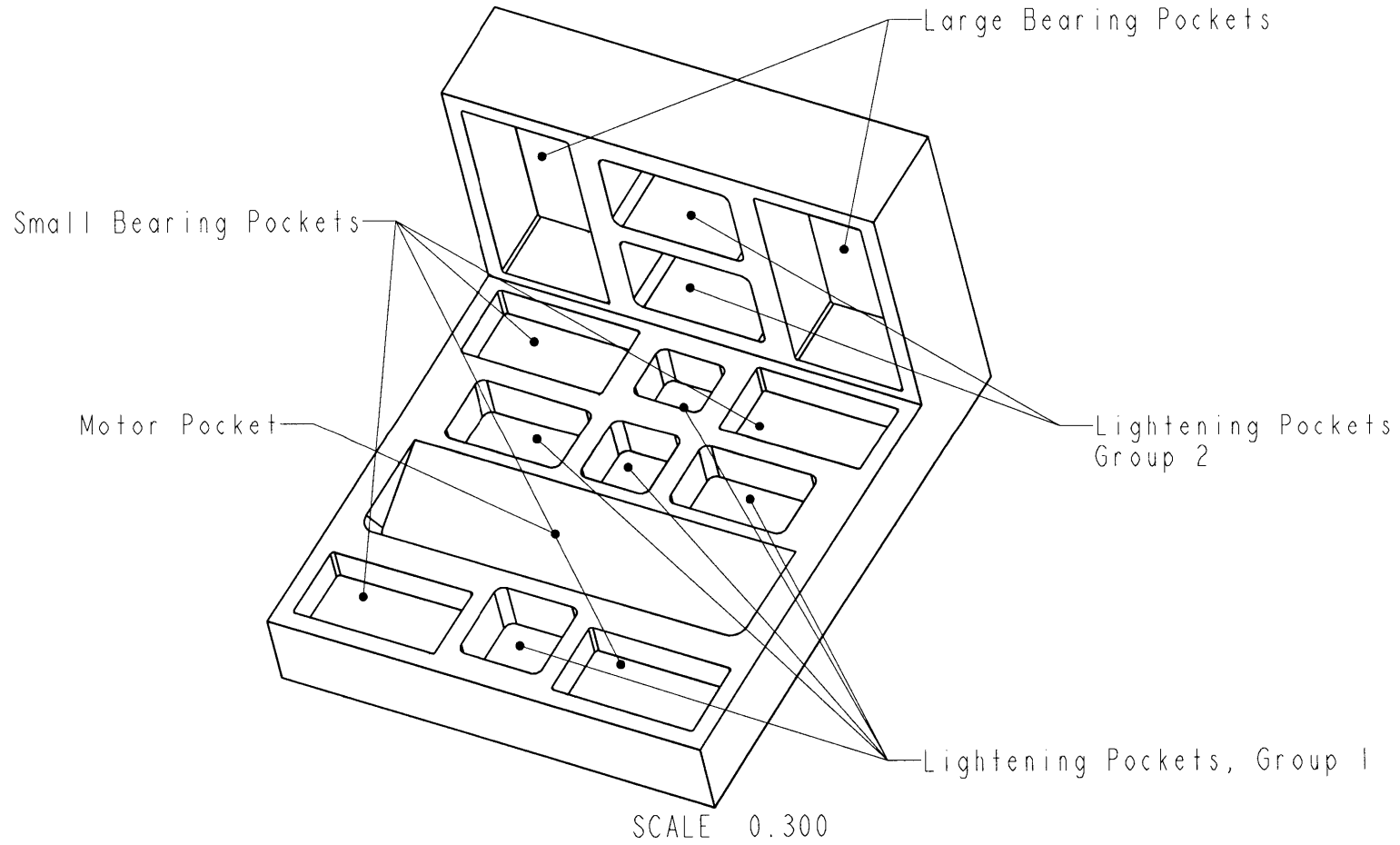
- Detail design of position encoder mounting hardware.
- Detail design of cable carrier mounting hardware.
- Detail design of the Z axis and spindle mount.
- Detail design of the bellows mounting hardware.

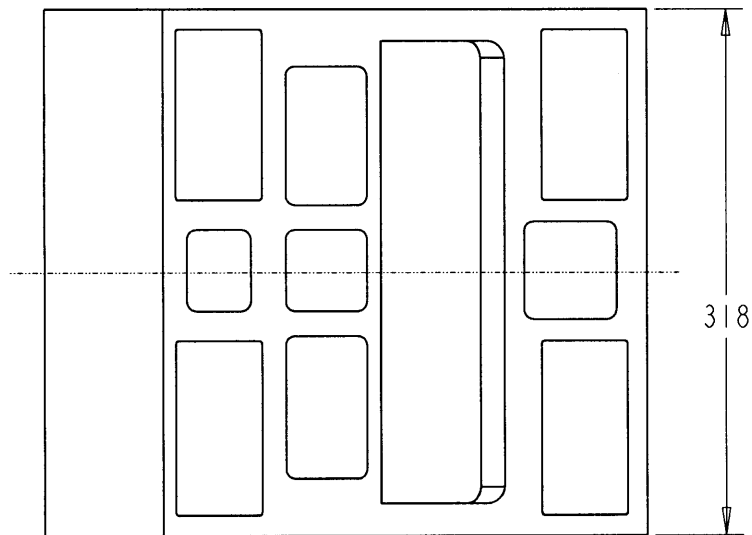
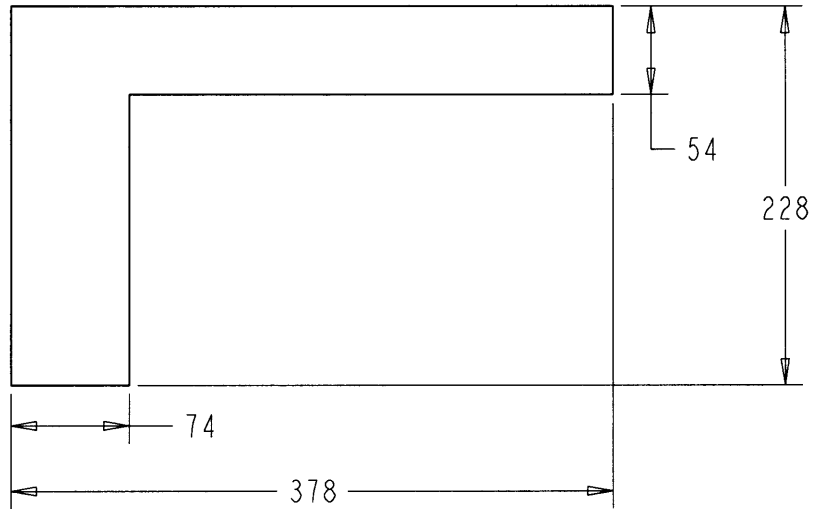
Chapter 3

AXTRUSION PART DRAWINGS

This chapter consists of the manufacturing drawings for the prototype Axtrusion and its fixturing. These are the drawings for the machine that was actually built. The next generation carriage should include a lot of improvements. A list of these suggested improvements and the reasons for them are included in Section A.3 on page 113 of the Appendix.

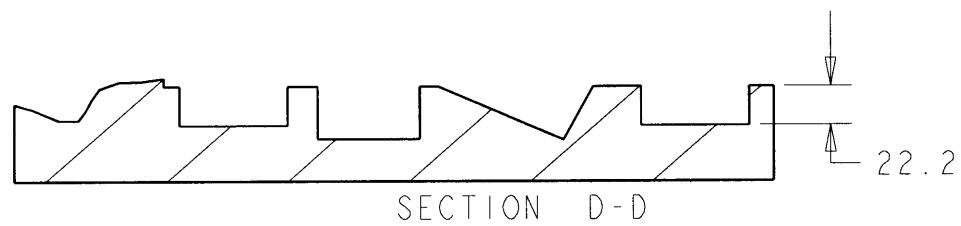
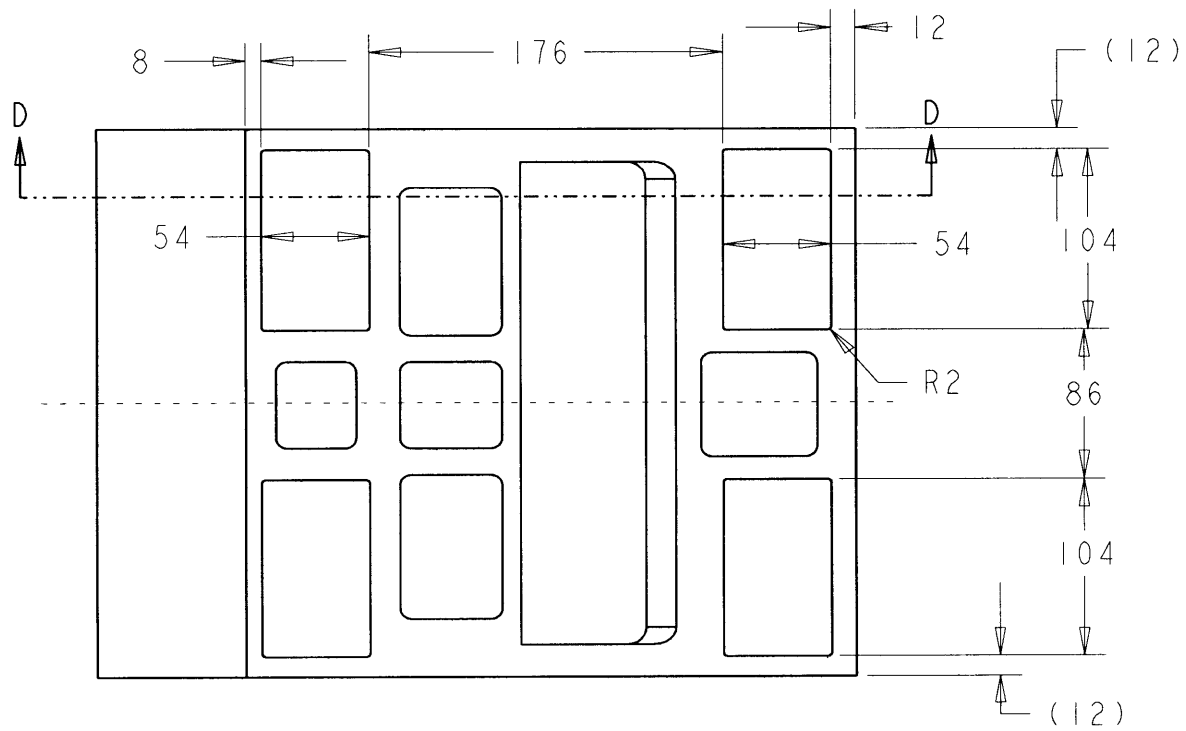
Part Overview





Overall Dimensions (mm)

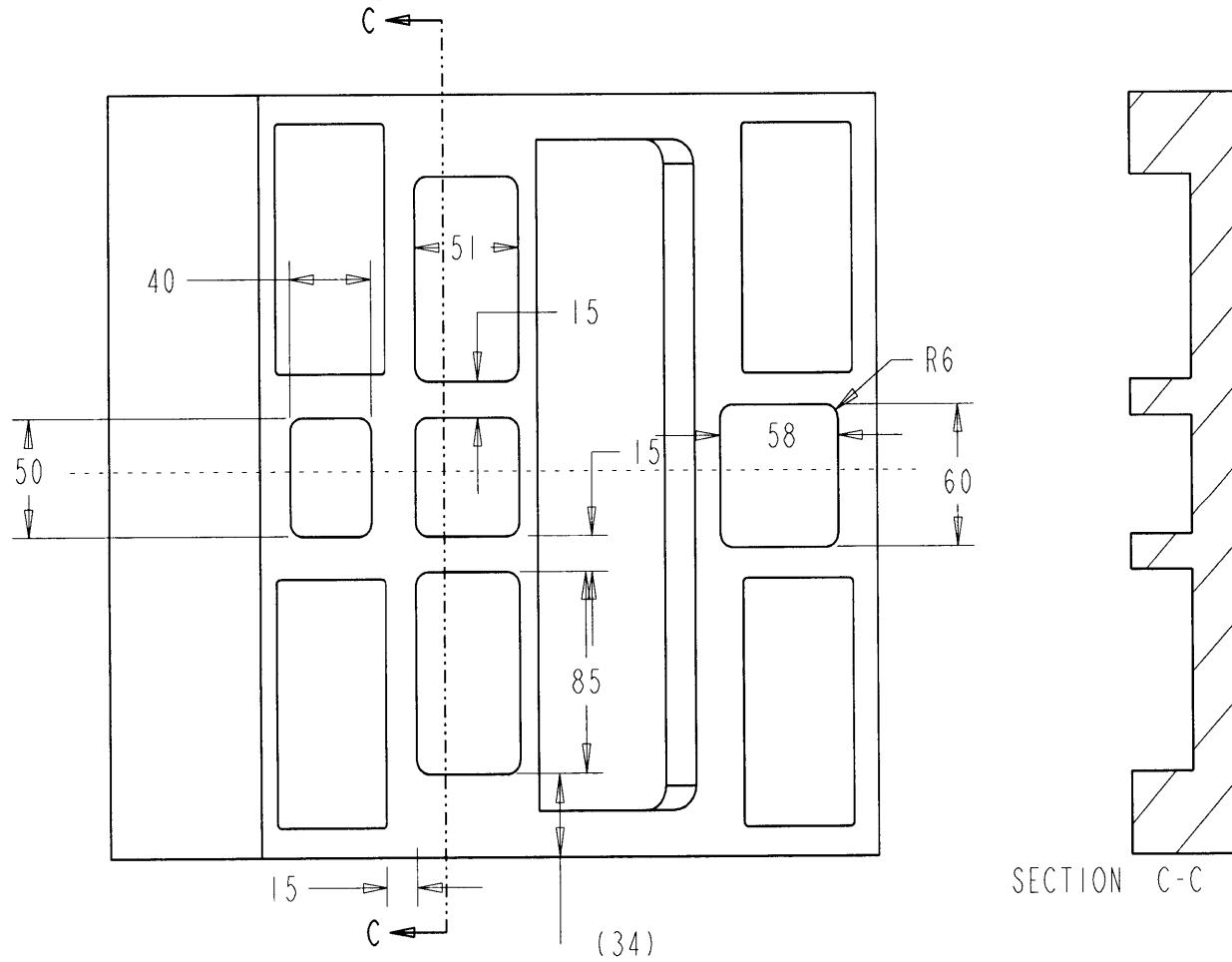
Small Bearing Pocket Dimensions



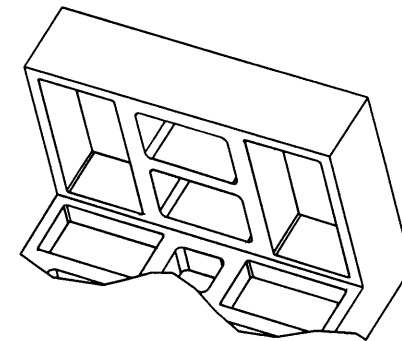
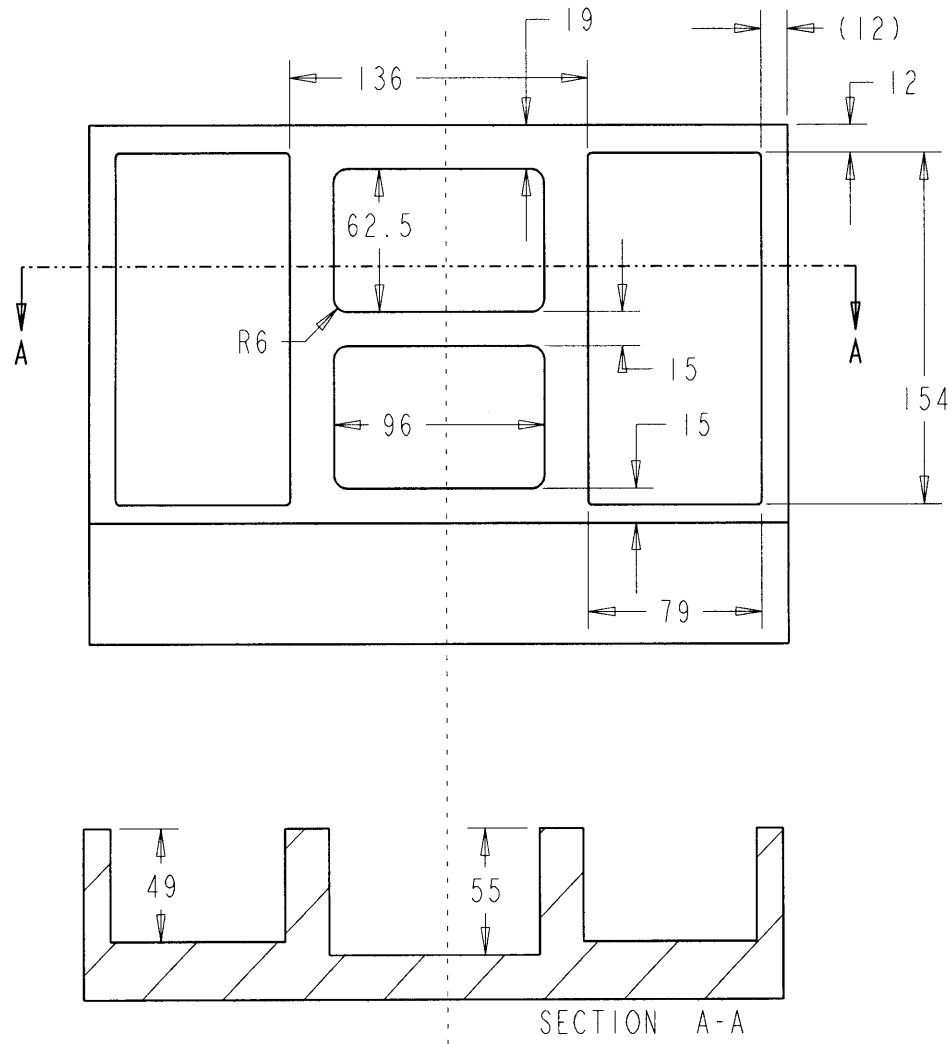
All Dimensions In mm

Lightening Pockets, Group 1 Dimensions (mm)

All 5 lightening Pockets are 30 mm deep from the main surface

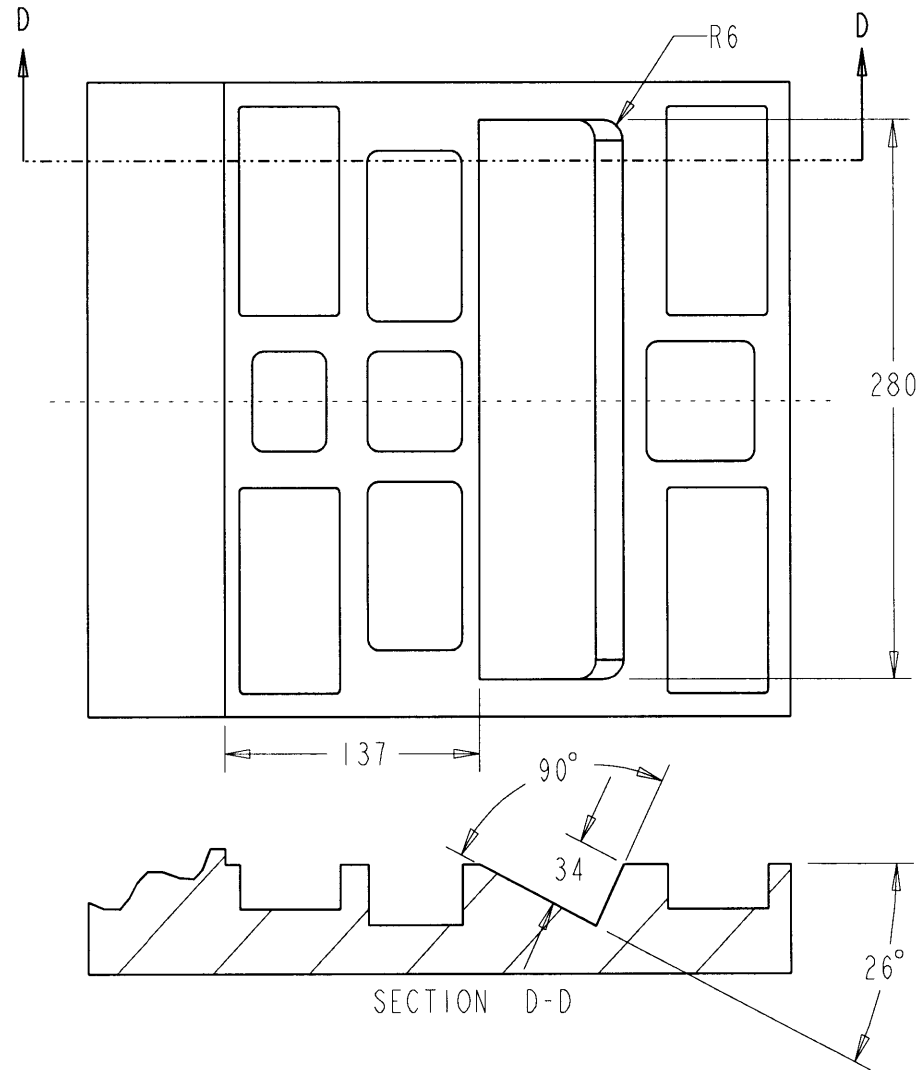


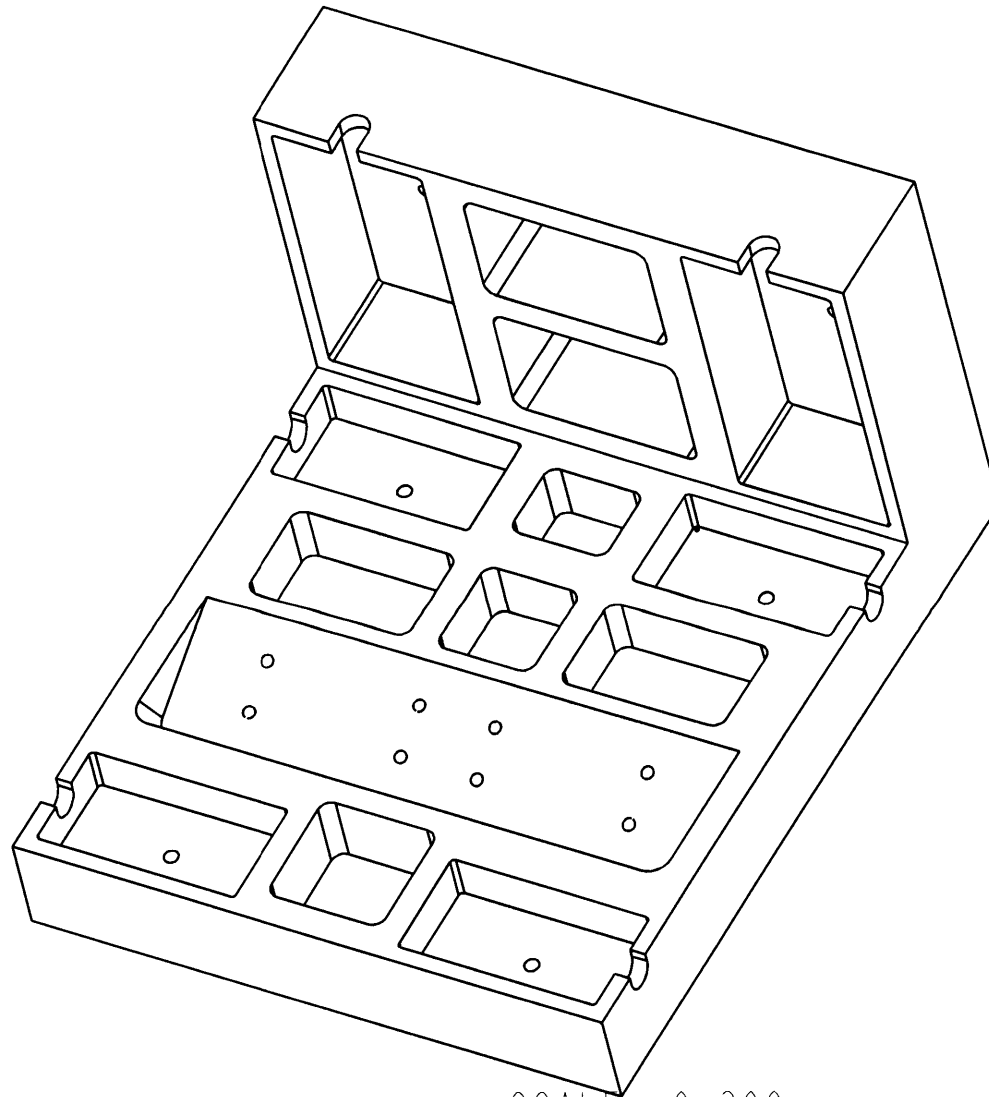
Big Bearing Pocket and Lightening Pockets (Group 2)



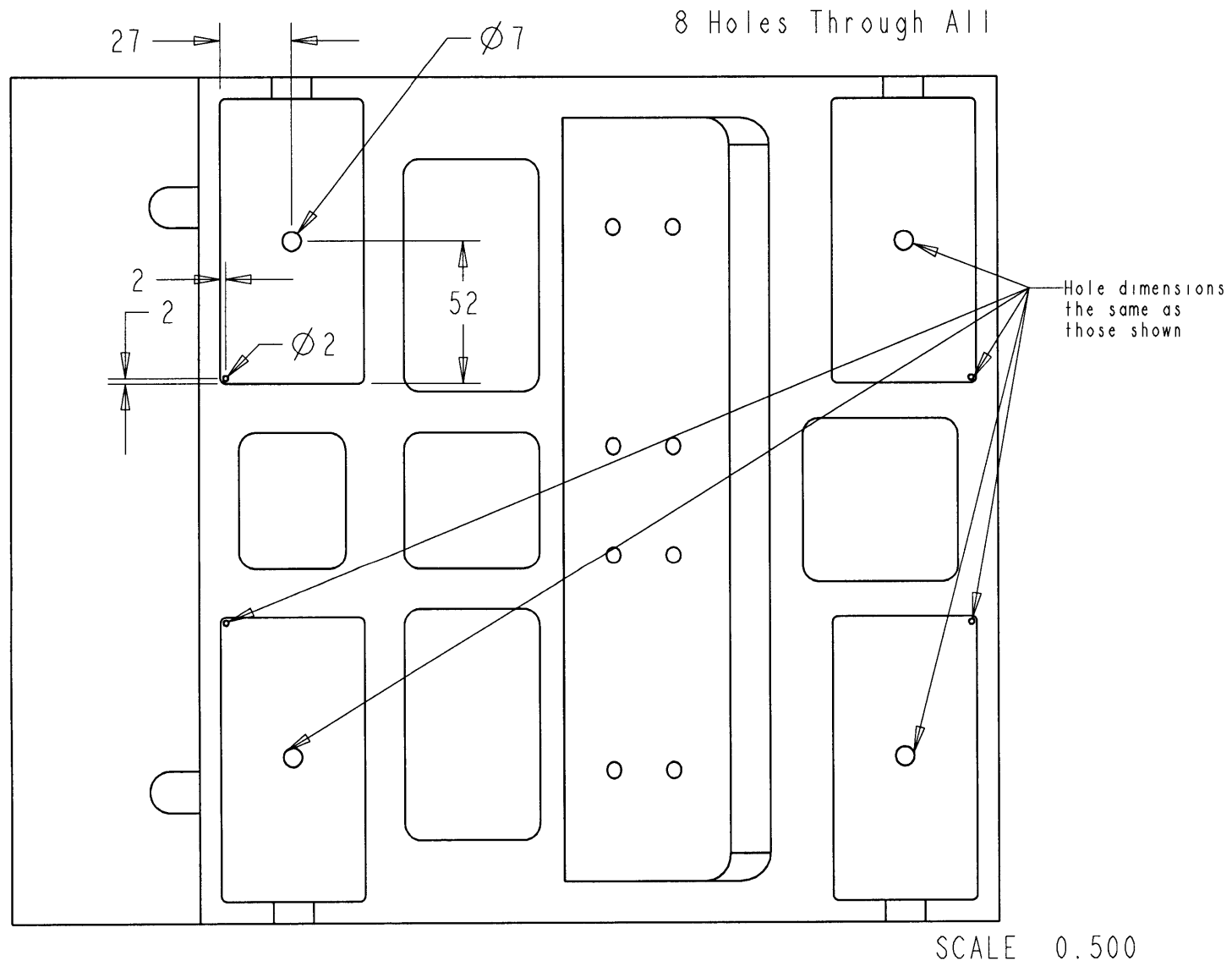
SCALE 0.200

Motor Pocket Dimensions (mm)



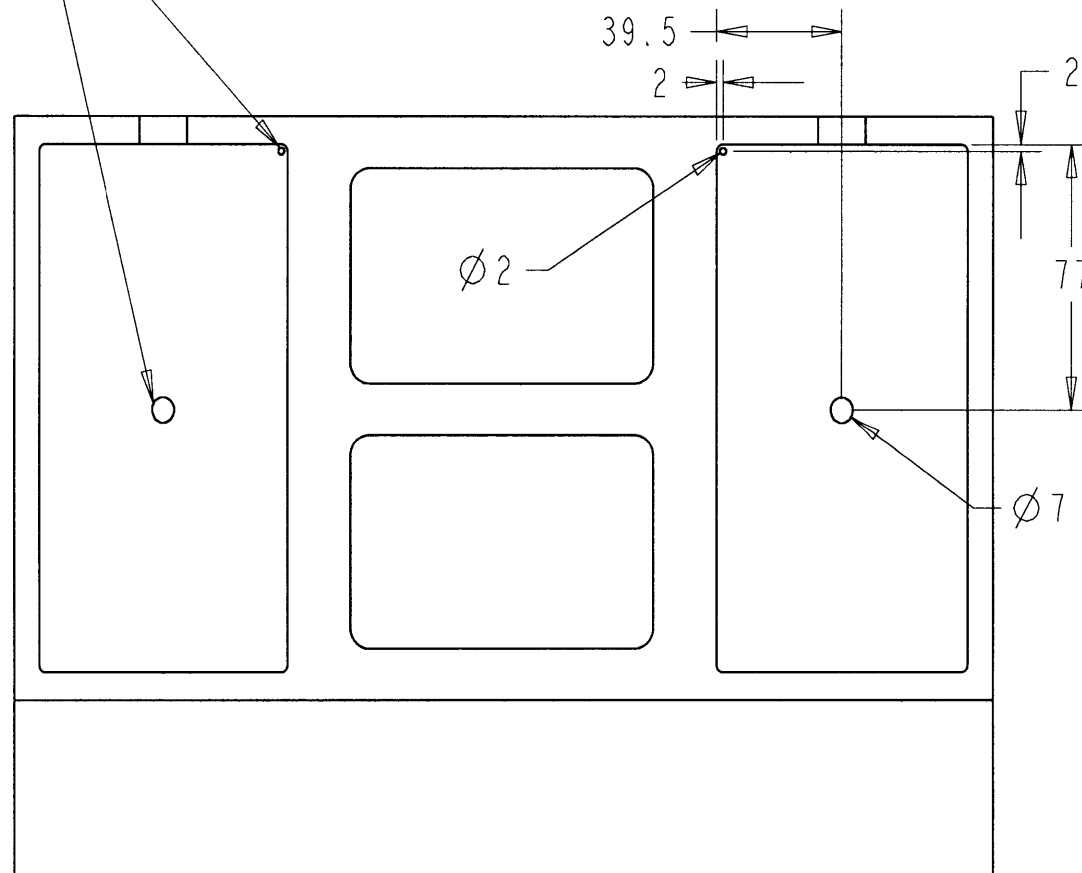


SCALE 0.300

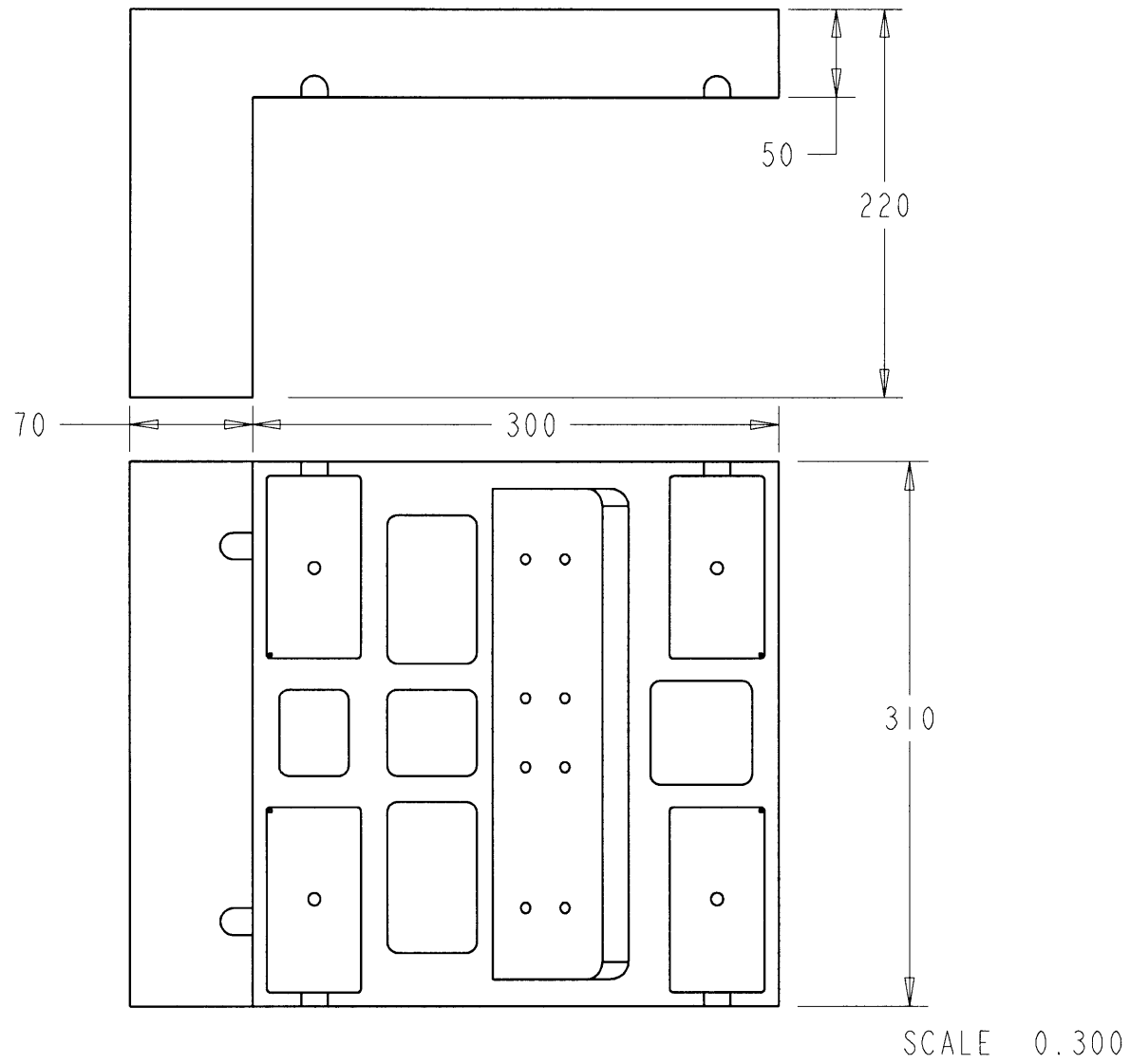


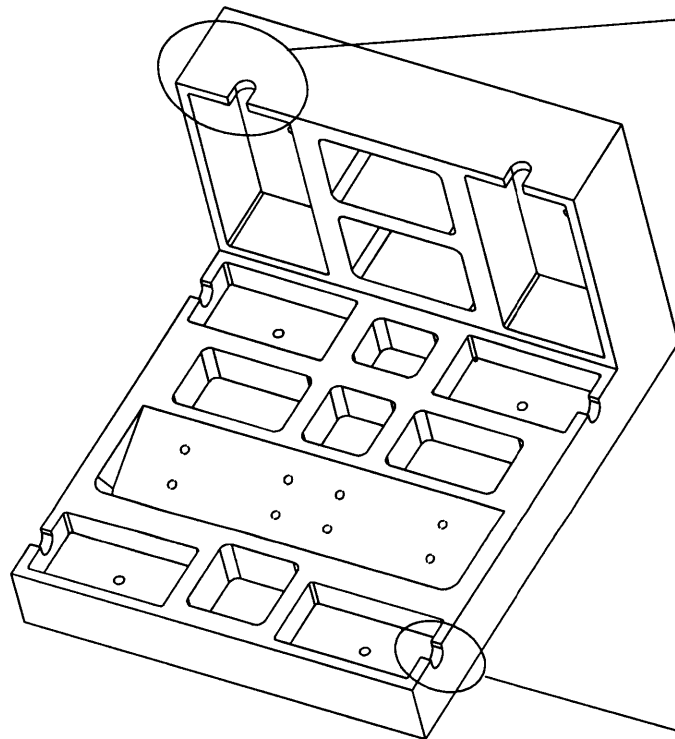
Hole dimensions
same as those shown

4 Holes Though All

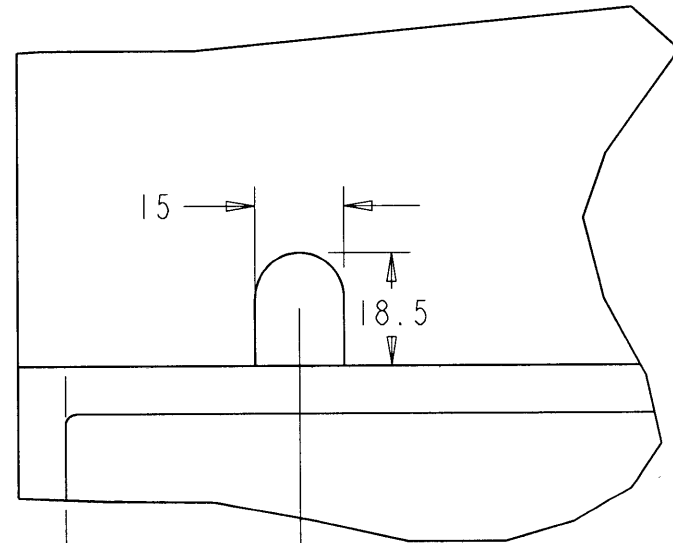


SCALE 0.500

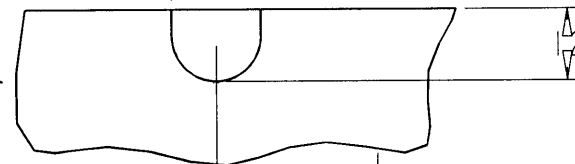




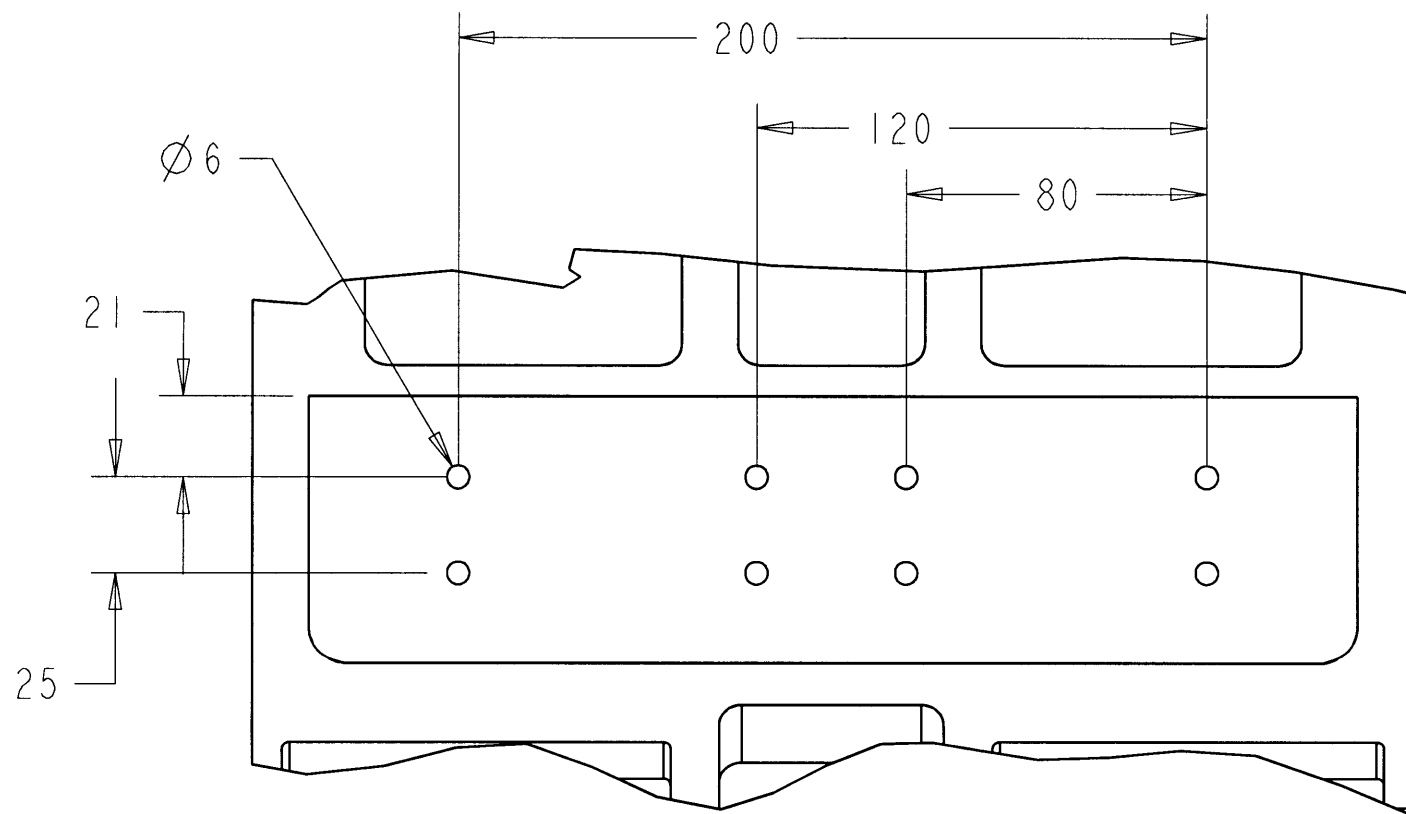
SCALE 0.250



39.5 15 SCALE 1.000

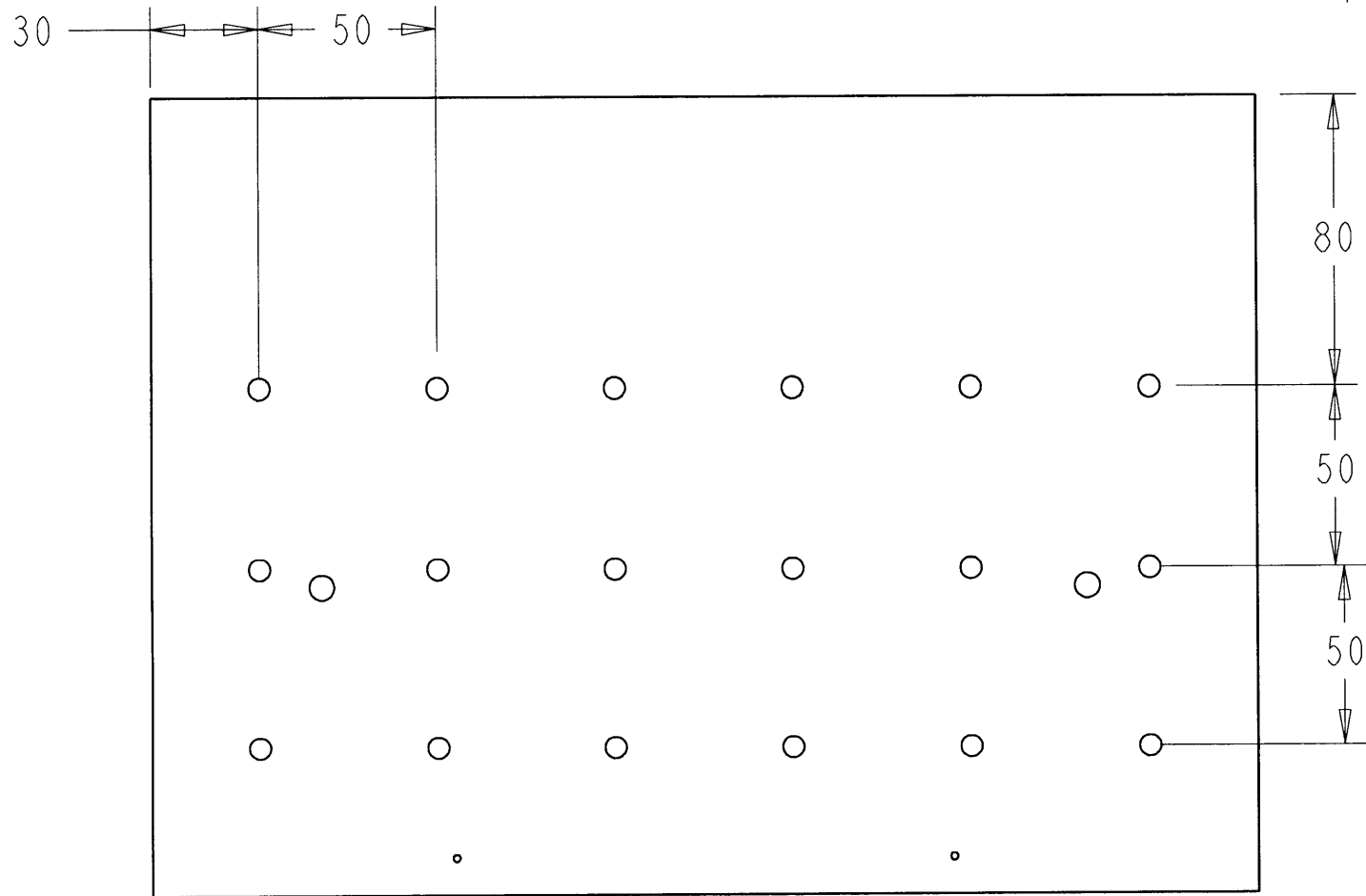


27 SCALE 1.000



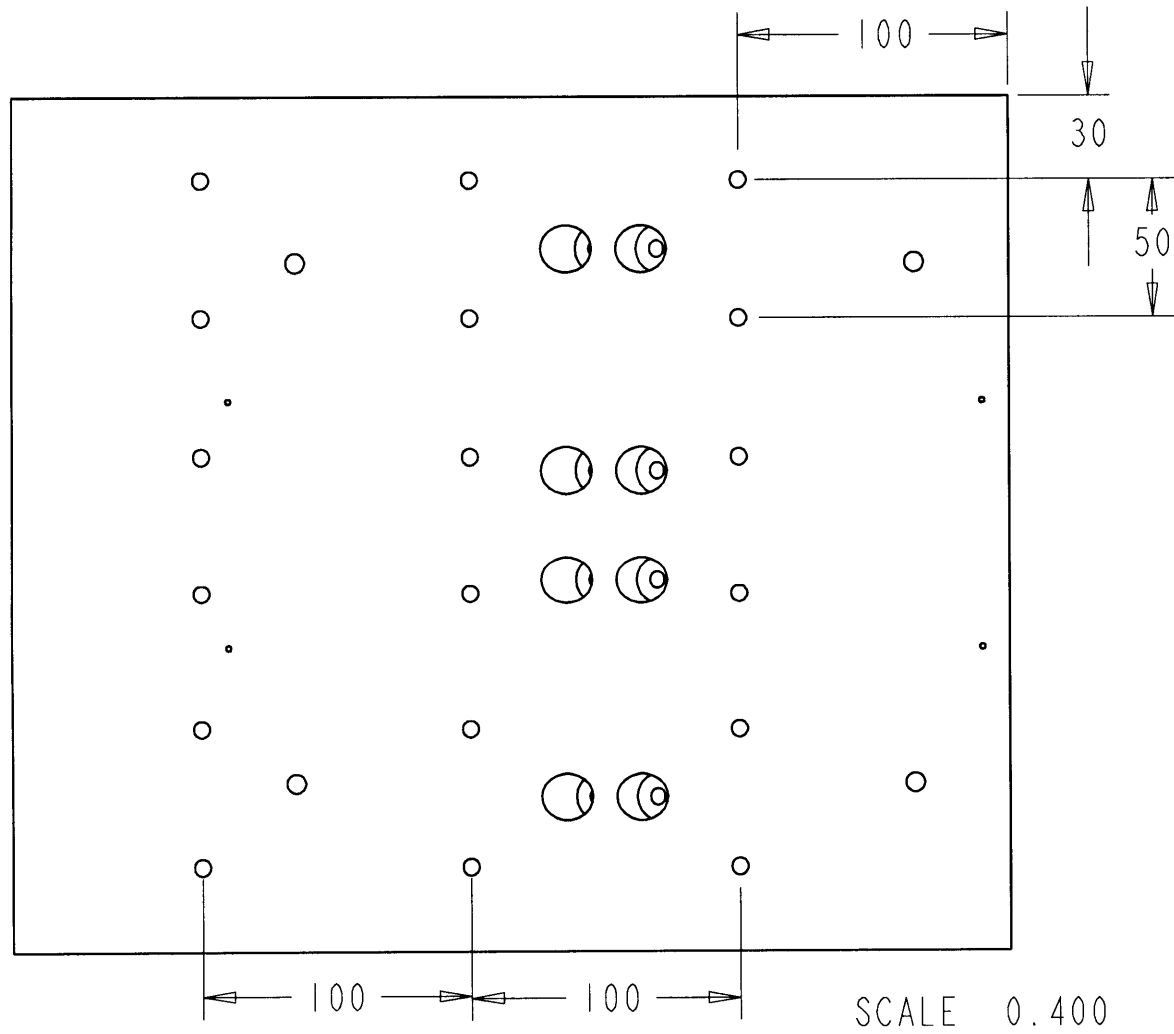
SCALE 0.500

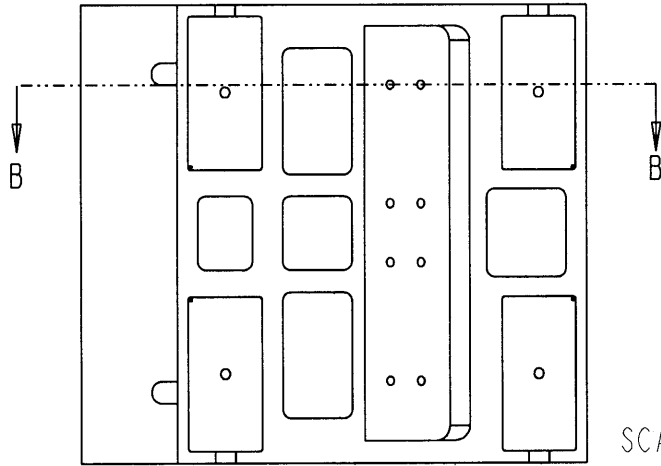
18 Holes with M6 threads 12 mm deep



SCALE 0.500

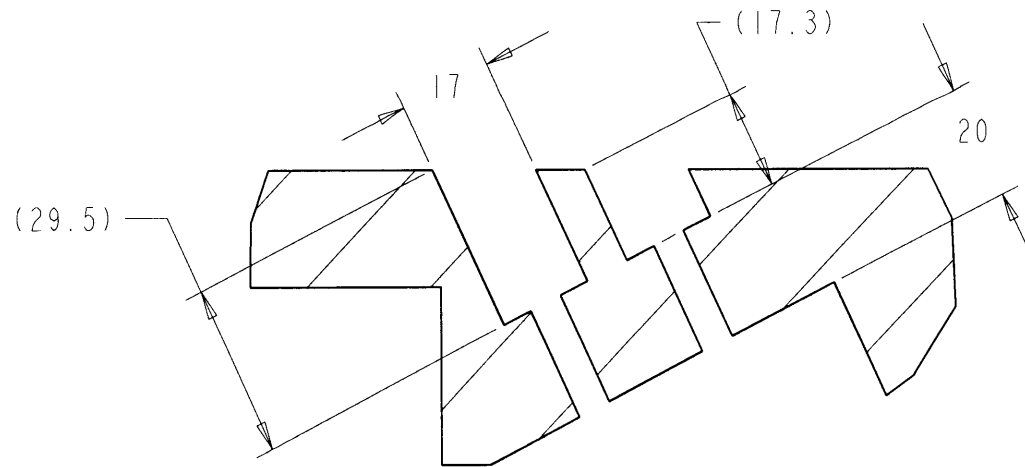
18 Holes with M6 threads 12 mm deep





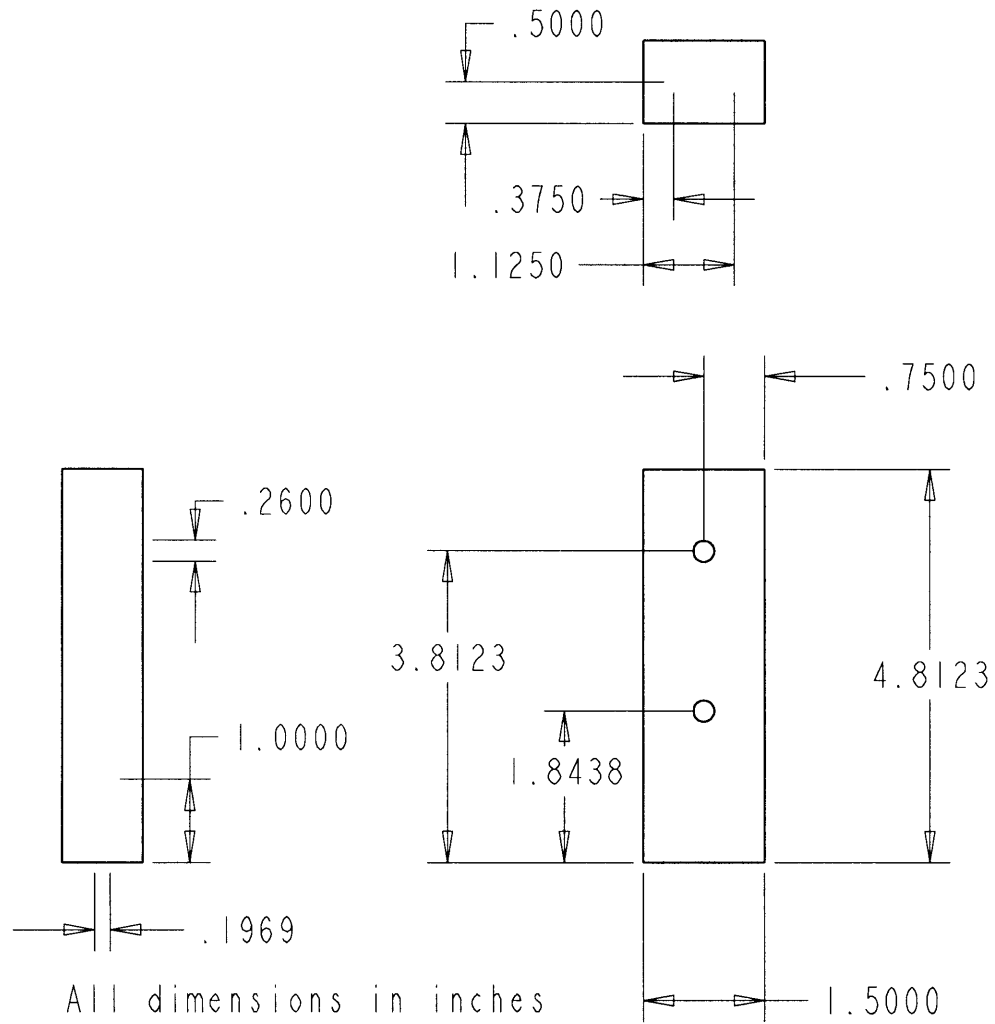
Dimensions for Angled
Counter Bored Holes

SCALE 0.250

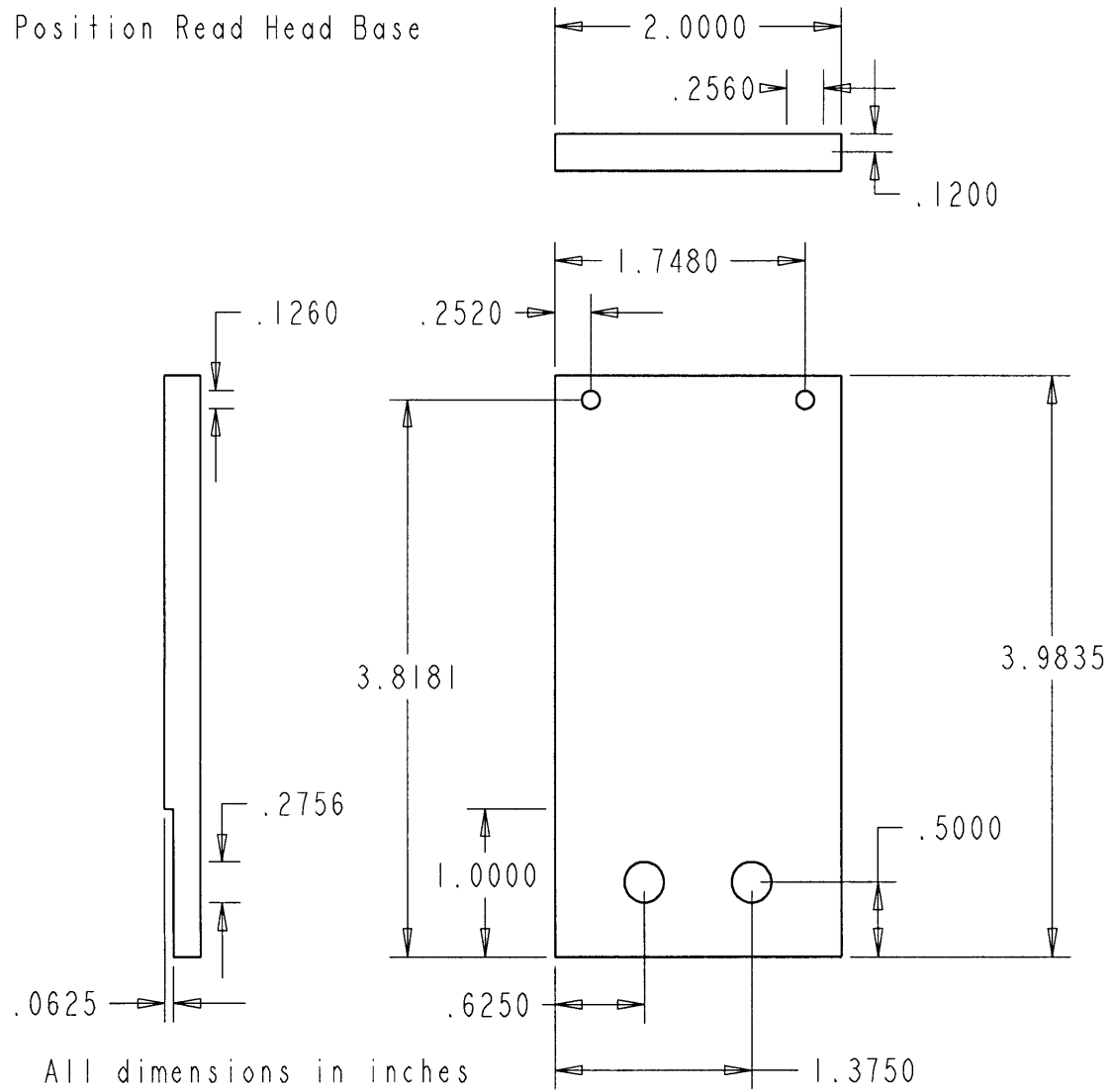


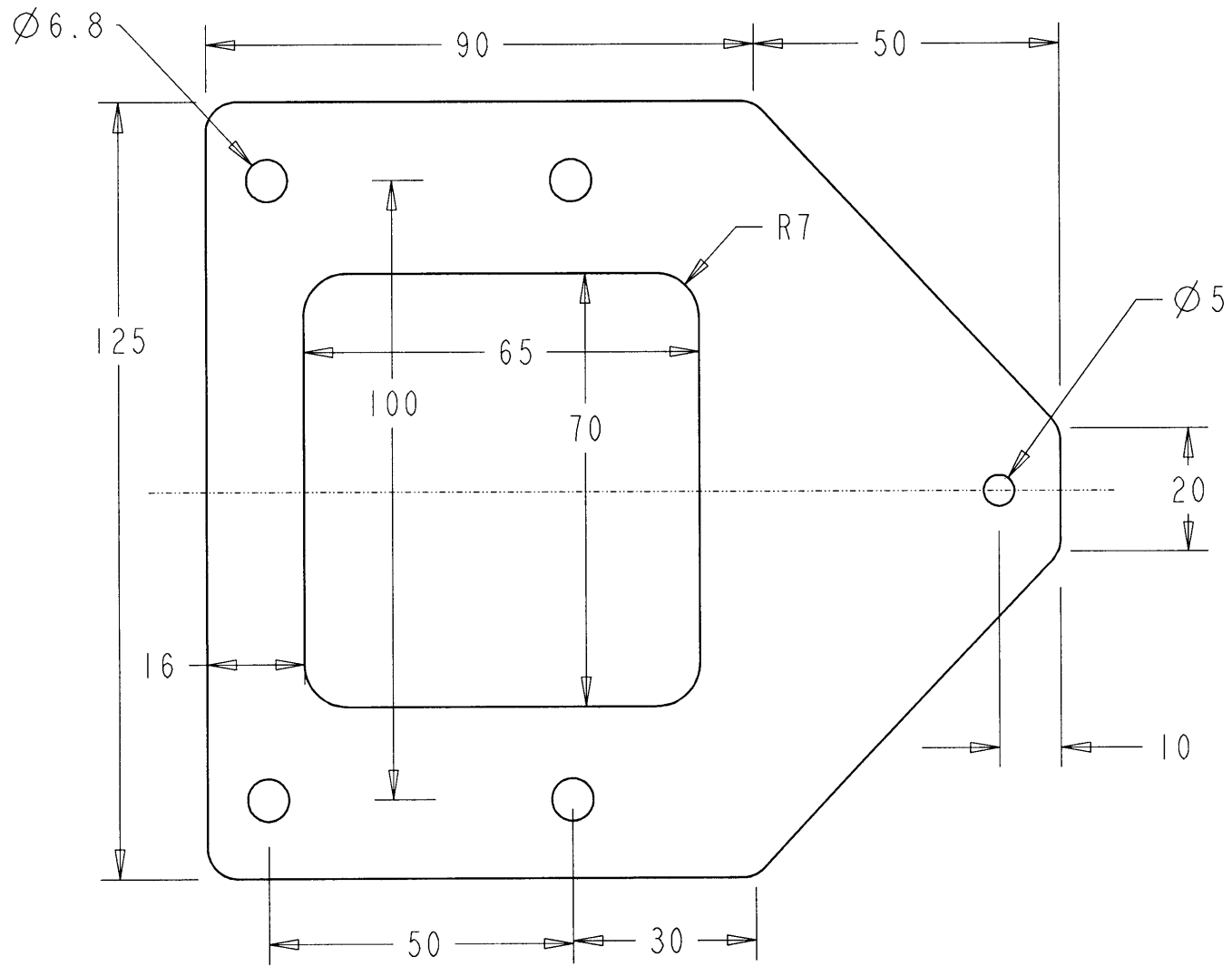
SECTION B-B
SCALE 1.000

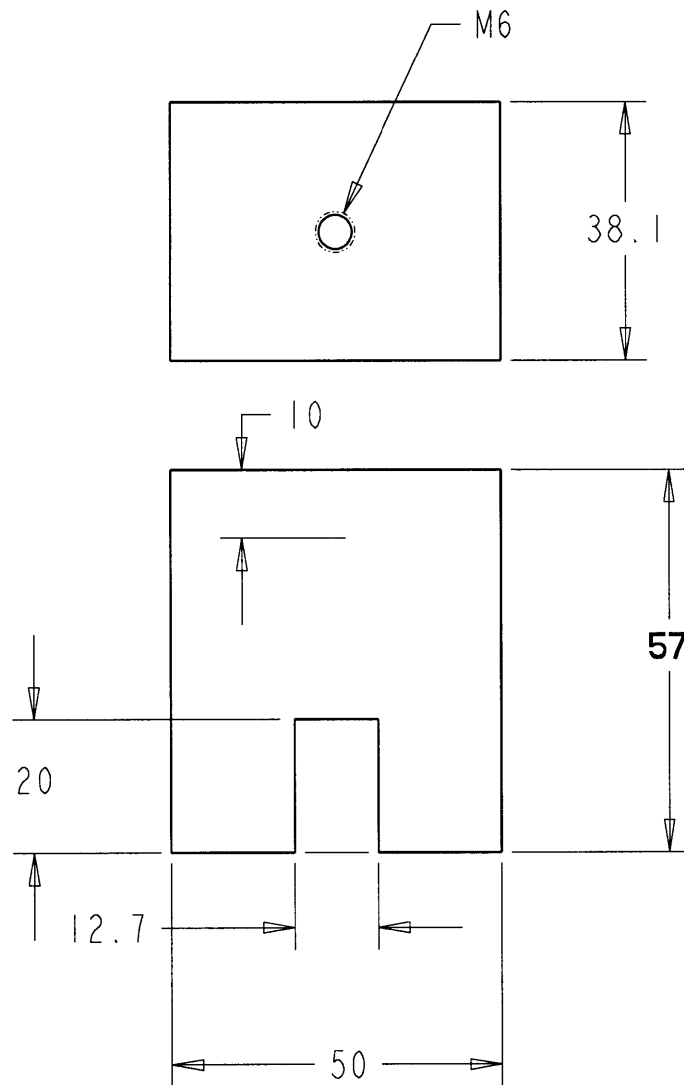
Position Read Head Mount



Position Read Head Base

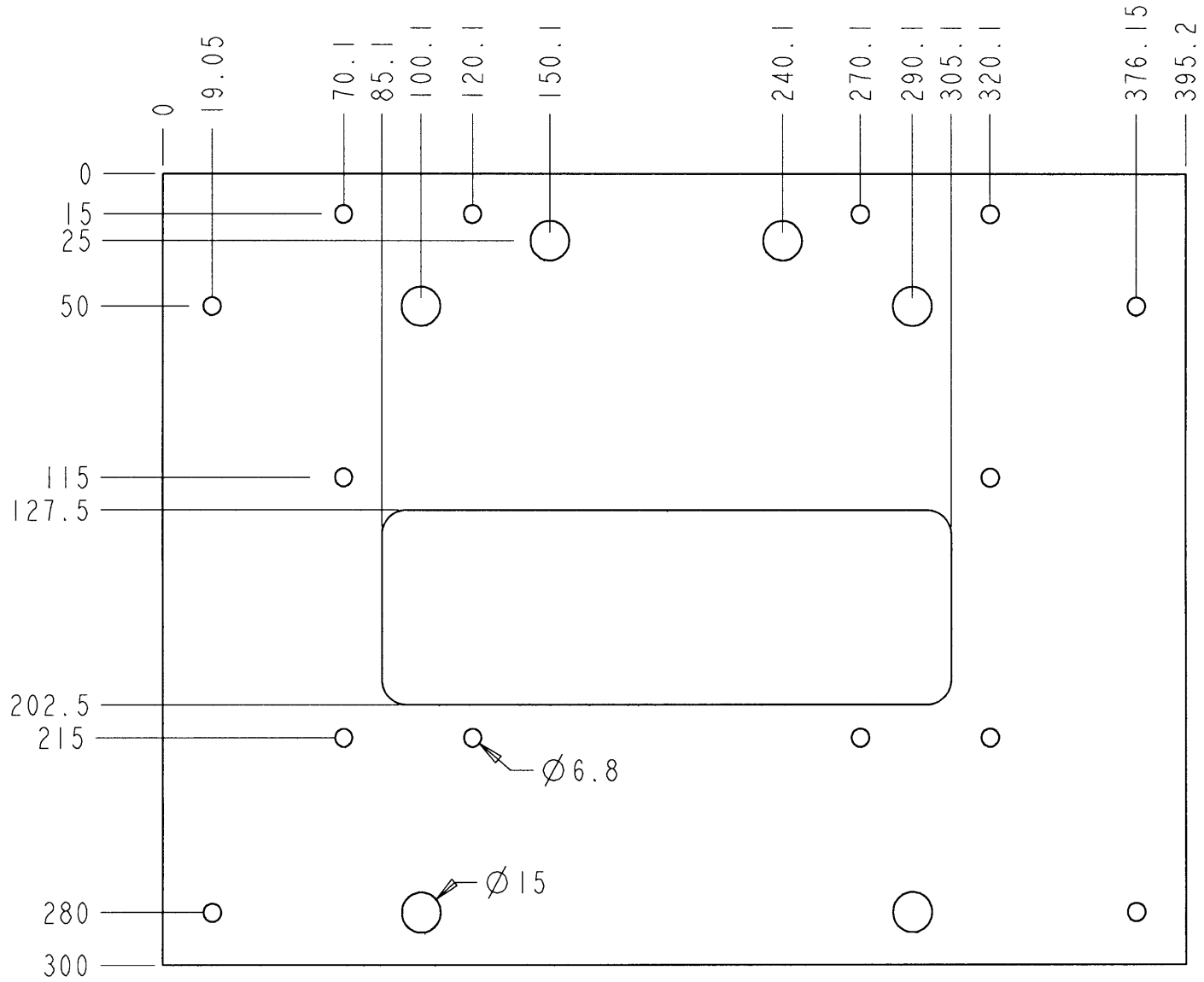




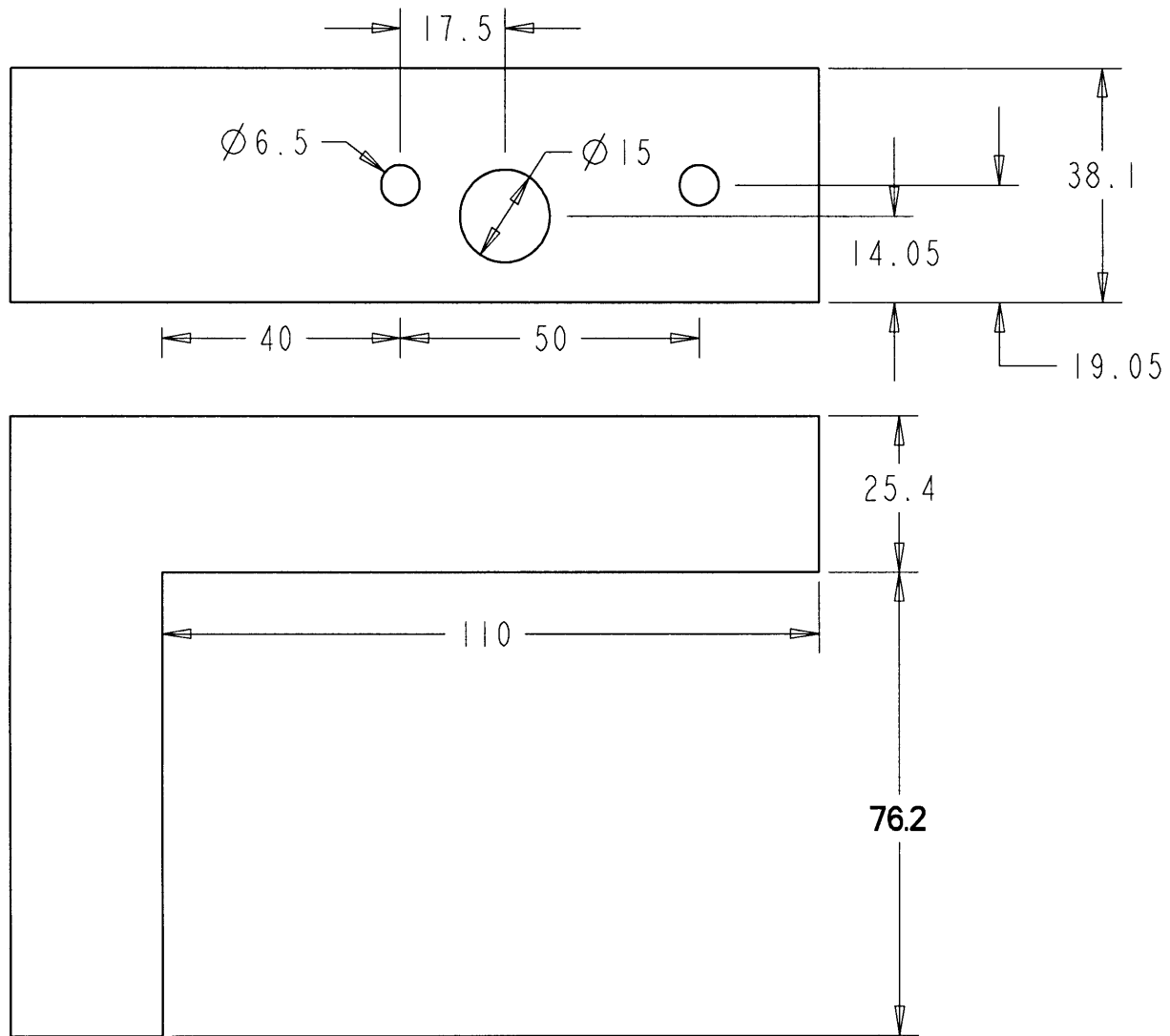


Fixture Block for Top
1.5" Aluminum Plate
all dimensions in mm

Axtrusion Top Fixturing Plate 3/4" Aluminum
 all dimensions in mm

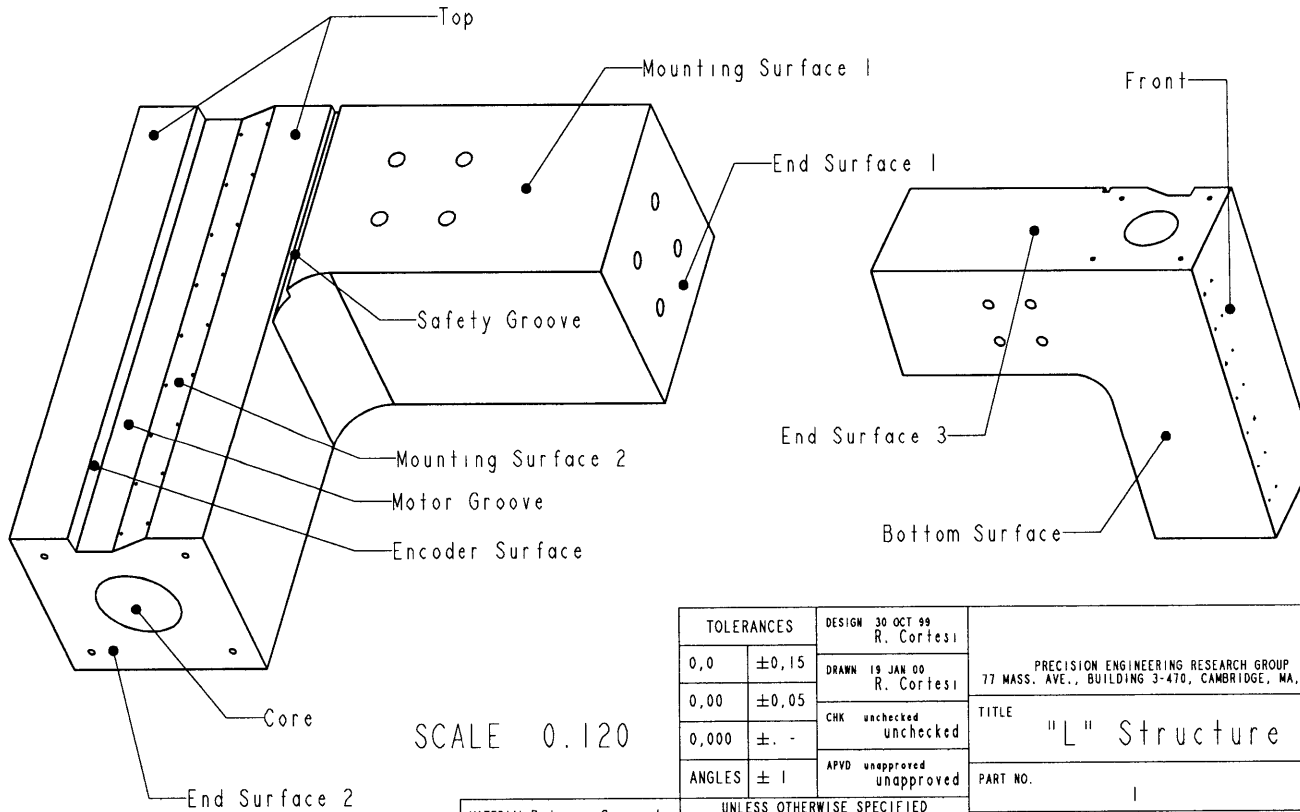


Fixture Block for the Front Face
1.5" Aluminum Plate
all dimensions in mm
make a lefthand and righthand version



Surface and Groove Names

DRW NO.		1		SH	1	REV	0.700
ZONE	REV	SCR NO.	DESCRIPTION	BY	DATE	APPROVED	
			NEW RELEASE				

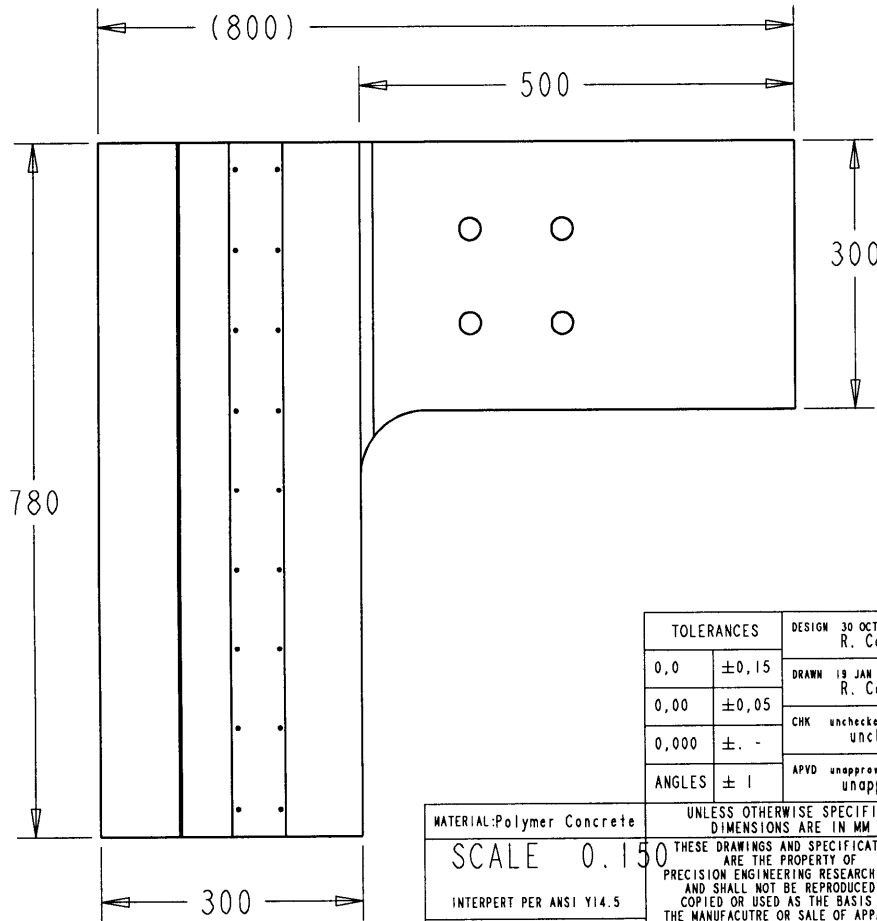


SCALE 0.120

TOLERANCES		DESIGN 30 OCT 99 R. Cortesi	PRECISION ENGINEERING RESEARCH GROUP 77 MASS. AVE., BUILDING 3-470, CAMBRIDGE, MA, 02139	DRAWING NO. 1	REV 0.700
0,0	±0,15	DRAWN 19 JAN 00 R. Cortesi			
0,00	±0,05	CHK unchecked unchecked			
0,000	±. -	APVD unapproved unapproved			
ANGLES	± 1				
MATERIAL: Polymer Concrete		UNLESS OTHERWISE SPECIFIED DIMENSIONS ARE IN MM		TITLE "L" Structure	
INTERPERT PER ANSI Y14.5		THESE DRAWINGS AND SPECIFICATIONS ARE THE PROPERTY OF PRECISION ENGINEERING RESEARCH GROUP AND SHALL NOT BE REPRODUCED OR COPIED OR USED AS THE BASIS FOR THE MANUFACTURE OR SALE OF APPARATUS WITHOUT THE WRITTEN PERMISSION OF PRECISION ENGINEERING RESEARCH GROUP		PART NO. 1	
CODE IDENT 31413		PRO/E DRAW FILE STRUCTURE_L		DRAWING NO. 1	
		SIZE A		SCALE 0.075	
				SHEET 1 OF 9	

DRW NO	1
SH	1
REV	0.700

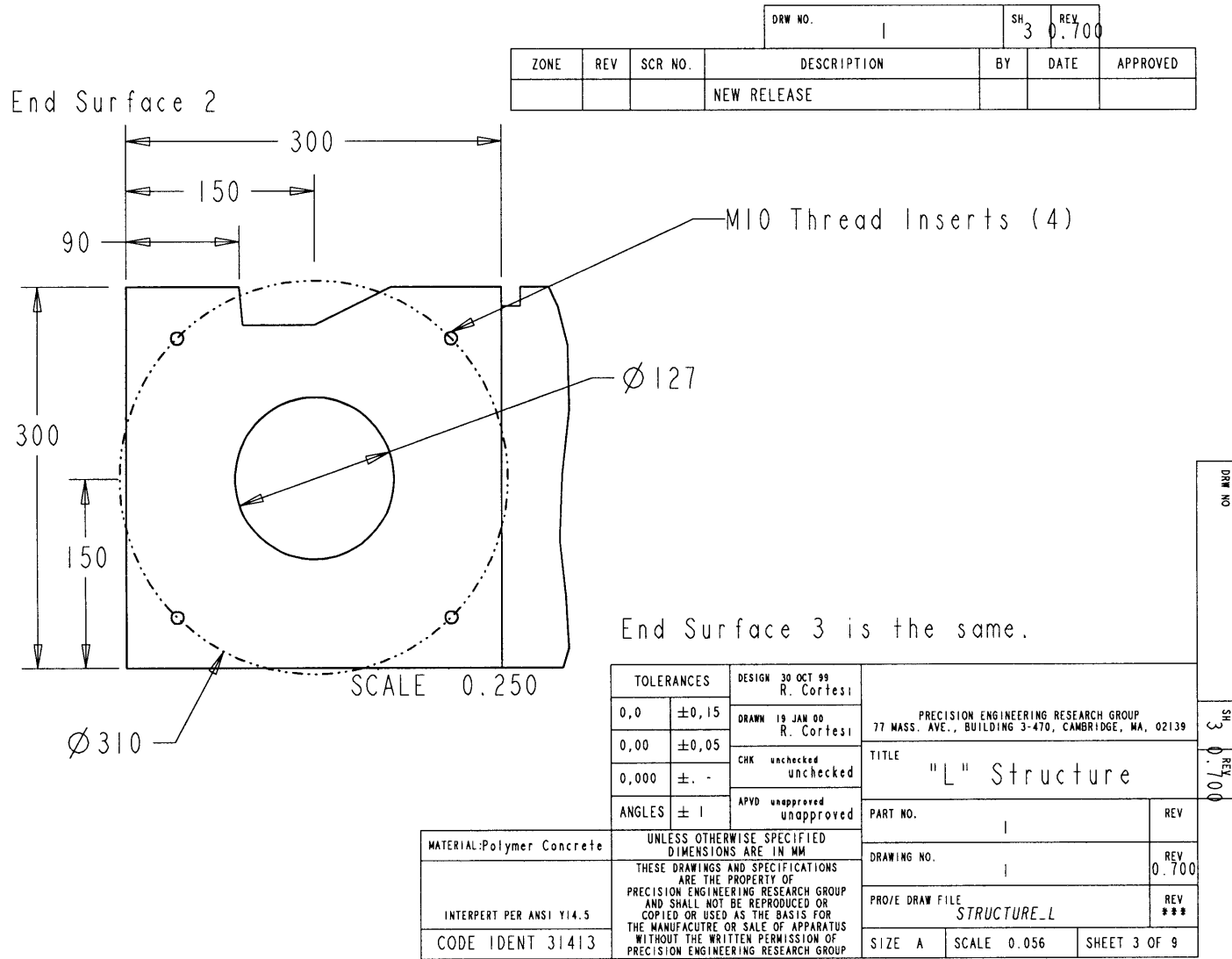
Overall Dimensions



DRW NO.		1		SH	2	REV	0.700
ZONE	REV	SCR NO.	DESCRIPTION	BY	DATE	APPROVED	
			NEW RELEASE				

TOLERANCES		DESIGN 30 OCT 99 R. Cortesi	PRECISION ENGINEERING RESEARCH GROUP 77 MASS. AVE., BUILDING 3-470, CAMBRIDGE, MA, 02139	DRAWING NO. 1	REV 0.700		
0,0	±0,15	DRAWN 19 JAN 00 R. Cortesi					
0,00	±0,05	CHK unchecked unchecked					
0,000	± -	APVD unapproved unapproved					
ANGLES	± 1		TITLE "L" Structure				
MATERIAL: Polymer Concrete		UNLESS OTHERWISE SPECIFIED DIMENSIONS ARE IN MM		PART NO.	1	REV	
SCALE 0.150		THESE DRAWINGS AND SPECIFICATIONS ARE THE PROPERTY OF PRECISION ENGINEERING RESEARCH GROUP AND SHALL NOT BE REPRODUCED OR COPIED OR USED AS THE BASIS FOR THE MANUFACTURE OR SALE OF APPARATUS WITHOUT THE WRITTEN PERMISSION OF PRECISION ENGINEERING RESEARCH GROUP		DRAWING NO.	1	REV	0.700
INTERPERT PER ANSI Y14.5				PROJ/E DRAW FILE	STRUCTURE_L	REV	***
CODE IDENT 31413				SIZE A	SCALE 0.056	SHEET 2 OF 9	

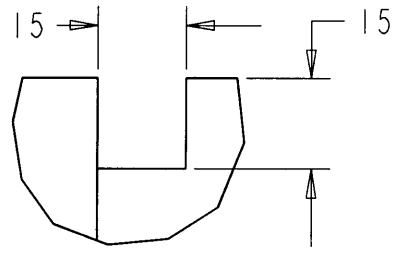
DRW NO.	
SH	2
REV	0.700



DRW NO.		1		SH.	3	REV.	0.700
ZONE	REV	SCR NO.	DESCRIPTION	BY	DATE	APPROVED	
			NEW RELEASE				

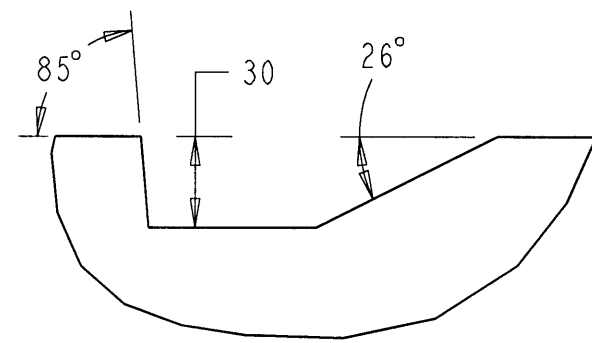
TOLERANCES		DESIGN 30 OCT 99 R. Cortesi	PRECISION ENGINEERING RESEARCH GROUP 77 MASS. AVE., BUILDING 3-470, CAMBRIDGE, MA. 02139	SH. 3 REV. 0.700
0,0	±0,15	DRAWN 19 JAN 00 R. Cortesi		
0,00	±0,05	CHK unchecked unchecked		
0,000	±. -	APVD unapproved unapproved		
ANGLES	± 1			
MATERIAL: Polymer Concrete		UNLESS OTHERWISE SPECIFIED DIMENSIONS ARE IN MM		
INTERPERT PER ANSI Y14.5		THESE DRAWINGS AND SPECIFICATIONS ARE THE PROPERTY OF PRECISION ENGINEERING RESEARCH GROUP AND SHALL NOT BE REPRODUCED OR COPIED OR USED AS THE BASIS FOR THE MANUFACTRE OR SALE OF APPARATUS WITHOUT THE WRITTEN PERMISSION OF PRECISION ENGINEERING RESEARCH GROUP		
CODE IDENT 31413		TITLE "L" Structure	PART NO. 1	REV
		DRAWING NO. 1		REV 0.700
		PRO/E DRAW FILE STRUCTURE_L		REV ***
SIZE A	SCALE 0.056	SHEET 3 OF 9		

Groove Dimensions

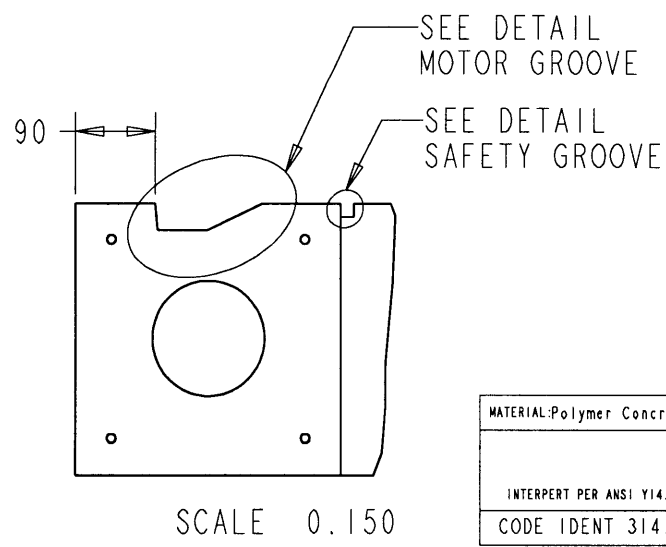


DETAIL SAFETY GROOVE
SCALE 1.000

DRW NO.		1		SH	4	REV	0.700
ZONE	REV	SCR NO.	DESCRIPTION	BY	DATE	APPROVED	
			NEW RELEASE				



DETAIL MOTOR GROOVE
SCALE 0.500

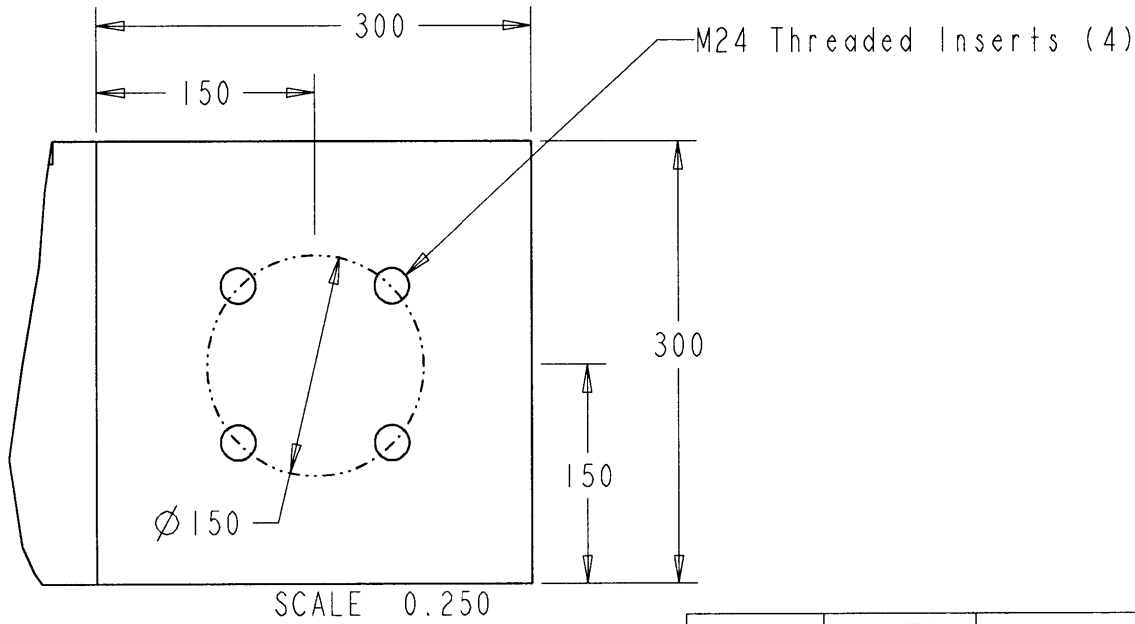


SCALE 0.150

TOLERANCES		DESIGN 30 OCT 99 R. Cortesi	PRECISION ENGINEERING RESEARCH GROUP 77 MASS. AVE., BUILDING 3-470, CAMBRIDGE, MA, 02139
0,0	±0,15	DRAWN 19 JAN 00 R. Cortesi	
0,00	±0,05	CHK unchecked unchecked	TITLE "L" Structure
0,000	± -	APVD unapproved unapproved	PART NO. 1
ANGLES	± 1		REV
MATERIAL: Polymer Concrete	UNLESS OTHERWISE SPECIFIED DIMENSIONS ARE IN MM		SH 4
INTERPERT PER ANSI Y14.5	THESE DRAWINGS AND SPECIFICATIONS ARE THE PROPERTY OF PRECISION ENGINEERING RESEARCH GROUP AND SHALL NOT BE REPRODUCED OR COPIED OR USED AS THE BASIS FOR THE MANUFACTURE OR SALE OF APPARATUS WITHOUT THE WRITTEN PERMISSION OF PRECISION ENGINEERING RESEARCH GROUP		REV 0.700
CODE IDENT 31413	DRAWING NO. 1		REV ***
	PROJE DRAW FILE STRUCTURE_L	SIZE A	SCALE 0.056
			SHEET 4 OF 9

ON M40
SH 4
REV 0.700

End Surface I Dimensions

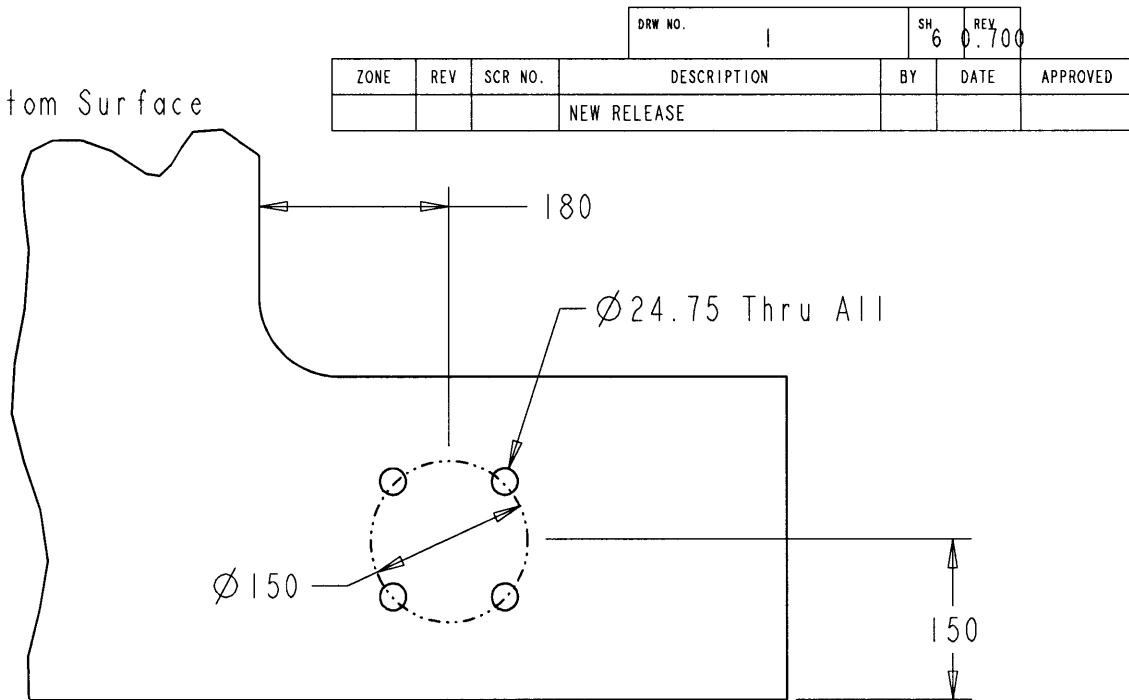


DRW NO.		1		SH	5	REV	0.700
ZONE	REV	SCR NO.	DESCRIPTION	BY	DATE	APPROVED	
			NEW RELEASE				

TOLERANCES		DESIGN	30 OCT 99 R. Cortesi	PRECISION ENGINEERING RESEARCH GROUP 77 MASS. AVE., BUILDING 3-470, CAMBRIDGE, MA, 02139	TITLE "L" Structure	PART NO. 1	REV
0,0	±0,15	DRAWN	19 JAN 00 R. Cortesi				
0,00	±0,05	CHK	unchecked unchecked				
0,000	±. -	APVD	unapproved unapproved				
ANGLES	± 1						
MATERIAL: Polymer Concrete	UNLESS OTHERWISE SPECIFIED DIMENSIONS ARE IN MM						
INTERPERT PER ANSI Y14.5	THESE DRAWINGS AND SPECIFICATIONS ARE THE PROPERTY OF PRECISION ENGINEERING RESEARCH GROUP AND SHALL NOT BE REPRODUCED OR COPIED OR USED AS THE BASIS FOR THE MANUFACTURE OR SALE OF APPARATUS WITHOUT THE WRITTEN PERMISSION OF PRECISION ENGINEERING RESEARCH GROUP			DRAWING NO. 1		REV 0.700	
CODE IDENT 31413				PRO/E DRAW FILE STRUCTURE_L		REV &pdmr ev	
		SIZE	A	SCALE	0.056	SHEET 5 OF 9	

DRW NO	1
SH	5
REV	0.700

Holes in Bottom Surface



SCALE 0.180

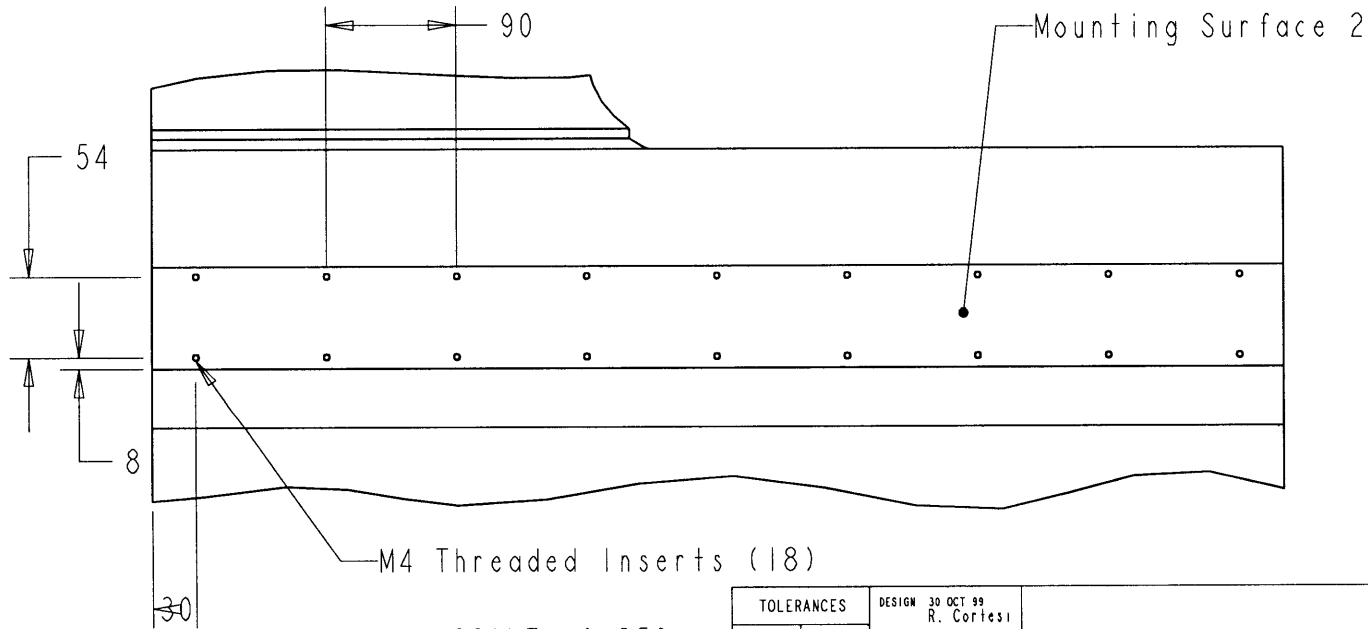
DRW NO. 1			SH 6	REV 0.700		
ZONE	REV	SCR NO.	DESCRIPTION	BY	DATE	APPROVED
			NEW RELEASE			

TOLERANCES		DESIGN 30 OCT 99 R. Cortesi	PRECISION ENGINEERING RESEARCH GROUP 77 MASS. AVE., BUILDING 3-470, CAMBRIDGE, MA, 02139	TITLE "L" Structure	PART NO. 1	REV
0,0	±0,15	DRAWN 19 JAN 00 R. Cortesi				
0,00	±0,05	CNK unchecked unchecked				
0,000	±. -	APVD unapproved unapproved				
ANGLES	± 1					
MATERIAL: Polymer Concrete	UNLESS OTHERWISE SPECIFIED DIMENSIONS ARE IN MM					
INTERPERT PER ANSI Y14.5	THESE DRAWINGS AND SPECIFICATIONS ARE THE PROPERTY OF PRECISION ENGINEERING RESEARCH GROUP AND SHALL NOT BE REPRODUCED OR COPIED OR USED AS THE BASIS FOR THE MANUFACTURE OR SALE OF APPARATUS WITHOUT THE WRITTEN PERMISSION OF PRECISION ENGINEERING RESEARCH GROUP		DRAWING NO. 1			REV 0.700
CODE IDENT 31413			PRO/E DRAW FILE STRUCTURE_L			REV &pdm rev
	SIZE A	SCALE 0.056	SHEET 6 OF 9			

ON M.J.O
SH 6
REV 0.700

Insert Location
on Mounting Surface 2

DRW NO.		1		SH	7	REV	0.700
ZONE	REV	SCR NO.	DESCRIPTION	BY	DATE	APPROVED	
			NEW RELEASE				



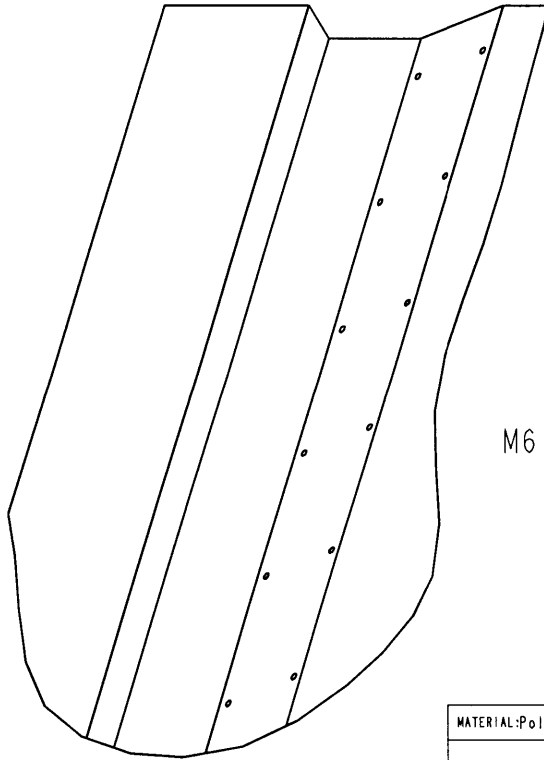
SCALE 0.250

TOLERANCES		DESIGN 30 OCT 99 R. Cortesi	PRECISION ENGINEERING RESEARCH GROUP 77 MASS. AVE., BUILDING 3-470, CAMBRIDGE, MA. 02139	TITLE "L" Structure
0,0	±0,15	DRAWN 19 JAN 00 R. Cortesi		
0,00	±0,05	CHK unchecked unchecked		
0,000	±. -	APVD unapproved unapproved		
ANGLES	± 1			

MATERIAL: Polymer Concrete	UNLESS OTHERWISE SPECIFIED DIMENSIONS ARE IN MM		PART NO.	1	REV	
INTERPERT PER ANSI Y14.5	THESE DRAWINGS AND SPECIFICATIONS ARE THE PROPERTY OF PRECISION ENGINEERING RESEARCH GROUP AND SHALL NOT BE REPRODUCED OR COPIED OR USED AS THE BASIS FOR THE MANUFACTURE OR SALE OF APPARATUS WITHOUT THE WRITTEN PERMISSION OF PRECISION ENGINEERING RESEARCH GROUP		DRAWING NO.	1	REV	0.700
CODE IDENT 31413			PROJE DRAW FILE	STRUCTURE_L	REV	***
	SIZE A	SCALE 0.056	SHEET 7 OF 9			

DRW NO.	
SH	7
REV	0.700

Insert Location
on Encoder Surface



SCALE 0.300

M6 Threaded Inserts (2)

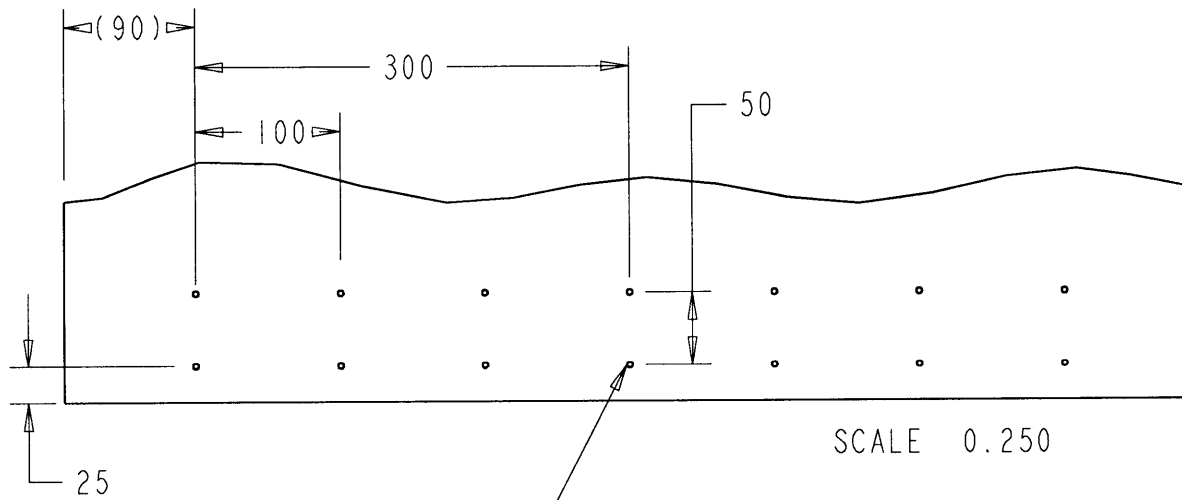
DRW NO.		1		SH	8	REV	0.700
ZONE	REV	SCR NO.	DESCRIPTION	BY	DATE	APPROVED	
			NEW RELEASE				

TOLERANCES		DESIGN 30 OCT 99 R. Cortesi	PRECISION ENGINEERING RESEARCH GROUP 77 MASS. AVE., BUILDING 3-470, CAMBRIDGE, MA, 02139	TITLE "L" Structure	PART NO. 1	REV
0,0	±0,15	DRAWN 19 JAN 00 R. Cortesi				
0,00	±0,05	CHK unchecked unchecked	DRAWING NO. 1		REV 0.700	
0,000	±. -	APVD unapproved unapproved	PROVE DRAW FILE STRUCTURE_L		REV 8pdmrev	
ANGLES	± 1		SIZE A	SCALE 0.056	SHEET 8 OF 9	
MATERIAL: Polymer Concrete		UNLESS OTHERWISE SPECIFIED DIMENSTONS ARE IN MM				
INTERPERT PER ANSI Y14.5		THESE DRAWINGS AND SPECIFICATIONS ARE THE PROPERTY OF PRECISION ENGINEERING RESEARCH GROUP AND SHALL NOT BE REPRODUCED OR COPIED OR USED AS THE BASIS FOR THE MANUFACTRE OR SALE OF APPARATUS WITHOUT THE WRITTEN PERMISSION OF PRECISION ENGINEERING RESEARCH GROUP				
CODE IDENT 31413						

DRW NO	
SH	8
REV	0.700

DRW NO.		1		SH	9	REV	0.700
ZONE	REV	SCR NO.	DESCRIPTION	BY	DATE	APPROVED	
			NEW RELEASE				

Insert Location for Hardware Mounting



SCALE 0.250

M4 Threaded Insert (14)

TOLERANCES		DESIGN 30 OCT 99 R. Cortesi	PRECISION ENGINEERING RESEARCH GROUP 77 MASS. AVE., BUILDING 3-470, CAMBRIDGE, MA. 02139 TITLE "L" Structure PART NO. 1 DRAWING NO. 1 PRO/E DRAW FILE STRUCTURE.L SIZE A SCALE 0.056 SHEET 9 OF 9	SH 9 REV 0.700
0,0	±0,15	DRAWN 19 JAN 00 R. Cortesi		
0,00	±0,05	CHK unchecked unchecked		
0,000	± -	APVD unapproved unapproved		
ANGLES	± 1			
MATERIAL: Polymer Concrete	UNLESS OTHERWISE SPECIFIED DIMENSIONS ARE IN MM			
INTERPERT PER ANSI Y14.5	THESE DRAWINGS AND SPECIFICATIONS ARE THE PROPERTY OF PRECISION ENGINEERING RESEARCH GROUP AND SHALL NOT BE REPRODUCED OR COPIED OR USED AS THE BASIS FOR THE MANUFACTURE OR SALE OF APPARATUS WITHOUT THE WRITTEN PERMISSION OF PRECISION ENGINEERING RESEARCH GROUP			
CODE IDENT 31413				

Appendix A

EXTRUSION SUPPLEMENTARY MATERIALS

A.1 Carriage Stiffness Estimates

This section describes the steps to predict the stiffness performance of the carriage. First an accurate stiffness model of the individual air bearings is generated. Next a model of the carriage (made up of several individual bearings) is generated. Finally a model is developed that will allow forces and displacements to be applied and measured at different points on the way with respect to the carriage

A.1.1 Air Bearing Stiffness Calculations

An approximate formula for estimating a bearing's stiffness is¹

$$K = \frac{P_s \cdot A}{2 \cdot h}, \quad (\text{A.1})$$

where P_s is the supply pressure, A is the area of the pad, and h is the gap thickness. This estimate is used initially to approximate the size of components.

A more accurate bearing model is needed to make a more accurate carriage stiffness model. A better bearing model uses the actual load curves for each size bearing used in the carriage. These curves are available from the Newway web site (<http://www.newwaybear->

1. Precision Machine Design page 583, Alexander H. Slocum, 1992, Society of Manufacturing Engineers, Dearborn Michigan.

ings.com/). The bearing load curves are approximated as a polynomial. The Newway™ 50 x 100 mm and 75 x 150 mm bearings are approximated by

$$L_{50x100} = 0.0065h^4 - 0.496h^3 + 14.598h^2 - 223.351h + 1937, \text{ and} \quad (\text{A.2})$$

$$L_{75x150} = 0.0394h^4 - 2.515h^3 + 61.32h^2 - 786.5h + 5306.3, \quad (\text{A.3})$$

where h is the bearing gap (lift) in microns, and L is the load capacity in Newtons. The stiffness of each air bearing is given by

$$K = \frac{dL}{dx}. \quad (\text{A.4})$$

Differentiating equations A.2 and A.3 with respect to x yield expressions for bearing stiffness [newtons per micron] as a function of gap height [microns]. The expressions for each size bearing are:

$$K_{50x100} = -0.0258h^3 + 1.489h^2 - 29.196h + 223.35 \quad (\text{A.5})$$

$$K_{75x150} = -0.158h^3 + 7.543h^2 - 122.644h + 786.51 \quad (\text{A.6})$$

Knowing the preload forces on each of the bearings allows the bearing gap and stiffness to be calculated. Section 1.7 explains how to calculate the preload force on each bearing. The preload value is added to the actual load. These load values are then used to estimate the gap size by taking the inverses of equations A.2 and A.3, yielding

$$h_{50x100} = (8.0046 \cdot 10^{-12})L^4 - (3.583 \cdot 10^{-8})L^3 + (6.937 \cdot 10^{-5})L^2 - 0.0751L + 39.725; \quad (\text{A.7})$$

$$h_{75x150} = (1.271 \cdot 10^{-13})L^4 - (1.096 \cdot 10^{-9})L^3 + (4.852 \cdot 10^{-6})L^2 - 0.0149L + 24.312. \quad (\text{A.8})$$

Once the gap sizes are known, equations A.5 and A.6 are used to solve for the stiffness of each of the bearings. The results of this substitution are plotted in Figure A.1.

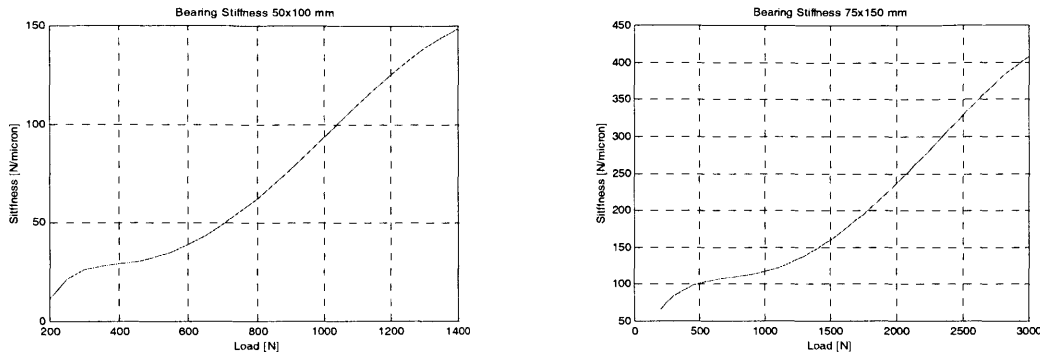


Figure A.1 A Plot of the derived bearings stiffness [Newtons/micron] vs. load [Newtons] for the New-way 50 x 100 mm (left) and 75 x 150 mm (right) air bearing running at 60 psi.

A.1.2 Estimating the Stiffness of the Axtrusion

Several assumptions are made in this analysis: 1) The actual carriage structure is infinitely stiff; all the displacement in the carriage comes from the compliance in the bearing pads. 2) The bearing stiffness is constant over the range of motion we are looking at. A compliance matrix is defined for the configuration shown below.

Figure A.2 The model used to estimate the deflection of the carriages due to tool loading forces. Each bearing was modeled as spring of constant stiffness in the direction normal to the bearing pad. The motor was modeled as spring of constant stiffness in the direction of travel.

Each pad is modeled as a spring of stiffness k_{top1} , k_{top2} , and k_{side} for the top inboard bearing pair, top outboard pair, and the side pair, respectively. The motor has a stiffness of k_{motor} in the direction of travel. A compliance matrix is calculated for this assembly.

$$\vec{C} = \begin{bmatrix} \frac{1}{k_{motor}} & 0 & 0 & 0 & 0 & 0 \\ 0 & \frac{1}{2k_{side}} & 0 & 0 & 0 & 0 \\ 0 & 0 & \frac{1}{2k_{top1} + 2k_{top2}} & 0 & 0 & 0 \\ 0 & 0 & 0 & \frac{1}{\frac{1}{2}L_y^2(k_{top1} + k_{top2}) + 2k_{side}L_{zz}^2} & 0 & 0 \\ 0 & 0 & 0 & 0 & \frac{1}{\frac{1}{2}L_x^2(k_{top1} + k_{top2})} & 0 \\ 0 & 0 & 0 & 0 & 0 & \frac{1}{\frac{1}{2}k_{side}L_{zx}^2} \end{bmatrix} \quad (A.9)$$

The compliance matrix is used to solve for the displacement and rotation of the carriage in response to forces and moments applied to the carriage's center of stiffness. The forces and moments applied to the center of stiffness are described by the vector

$$\vec{F} = \begin{bmatrix} F_x \\ F_y \\ F_z \\ M_x \\ M_y \\ M_z \end{bmatrix}. \quad (A.10)$$

The displacement and rotation of the carriage can be solved by

$$\vec{D}_{carrage} = \vec{C} \cdot \vec{F} = \begin{bmatrix} \delta x \\ \delta y \\ \delta z \\ \theta_x \\ \theta_y \\ \theta_z \end{bmatrix}, \quad (A.11)$$

where $D_{carrage}$ is the displacement of the carriage (in translation and rotation).

A.1.3 Translation and Rotation of Points Not at the C.O.S.¹

If the translation and rotation of the carriage is known, then the motion of any point fixed to the carriage can be calculated using a Homogeneous Transformation Matrix (HTM). To calculate the HTM for the displacement $D_{carriage}$ use

$$\overrightarrow{HTM} = \begin{bmatrix} C\theta_y C\theta_z & -C\theta_y S\theta_z & S\theta_y & \delta x \\ S\theta_x S\theta_y C\theta_z + C\theta_x S\theta_z & C\theta_x C\theta_z - S\theta_x S\theta_y S\theta_z & -S\theta_x C\theta_y & \delta y \\ -C\theta_x S\theta_y C\theta_z + S\theta_x S\theta_z & S\theta_x C\theta_z + C\theta_x S\theta_y S\theta_z & C\theta_x C\theta_y & \delta z \\ 0 & 0 & 0 & 1 \end{bmatrix}, \quad (\text{A.12})$$

where S = sine and C = cosine. To find the displacement at a point, the location of the point with respect to the coordinate system of the *HTM* must be known. This location *P* has the form

$$\vec{P} = \begin{bmatrix} x \\ y \\ z \\ 1 \end{bmatrix}, \quad (\text{A.13})$$

where *x*, *y*, and *z* are the coordinates of the point with respect to the HTM. The displacement at the point is given by

$$\vec{E} = \overrightarrow{HTM} \cdot \vec{P} = \begin{bmatrix} \epsilon_x \\ \epsilon_y \\ \epsilon_z \\ 1 \end{bmatrix}. \quad (\text{A.14})$$

A.2 Detail Bearing Replication Steps

This is how the bearings were replicated in place in the carriage:

1. Clean and degrease the carriage pockets and way surfaces. It is important to completely remove any particles or materials that will compromise the bond between the epoxy and the carriage pockets. The way should also be cleaned

1. Precision Machine Design page 66, Alexander H. Slocum, 1992, Society for Manufacturing Engineers, Dearborn Michigan

of particles and degreased so the bearings lie flat on the way and are not damaged by grit sliding between them and the way



Figure A.3 Drew Devitt (Newway Bearings) degreasing the way.

2. If the fill holes in the carriage are in the center of the pockets, then the hemispherical mounting feature in the back of each bearing should be covered with a small piece of tape. This will dramatically reduce the amount of epoxy needed to replicate each bearing in place.
3. If there are multiple inlet ports in the bearings, plug the ports that are not going to be connected to the air system with set screws or five minute epoxy. If the unused ports are not plugged then the air will not support the bearings.
4. Perform a test of the vacuum system to ensure that all the bearings can be secured to the way. Drawing a vacuum through the bearings ensures that they are aligned with the way and it prevents them from moving while the epoxy is curing.
5. Apply mold release to the linear motor coil. This will allow it to be removed from the carriage later.
6. Attach the motor coil to the carriage with the mounting screws. Draw the motor completely into the pocket. This will increase the air gap between the motor coil and magnet track from about 0.8 mm to about 3 mm, which reduces the preload force to a manageable level.
7. Attach the fixturing to the carriage.
8. Rough position the top bearings on the way.

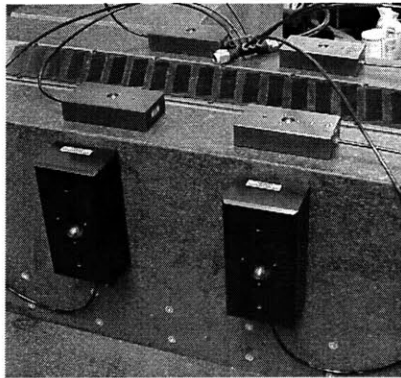


Figure A.4 Testing the vacuum system ensures that there are no leaks in the air system prior to squirting the epoxy. Notice the side bearing pads clamped to the way by the vacuum.



Figure A.5 The top bearings in their approximate locations on the Way.

9. Lower the carriage on the way. Fit the top bearings into their pockets.
10. Draw a vacuum through the top bearings. This holds them in place during the rest of the replication process.
11. Remove the carriage, leaving the top bearings on the way.
12. Degrease the replicating surfaces of all the bearings.
13. Place the side bearings in their pockets on the carriage.
14. Place the carriage back on the way.

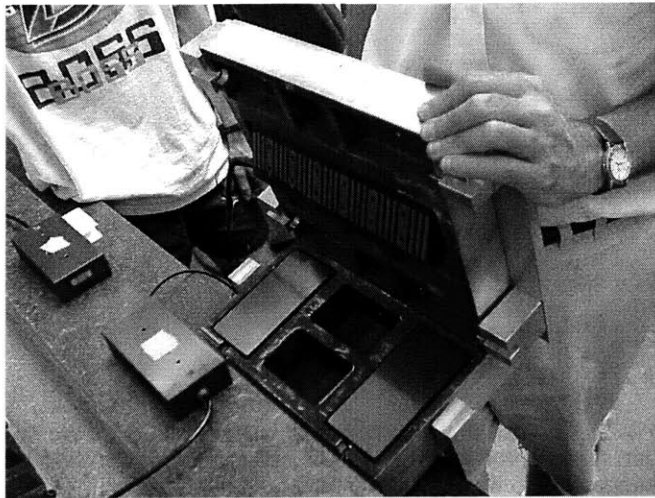


Figure A.6 The side bearings placed in their pockets before the carriage is put on the way.

15. Center the side bearings in their pockets if needed.
16. Draw a vacuum through the side bearings to hold them in place.
17. Place a piece of non-ferrous shim stock (cardboard, plastic, etc.) between the motor coil and magnet track. The shim stock's thickness should be the required air gap for the motor.
18. Lower the motor onto the shim stock and then back it off until the shim can be removed.
19. Visually inspect the air gap between the motor coil and magnet track to ensure that there is no contact between them.
20. Calculate the needed volumes of epoxy to fill each pocket. This prevents the pockets from being over filled. Overfilling could cause the epoxy to leak, and possibly even glue the carriage to the way.
21. Mix the epoxy.
22. Slowly inject the required amount of epoxy into each pocket.
23. The vacuum pump should continue to be run for about 12 hours to allow the epoxy to cure.

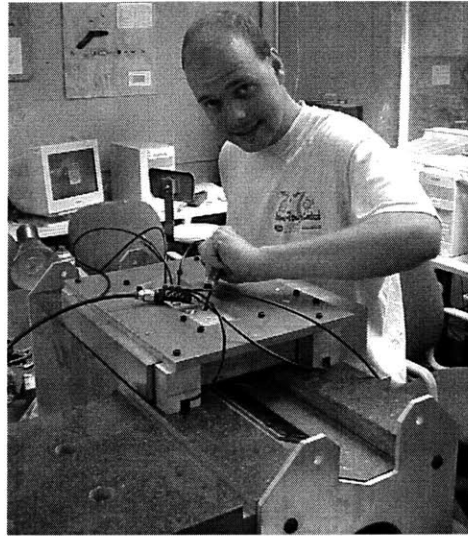


Figure A.7 Roger lowering the motor down onto the shim stock.



Figure A.8 The epoxy being mixed

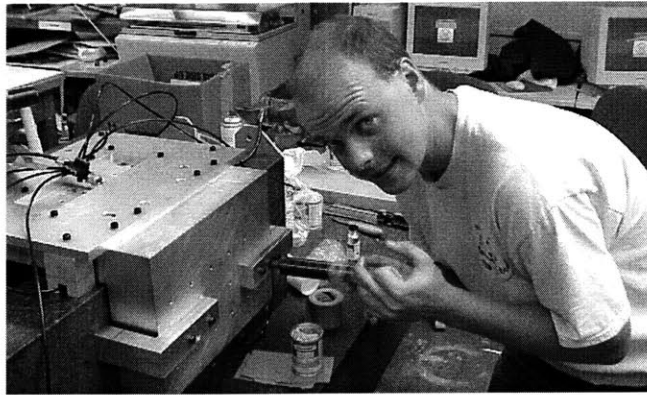


Figure A.9 Roger injecting epoxy into one of the side pockets.

A.3 Performance Data from the Prototype

Five tests were done on the prototype to assess its performance:

- Carriage Pitch
- Carriage Yaw
- Carriage Linear Position Accuracy
- Carriage Straightness
- Carriage Stiffness

A.3.1 Carriage Pitch Data

The pitch measurements were made with a Hewlett Packard 5519A Laser System. Four data sets were taken for both pitch and yaw. The first three data sets consisted of six (6) passes, three (3) in each direction, using 320 mm of travel (the carriage has a total travel of 330 mm). The measurements were taken every 10 mm. Two data sets were run with the carriage at continuous speeds of 10 mm/s, 40 mm/s. A third data was run with the carriage stopping every 10 mm to take a measurement at rest. Finally a fourth pass was made to take measurements every 0.1 seconds, while the carriage traveled at a continuous speed of 10 mm/s. This provided a higher resolution image of what the carriage was doing in pitch. The results are summarized and plotted below.

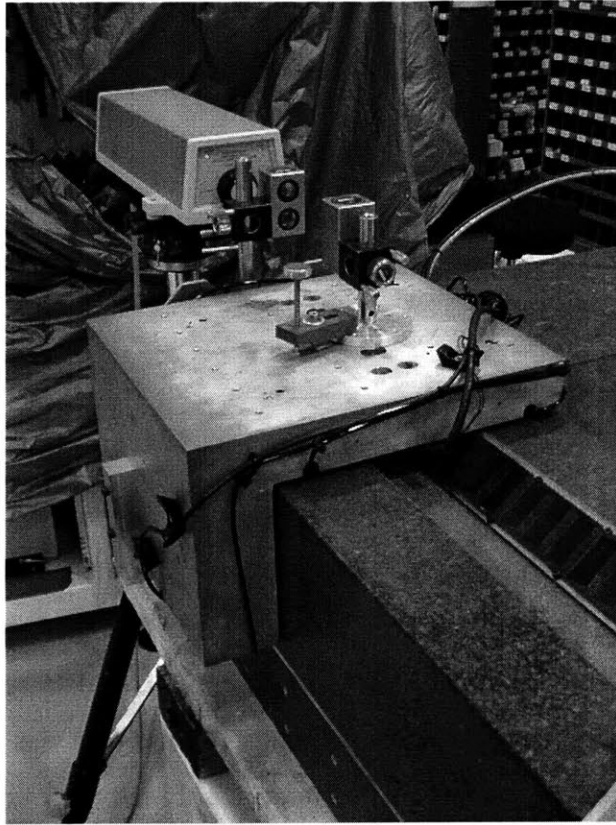


Figure A.10 The pitch measurement setup.

TABLE A.1 Carriage Pitch Data Results

	10 mm/s	40 mm/s	10 mm/s @ 10mm increments
Raw Accuracy [arc sec.]	2.44	2.57	2.38
Raw Repeatability [arc sec.]	0.50	1.63	0.56
Raw Accuracy Forward [arc sec.]	2.44	2.57	2.32
Raw Repeatability Froward [arc sec.]	0.19	1.63	0.25
Raw Accuracy Reverse [arc sec.]	2.38	2.19	2.32
Raw Repeatability Reverse [arc sec.]	0.19	0.25	0.50

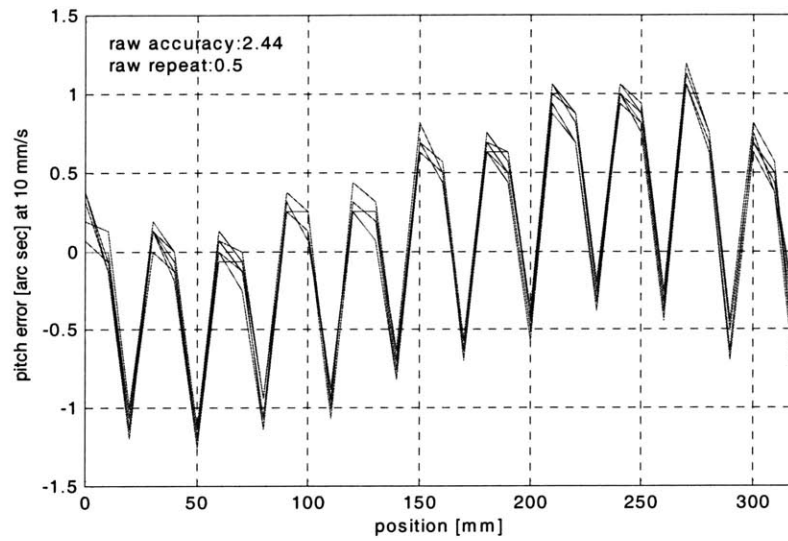


Figure A.11 Carriage Pitch [arc seconds] vs. Carriage position [mm] when the carriage is traveling at 10 mm/s. Measurements made every 10 mm. All six (6) passes are plotted.

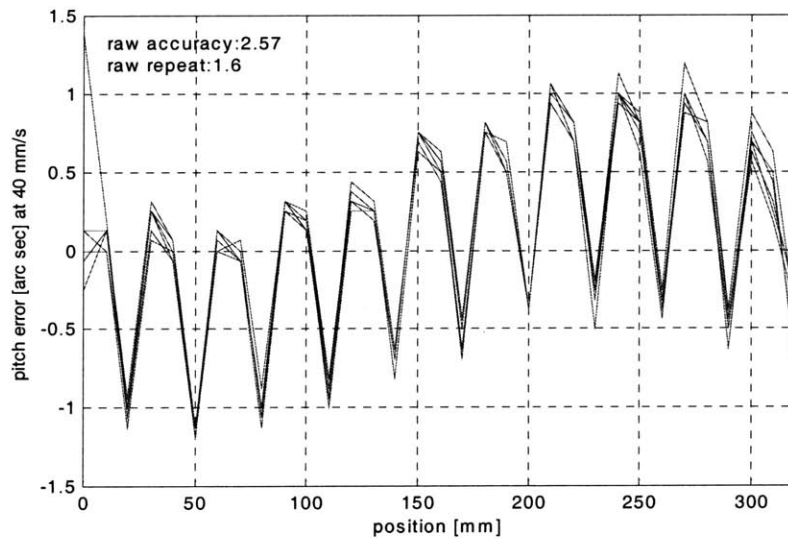


Figure A.12 Carriage Pitch [arc seconds] vs. Carriage position [mm] when the carriage is traveling at 40 mm/s. Measurements made every 10 mm. All six (6) passes are plotted.

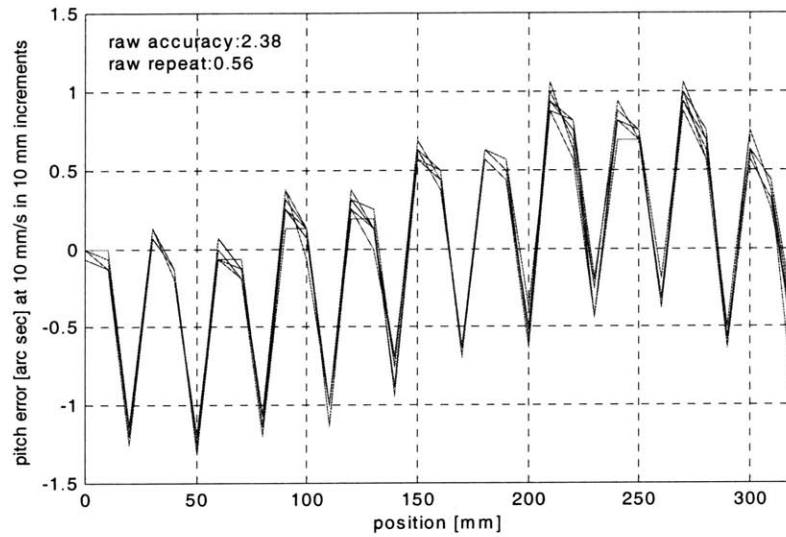


Figure A.13 Carriage Pitch [arc seconds] vs. Carriage position [mm] when the carriage is traveling at 10 mm/s stopping in 10 mm increments and the data taken after the carriage had stopped. Measurements made every 10 mm. All six (6) passes are plotted.

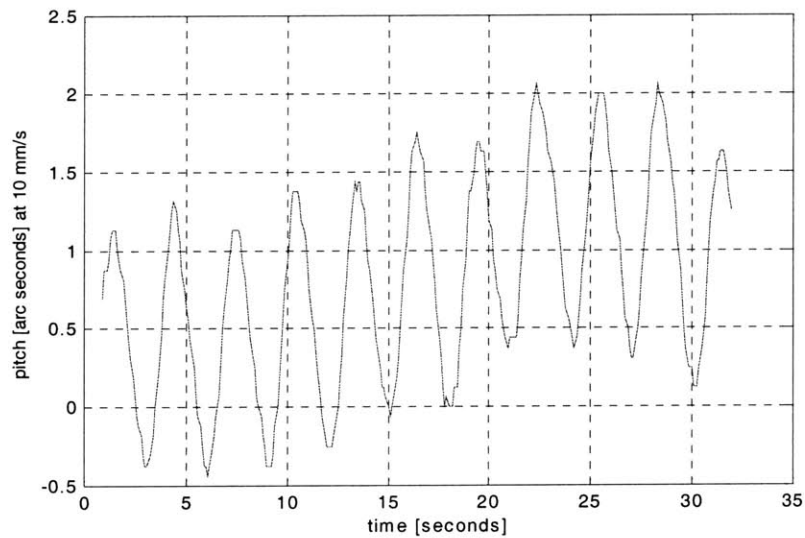


Figure A.14 Carriage Pitch [arc seconds] vs. Time [seconds]. Measurements were made every 0.1 seconds while the carriage was moving at 10 mm/s in the forward direction.

A.3.2 Carriage Yaw Data

The testing procedure for carriage yaw was identical to the testing procedure for the carriage pitch except that the interferometer was reconfigured to measure yaw. When the data was taken a very strong linear trend was observed. It is not clear if this linear trend is due to the instrumentation or an actual error in yaw. If it is an error in yaw, the linear component is trivial to remove by mapping of an orthogonal axis. If the error is an artifact of the instrumentation then the linear trend is of no concern. Data is presented in both its raw format and with the linear trend removed.

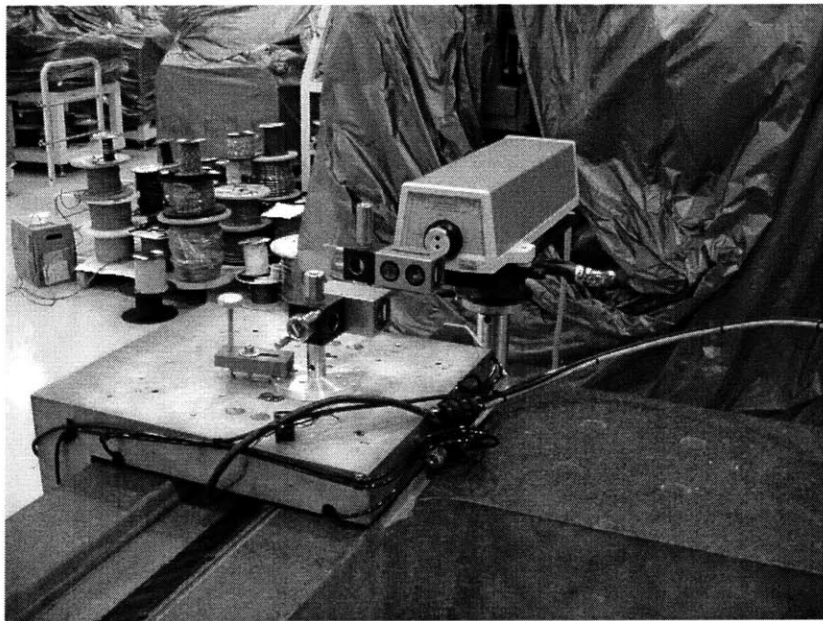
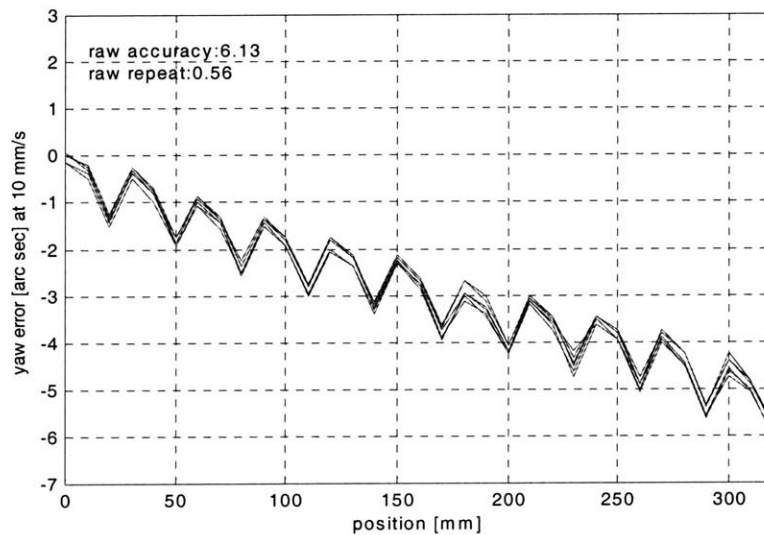


Figure A.15 The yaw measurement setup. This is identical to the pitch set up shown in Figure A.10 on page 124 except the pair of interferometer lenses have been rotated 90 degrees to measure yaw instead of pitch.

TABLE A.2 Carriage Yaw Data Results

	Pitch [arc seconds]		
	10 mm/s	40 mm/s	10 mm/s @ 10mm increments
Raw Accuracy, Linear Trend Removed	1.59	1.66	1.70
Raw Repeatability, Linear Trend Removed	0.56	0.43	0.26
Raw Accuracy	6.13	6.13	6.07
Raw Repeatability	0.56	0.38	0.25
Raw Accuracy Forward	6.07	5.88	6.01
Raw Repeatability Forward	0.44	0.19	0.19
Raw Accuracy Reverse	6.07	6.13	5.94
Raw Repeatability Reverse	0.56	0.25	0.25

**Figure A.16** Carriage Yaw [arc seconds] vs. Carriage position [mm] when the carriage is traveling at 10 mm/s. Measurements made every 10 mm. All six (6) passes are plotted

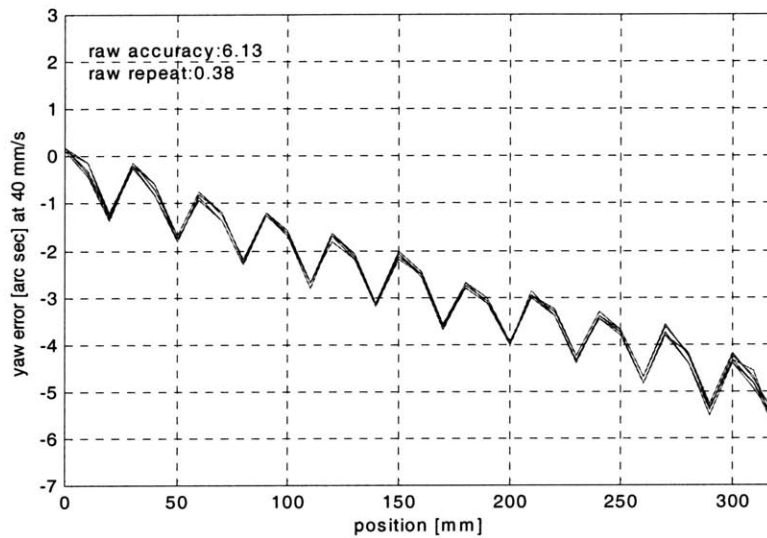


Figure A.17 Carriage Yaw [arc seconds] vs. Carriage position [mm] when the carriage is traveling at 40 mm/s. Measurements made every 10 mm. All six (6) passes are plotted

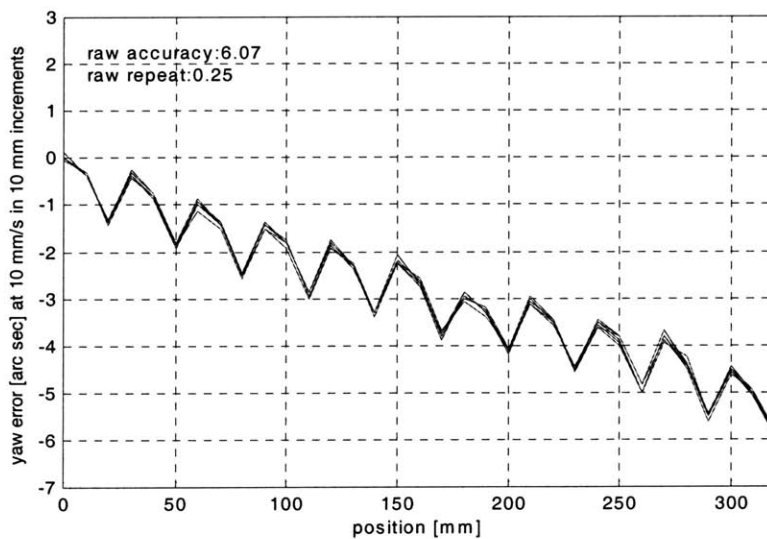


Figure A.18 Carriage Yaw [arc seconds] vs. Carriage position [mm] when the carriage is traveling at 10 mm/s stopping in 10 mm increments and the data taken after the carriage had stopped. Measurements made every 10 mm. All six (6) passes are plotted.

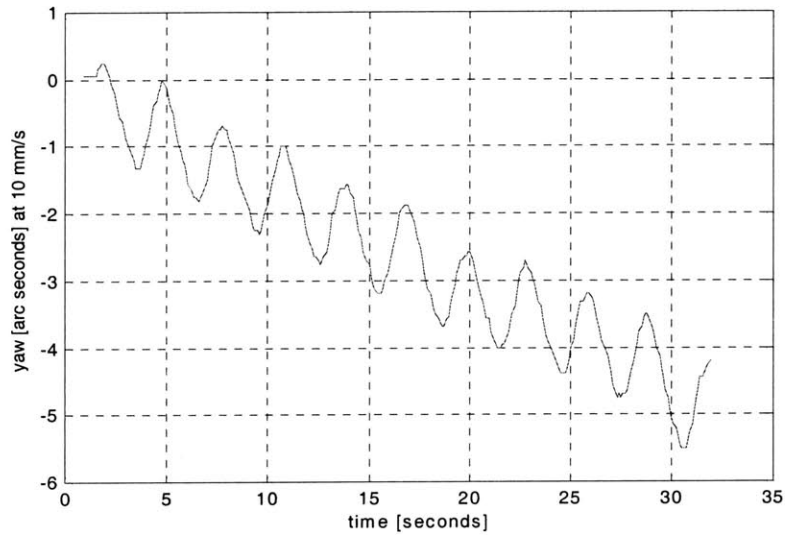


Figure A.19 Carriage Yaw [arc seconds] vs. Time [seconds]. Measurements were made every 0.1 seconds while the carriage was moving at 10 mm/s in the forward direction.

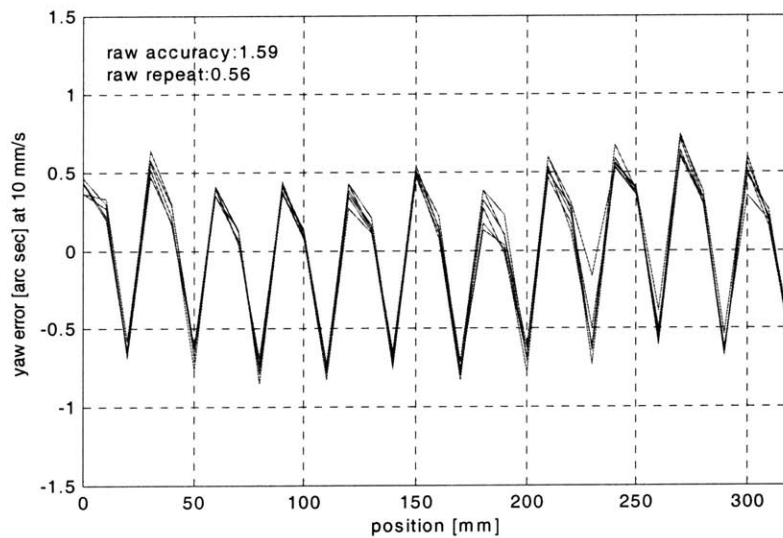


Figure A.20 Carriage Yaw [arc seconds] vs. Position [mm] with the linear trend in the data removed for the 10 mm/s test. Notice the dramatic increase in performance.

A.3.3 Linear Position Accuracy Data

This test was also done with the HP laser interferometer. The linear position accuracy was used to determine the amount of error between where the controller thought the carriage was and the carriage's actual position. The carriage was moved in 10 mm steps and its position recorded. Like the yaw data, the linear position accuracy data has a very strong linear component. If this component is removed (by the controller for example) the performance of the Axtrusion is improved by an order of magnitude. The results are summarized and plotted below.

TABLE A.3 Linear Position Accuracy Results

Raw Accuracy, Linear Trend Removed [microns]	1.34
Raw Repeatability, Linear Trend Removed [microns]	0.33
Raw Accuracy [microns]	9.808
Raw Repeatability [microns]	0.454
Raw Accuracy Forward [microns]	9.785
Raw Repeatability Forward [microns]	0.323
Raw Accuracy Reverse [microns]	9.773
Raw Repeatability Reverse [microns]	0.315

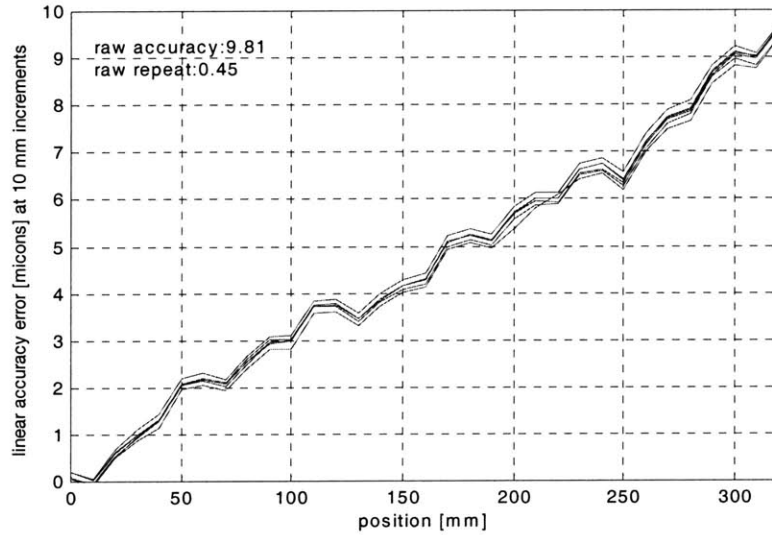


Figure A.21 Linear Position Accuracy [microns] vs. Position [mm] for the carriage. Three (3) passes in each direction are plotted.

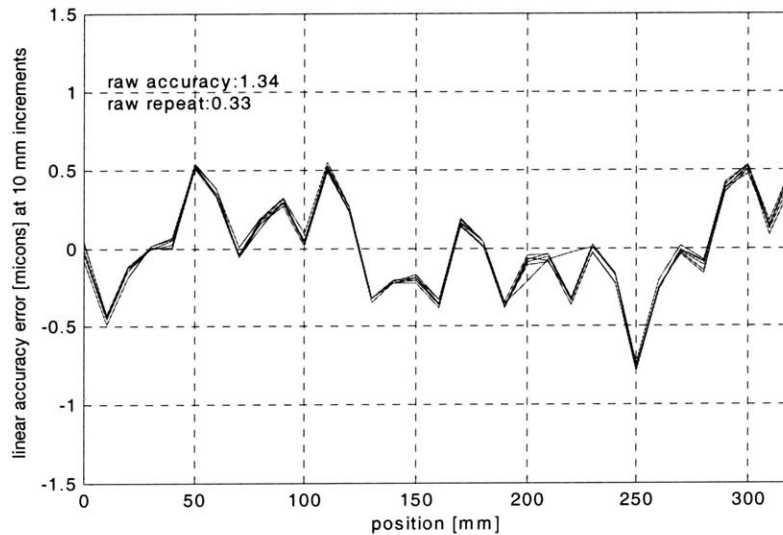


Figure A.22 Linear Position Accuracy [microns] vs. Position [mm] for the carriage, with the linear trend in the data removed. Performance is greatly increased. Three (3) passes in each direction are plotted.

A.3.4 Straightness Data

The straightness data was taken in the vertical direction only. There was not adequate fixturing to allow the measurements to be made easily in the horizontal direction. A straight edge mirror was placed on the carriage and a capacitance probe was suspended above it. As the carriage was moved the probe recorded the change in height. Since the straight edge could not be leveled perfectly the raw data would show a large linear change in the vertical position of the carriage over its length of travel. This trend was removed mathematically from the data.

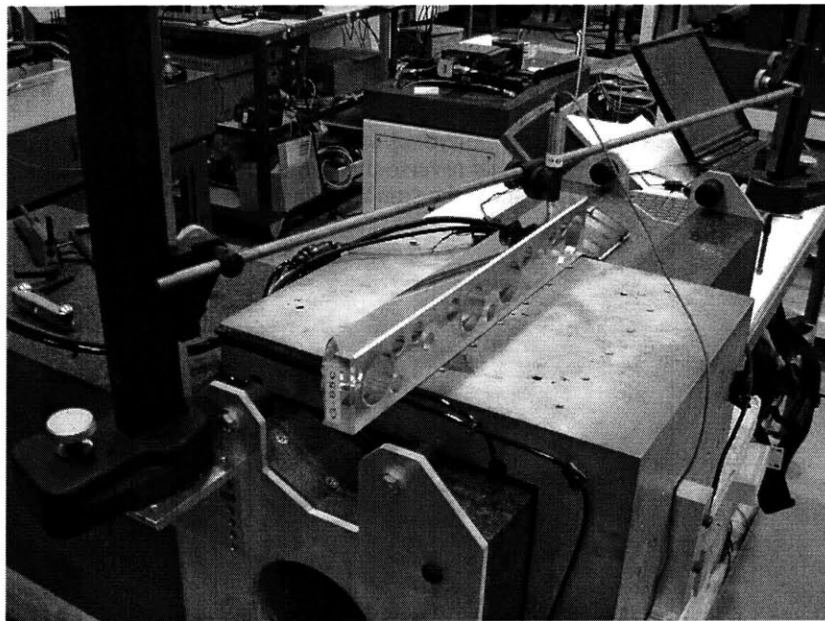


Figure A.23 The straightness measurement setup. Notice the straight edge mirror and capacitance probe suspended above it.

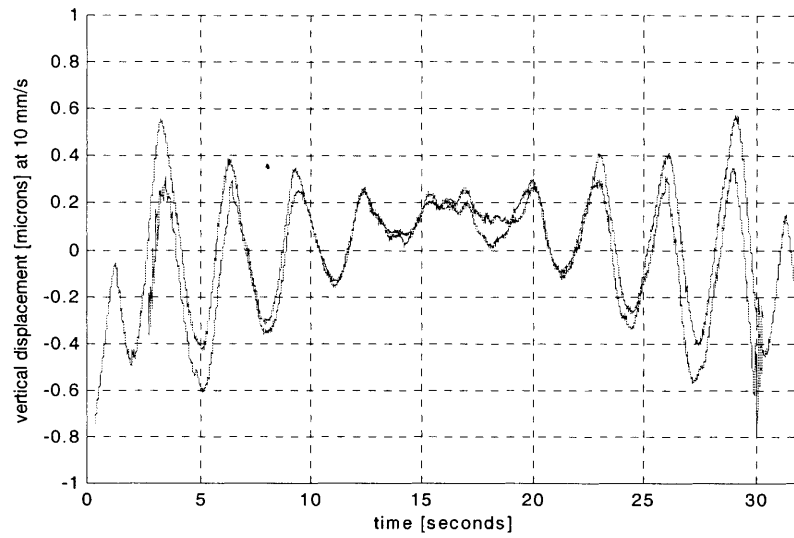


Figure A.24 Vertical Displacement [microns] vs. Time [seconds] for the carriage as it moves down the way in the forward and reverse direction. The data for the reverse direction has been flipped and shifted to show the similarity between the two curves.

A.4 The Stiffness Data

The initial stiffness measurements were fairly crude. The carriage was held in a position by the control system while dial indicator was placed on four of the points used in the modal analysis. These four points are approximately in the centers of each top bearing pads. The air bearings were run at a pressure of 4.13 Bar (60 psi). The carriage was loaded in the top center with 25 lbs and then with 50 lbs (111.2 N and 222.4 N). The displacement of each corner under both loads was recorded.

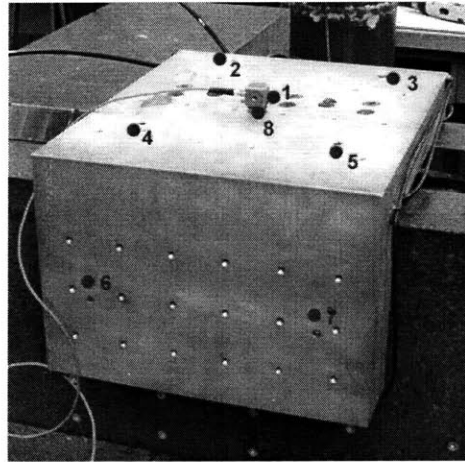


Figure A.25 Points 2, 3, 4, and 5 were used to measure the vertical displacement of the carriage when loads were applied to point 1. From this data the stiffness of the carriage was calculated.

TABLE A.4 Vertical Carriage Displacements Under Load

Carriage Location See Figure A.25	Displacement [microns] at 111.2 N (25 lbs)	Displacement [microns] at 222.4 N (50 lbs)
2	0.15	0.4
3	0.4	1.0
4	0.2	0.4
5	0.5	0.9

The approximate stiffness can be calculated from the known loads and displacements.

TABLE A.5 Vertical Carriage Stiffness Data

Carriage Location See Figure A.25	Stiffness at 111.2 N (25 lbs) [N/micron]	Stiffness at 222.4 N (50 lbs) [N/micron]	Average Point Stiffness [N/micron]
2	741	556	649
3	278	222	250
4	556	556	556
5	222	247	235

Therefore, the average stiffness for the carriage in the vertical direction is 422 Newtons per micron.

22410-64